THE RELATIONSHIP BETWEEN TOR ACTIVITY AND THE CIRCADIAN CLOCK OF *NEUROSPORA CRASSA*

GOLNOUSH AKHTARI

A THESIS SUBMITTED TO THE FACULTY OF GRADUATE STUDIES
IN PARTIAL FULFILMENT OF THE REQUIRMENT FOR THE DEGREE
OF MASTER OF SCIENCE

GRADUATE PROGRAM IN BIOLOGY
YORK UNIVERSITY
TORONTO, ONTARIO

APRIL 2023

Abstract

Circadian cycles are 24-hour rhythms that are present in almost all eukaryotes and some prokaryotes. These rhythms are believed to be driven by a Transcription-Translation Feedback Loop (TTFL) including *frq*, *wc-1*, and *wc-2* genes in our model organism, *Neurospora crassa*. However, evidence showed that other oscillators (FLO), can drive these rhythms in *Neurospora*.

Our lab previously found mutants in the TOR (Target of Rapamycin) pathway that affect the FLO. Thus, we became interested in the TOR pathway as a potential FLO. I measured 40S ribosomal protein S6 phosphorylation as an assay of TOR activity. I found that TOR activity is rhythmic with a circadian period in the wildtype and is rhythmic with different periods in TOR-mutant and clock-mutant strains. Rhythmic TOR activity correlates with conidiation (spore formation), which is under the control of the clock.

Acknowledgements

I would like to express my sincerest appreciation and gratitude to my supervisor Dr. Patricia Lakin-Thomas for being such a wonderful mentor and giving me the opportunity to research in her lab. Dr. Pat, you are an amazing teacher and a very supportive advisor. Without your guidance and encouragement, I would never be able to go through this journey. I have learnt a lot from you and your lab, and I am extremely grateful for the opportunity I had to be your student. Being an international student without family in a new country, it is very hard to study and work and be able to keep the balance of all the emotions and put up with a huge load of stress, but you were always there for me to help me over come the obstacles in this stage of my life. You are not only an amazing knowledgeable scientist, but you also care about your students like a mother.

I would like to extend my gratitude to my advisor, Dr. Mark Bayfield for his critical feedbacks and encouragement. Your advice and expertise helped me tremendously in understanding my project better and becoming a better researcher.

I am really thankful to Dr. Rosa Eskandari, our former PhD student, for teaching me most of the techniques that I used for conducting my research. The first months of my master's program, when there was no one in the University due to the pandemic, Rosa was in the lab to teach me how to do experiments and make me familiar with everything. Rosa, you were the first friend I made in Canada and without your help and support, I wouldn't pass through all the very hard moments I had during these two years. I will always remember the good memories we had together in the lab.

Finally, I would like to thank my family back in Iran for their support and encouragement. Although they were not here physically, their energy and encouragement warmed my heart all the time.

Table of Contents

List of Figures

List of Tables

List of Abbreviations

AD	Alzheimer's disease
BSA	Bovine Serum Albumin
ccgs	Clock Controlled Genes
CLK	Clock
CHK-2	Checkpoint kinase 2
CHX	Cycloheximide
CK1	Casein Kinase 1
CYC	Cycle
DAG	Sn-1,2-diacylglycerol
DBT	Double-Time
DD	Constant darkness
FFC	FRQ/FHR Complex
FGSC	Fungal Genetics Stock Centre
FHR	Frequency Interacting RNA Helicase
FLO	FRQ-less Oscillator
FRQ	Frequency
FWO	FRQ-WCC Oscillator
IDP	Inherently Disordered Protein
IP	Immuno-precipitation
LL	Constant light
MA	Maltose-Arginine Media
MAPKs	Mitogen-activated protein kinase
mTOR	Mammalian/Mechanistic TOR
Per	Period
PTO	Post translational Oscillator

RICTOR	Rapamycin-insensitive companion of mTOR
RPS6	Ribosomal Protein S6
S6K	S6 Kinase
SCN	Suprachiasmatic Nucleus
TOR	Target of Rapamycin
TORC1	TOR Complex 1
TORC2	TOR Complex 2
TTFL	Transcription/Translation Feedback Loop
VTA	Vacuolar TOR-associated
WC-1	White-Collar 1
WC-2	White-Collar 2
WCC	White Collar Complex
WT	Wildtype

Chapter 1: Introduction

Every living organism needs to adapt to its environment and be able to predict the changes in resources to survive. During evolution, natural selection favored the biological circuits which are able to keep track of time and synchronize the organisms' behavioural, biochemical, and physiological states with the cycles in nature including celestial periods (Bhadra et al., 2017). There are four types of cycles generally, ultradian (less than 24 hours), circadian (close to 24 hours), infradian (more than 24 hours), and circannual rhythms (about 1 year). The very interesting aspect of these rhythms is that they are present even in the absence of the environmental cues. These rhythms persist in constant conditions and eventually become "free-runing" with a constant period (Wollnik, 1989).

1.1 Circadian Cycles

Circadian cycles are approximately 24-hour rhythms which are present in almost all eukaryotes and some prokaryotes. Circadian has a Latin root 'circa diem' which means about a day (Pittendrigh & Miller, 1993). These rhythms regulate many biological processes in organisms including physiological, behavioral, and metabolic activities (Lakin-Thomas, 2019). Several behavioral and physiological activities are under the control and regulation of circadian rhythms including sleep-wake patterns, plant flowering, body temperature, blood pressure, hibernation, birds and butterflies' migration, and many other activities (Harmer et al., 2001). They also synchronize the organism with the environment.

Circadian rhythms are endogenous, but they have the ability of being entrained by the environmental cues such as light-dark cycle, food availabilities, and temperature (Dunlap,

1999). In addition, these cycles have temperature compensation, which means that the period of these cycles stays stable in a range of different temperatures (Lakin-Thomas, 2006b). However, they are not insensitive to the changes in temperature. This characteristic differentiates the circadian rhythms from the other biological rhythms that are happening in the cells like the cell cycle (Baker et al., 2012). These rhythms are present in many tissues, multicellular organisms, and individual cells and almost all organisms form bacteria to humans (Cumming & Wagner, 1968; McClung, 2006). The genetic circuits of these rhythms are conserved from bacteria to complex organisms like humans, although the components or the clock-controlled genes (ccgs) differ (Bhadra et al., 2017).

1.2 Molecular Basis of Circadian Rhythms

After many years of research on circadian rhythms in different organisms, it became clear that there should be a main oscillator for these rhythms at the cellular level. In 2017, the Nobel Prize in Physiology or Medicine was awarded to Jeffery C. Hall, Michael Rosbash, and Michael W. Young for the discovery of the molecular oscillator of circadian rhythms in cells which is referred to as the transcription/translation feedback loop (TTFL). However, some anomalous observations in different organisms challenged this notion later.

1.2.1 Transcription/Translation Feedback Loops (TTFL)

The molecular basis of the circadian rhythms in cells is based on transcription/translation feedback loops (TTFL) (Figure 1.1). The canonical clock genes are not completely conserved among different species, but the general interactions between the clock genes and their protein products are the same. TTFL consists of positive and negative regulators (Dunlap, 1999; Lakin-Thomas, 2006b).

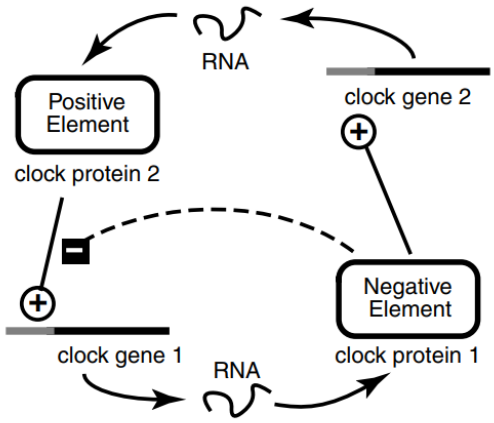

Figure 1.1 A general model for TTFL in organisms. TTFLs can contain one or more interlocked feedback loops. Adapted from Lakin-Thoms (2006b)

The positive elements of the clock usually act as transcriptional activators and promote the transcription of the negative elements by binding to the promoter of their genes. After accumulation of the negative-elements proteins upon translation, these proteins inhibit the transcriptional activity of the positive element in the nucleus, thereby they suppress their own transcription (Li et al., 2023). The period of this process is approximately 24 hours (Kippert, 2001). Thus, this way the feedback loops are able to maintain the rhythms at the molecular level.

1.2.2 Prokaryotes Clock

Circadian rhythmicity is not a property of eukaryotic cells only. Cyanobacteria, the photosynthetic prokaryotes that are known to be responsible for oxygenating the atmosphere of the earth, possess a circadian clock. The circadian clock of cyanobacteria controls many physiological processes in these unicellular organisms such as the timing of cell division and

compaction of the chromosome. The balance between photosynthesis and respiration is crucial for their survival which is regulated by the circadian clock (Kim et al., 2020).

Synechococcus elongatus is a freshwater-living strain of cyanobacteria whose circadian clock has been studied broadly. The three core genes of the circadian oscillator of *S. elongatus* clock are: *kaiA*, *kaiB*, and *kaiC*. Deletion of any of these genes abolishes the rhythms and mutation in any of them changes the period. All these three genes are an operon and transcribed together (Tomita et al., 2005).

The circadian clock of cyanobacteria is unique, since rhythmic gene expression (or transcription/translation feedback loop) is not essential for maintaining the rhythms, and the rhythms are generated by the post-translational modifications, thus this oscillator is called a posttranslational oscillator (PTO). KaiABC proteins together with CikA (involved in transmitting the environmental cues), and SasA and RpaA (involved in output pathways) drive the rhythms in cyanobacteria (Swan et al., 2018). Two studies that tested the essentiality of the TTFL in cyanobacteria showed that the rhythms continue independent of transcription and translation, and robust self-sustained, temperature compensated rhythms are observed when the three core proteins (KaiABC) plus ATP are added at the appropriate ratios in a test tube (Nakamichi et al., 2022; Tomita et al., 2005).

KaiC is an autokinase, autophosphatase, and an ATPase, whose daily phosphorylation rhythms are the key features of the timekeeping mechanism. kaiC is a hexameric protein with two domains: CI and CII (Figure 1.2). During the subjective day, KaiA upon binding to the A-loop on the CII domain of KaiC, promotes the autokinase activity

of the KaiC which results in the phosphorylation of Thr432 and then Ser431. This phosphorylation changes the conformational state of the KaiC protein and exposes the B-loop of the CI domain. Then during the subjective night, KaiB protein binds to the B-loop which results in the detachment of KaiA from the A-loop and promotes the autodephosphorylation activity of the KaiC protein. Dephosphorylation occurs firstly for Thr432 and then for Ser431 which results in a nonphosphorylated KaiC and completing one 24-hour cycle (Cohen & Golden, 2015).

Circadian rhythms have been observed in other bacteria as well. In the nonphotosynthetic bacterium *Bacillus subtilis*, free-running, temperature-compensated oscillations in PAS domain-containing gene expression with a period close to 24 hours have been observed, although this bacterium does not posses the *KaiA*, *KaiB*, and *KaiC* orthologs. In addition. under constant conditions, the circadian rhythms are detected in biofilm populations of *B. subtilis* (Eelderink-Chen et al., 2021).

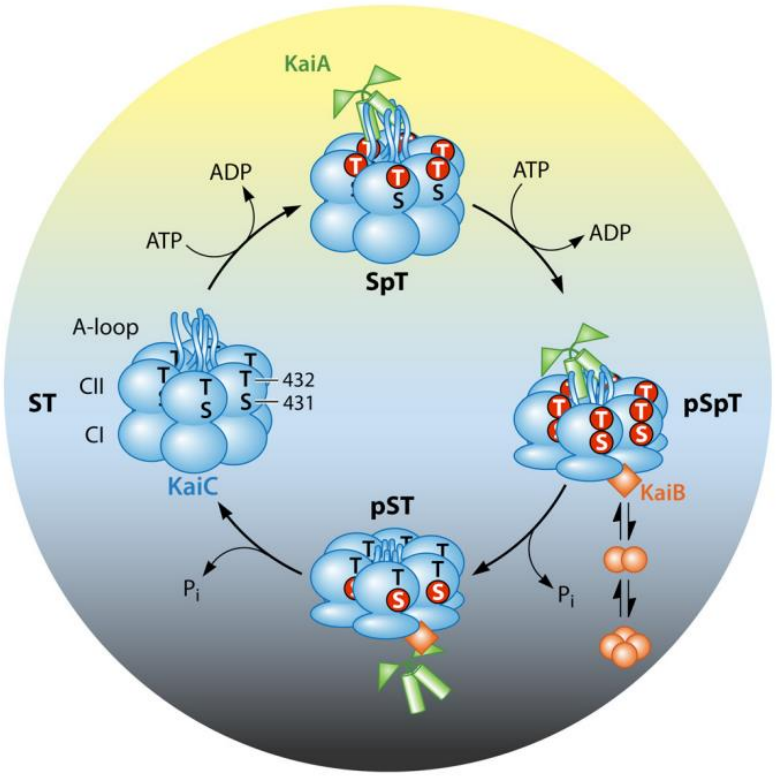

Figure 1.2 The cyanobacterial oscillation mechanism. KaiC is a hexameric protein with two domains. KaiA protein binds to A-loop on the c terminal of the CII domain and promotes the phosphorylation of Thr432 (SpT) and then Ser431(pSpT), which are located in the CII domain. When the KaiC protein is phosphorylated on both sites, it undergoes a conformational change which exposes the B-loop. KaiB also undergoes a conformational change and acquires a fold switch and then binds to the B-loop and promotes the dephosphorylation of KaiC. Adapted from Cohen & Golden (2015).

1.2.3 Molecular clocks in Mammals

Many behavioral and physiological processes in the body like body temperature, hormone secretion, protein synthesis, cell division, and sleep-wake patterns are under the control of the circadian rhythms. During evolution, organisms including mammals adapted their activities to the planet's daily movements to survive (Evans & Gorman, 2016). In mammals the dominant pacemaker of the whole body clock is located in the brain. The

suprachiasmatic nucleus (SCN) in the anterior part of the hypothalamus is responsible for synchronizing the clocks in the different parts and organs of the body. The SCN is comprised of a network of neurons which receive the input (light) from the retina in the eyes (Brown, 2016; Evans & Gorman, 2016). The neural network between the SCN neurons is coupled which results in a robust rhythm in the body. Other peripheral organs of the mammals' bodies have an independent clock, but some of these peripheral clocks are less robust which means they can be more affected by the internal cues (Partch et al., 2014). The mechanism that this master pacemaker uses to orchestrate and differentiate various clocks in different organs of the mammals' bodies is not yet fully understood (Paul et al., 2020).

Almost all the individual cells in mammals (Welsh et al., 2004), including the SCN neurons, have some interlocked feedback loops which make the main foundation of the circadian rhythms at the cellular level. Transcription/translation feedback loops are made of a few key genes in mammals (Figure 1.3). *Clock*, *Bmal1*, *Period* (*per1 &2*) and *Cryptochrome* (*cry1 &2*) are the main genes involved in mammals' molecular clock in cells. The protein products of *Clock* and *Bmal1* (CLOCK and BMAL1) are the positive elements of the clock which upon binding to E-box regulatory sequences upstream of the *Per* and *Cry* genes, promote the transcription of *Per* and *Cry* genes and eventually increase the amount of PER and CRY proteins in the cell. In turn, PER and CRY act as inhibitors (negative elements of the clock) and suppress their own transcription. This process takes approximately 24 hours to be completed (Ono, 2022). PER and CRY proteins then degrade by ubiquitination in the cytoplasm after accumulation. There are some other feedback loops that are interlocked with the main PER,CRY/BMAL1,CLOCK. The most prominent among these is the feedback loop

between *Bmal1*/*Clock* and *Rev-erbα* and *Rorα*. BMAL1/CLOCK complex promotes the transcription of *Rev-erbα* and *Rorα*, and the protein products of them, REV-ERBs and RORs inhibit their own transcription (Mohawk et al., 2012).

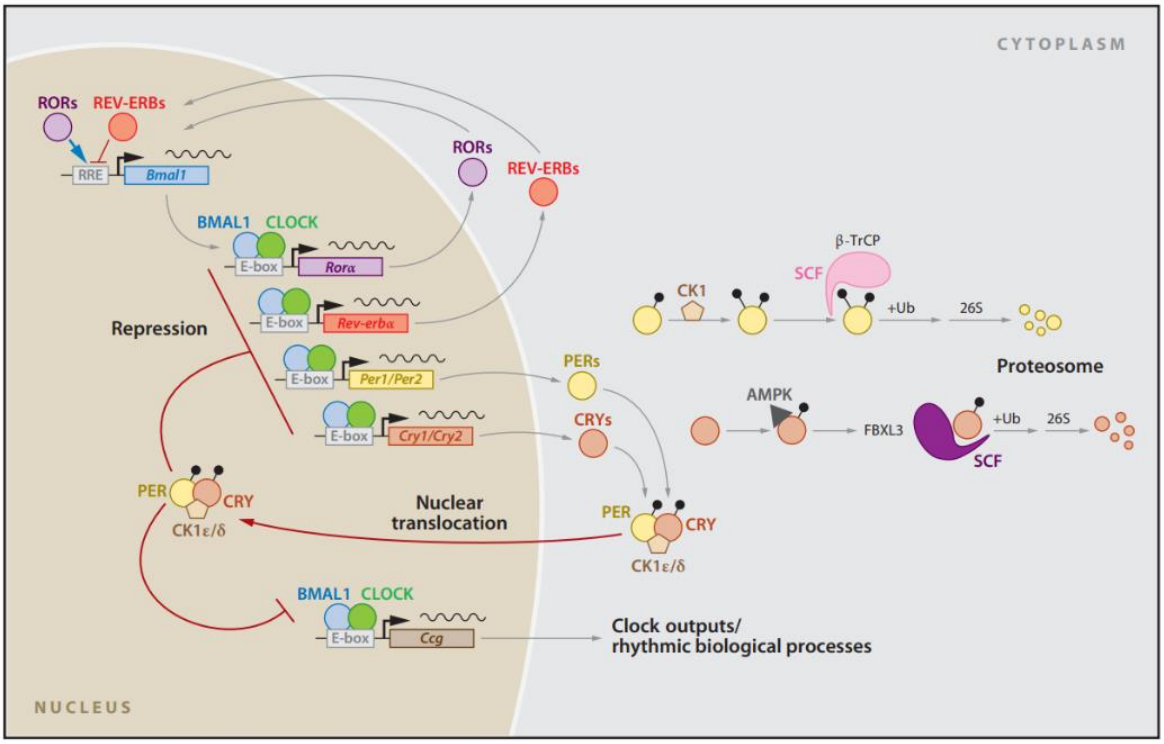

Figure 1.3 Molecular Circadian Clock in mammals. The interaction between the clock genes and their protein products are shown on the figure. Adapted from Mohawk et al. (2012)

1.2.4 Molecular Clocks in *Drosophila melanogaster*

The main pacemaker in the fly *Drosophila melanogaster* is located in the brain. There are 150 neurons in the brain that are considered the central pacemaker. These 150 neurons are classified into subgroups based on their location in the brain: the small and large ventral

lateral neurons (sLNvs, lLNvs), dorsal lateral neurons (LNds), three groups of dorsal neurons (DN1s, DN2s, DN3s), and lateral posterior neurons (LPNs). The mechanism by which the central clock orchestrates all the other peripheral clocks is not very well understood yet (Yildirim et al., 2022).

The molecular clock in Drosophila cells is a TTFL that has some key genes, some positive and some negative elements (Figure 1.4). The proteins CLK (Clock) and CYC (Cycle) are the positive arms of the clock which enter the nucleus and make a heterodimer complex that acts as the stimulatory transcription factor for the *per* (Period) and *tim* (Timeless) genes. The products of these genes, PER and TIM, inhibit their own transcription in return by repressing CLK/CYC complex after accumulating in the cytoplasm and localizing to the nucleus (Patke et al., 2020; Yildirim et al., 2022). There is also another feedback loop which is an interlocked loop that controls the transcription of the *clk* gene. Light dependent degradation of TIM happens during the day by the activity of the photoreceptor CRY (Cryptochrome) and E3 ubiquitin ligase jetlag (JET), which also degrades CRY. In the absence of TIM, PER becomes destabilized by DBT (Double-Time) which is the orthologue of CK1 (casein kinase1) in mammals. This decrease in the levels of TIM and PER resets the clock (Patke et al., 2020). There is also a second interlocked loop that controls the transcription of *clk* mRNA. CLK-CYC binds to the E-boxes of the genes *vri* (Vrille) and *pdp1ε* (PAR domain protein 1ε), and the products of these genes control the transcription of the *clk* gene. VRI protein binds to the VRI/PDP1ε boxes in the enhancer of the *clk* gene and inhibits its transcription, whereas the PDP1ε promotes the transcription upon

binding to the enhancer (Patke et al., 2020). Although this TTFL controls the transcription of the *clk* gene, it is not essential for the rhythmic behaviour of the fly (Lakin-Thomas, 2006b).

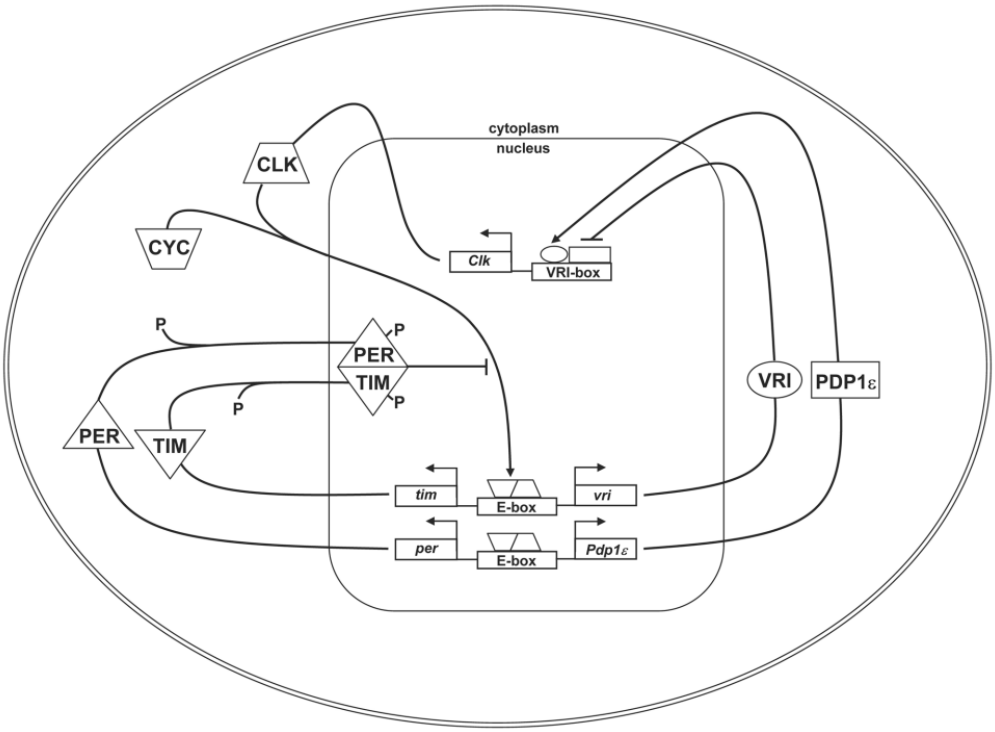

Figure 1.4 The TTFL in *D. melanogaster*. All the key genes of the feedback loops and their interactions are depicted on this figure. Adapted from Hardin (2004)

1.2.5 Molecular Clock in Plants

Several physiological processes like photosynthesis activities, metabolism, hormone secretion, leaf movements, pathogen responses, flowering, and fragrance emission are under the control of the circadian clocks in plants (Oakenfull & Davis, 2017). *Arabidopsis* is one of the most studied organisms among plants. One third of *Arabidopsis'* genes are regulated by the circadian clock (Nakamichi et al., 2022). There is evidence that shows that tissue-specific timekeeping exists in plants (Swift et al., 2022). Two of the most effective

environmental cues (Zietgebers) for the plants clocks are light and temperature. Light enables the plants to reset their clock at dawn and this way they can synchronize with their environment (Oakenfull & Davis, 2017).

The clock of *Arabidopsis* consists of a core feedback loop which is interconnected with the morning and evening loops (Figure 1.5). The repressors of the TTFL are the morning-expressed MYB-like transcription factors CIRDACIAN CLOCK ASSOCIATED1 (CCA1), LATE ELONGATED HYPOCOTYL (LHY), whose protein and transcript levels are abundant in the morning and which interact with each other physically, and the members of PSEUDO RESPONSE REGULATOR (PRR) protein family PRR7 and PRR9. These morning PRR are repressed in the evening by the evening complex (EC) which is composed of EARLY FLOWERING 3 (ELF3), ELF4, and LUX (ARRHYTHMO/PHYTOCLOCK1) (Cervela-Cardona et al., 2021). CCA1 and LHY repress an evening component called TIMING OF CAB EXPRESSION 1 (TOC1) that is also known as PRR1 by binding to the evening element (EE) of the TOC1 gene promoter. In turn, TOC1 also represses CCA1 and LHY directly. CCA1 and LHY also repress several other evening phase genes including GIGANTEA (GI), LUX, BROTHER OF LUX ARRYTHMO (BOA), ELF3, and ELF4. Besides the repression activity of CCA1 and LHY, the evidence shows that these two transcription factors act as activator for the day phase components PRR9 and PRR7. Day-phased components PRRs play an important role in the clock. PRR9 increases earliest just after dawn, followed by PRR7, PRR5, and TOC1 in the evening. PRR9, PRR7, and PRR5 together regulate the activation of CCA1 and LHY. There is another afternoon-phased transcription family, RVE4 (REVEILLE), RVE6, and RVE8 that are repressed by PRR9,

PRR7, and PRR5, and in turn they activate PRR5, TOC1, and the evening complex components LUX, ELF4, and ELF3 (Hsu & Harmer, 2014).

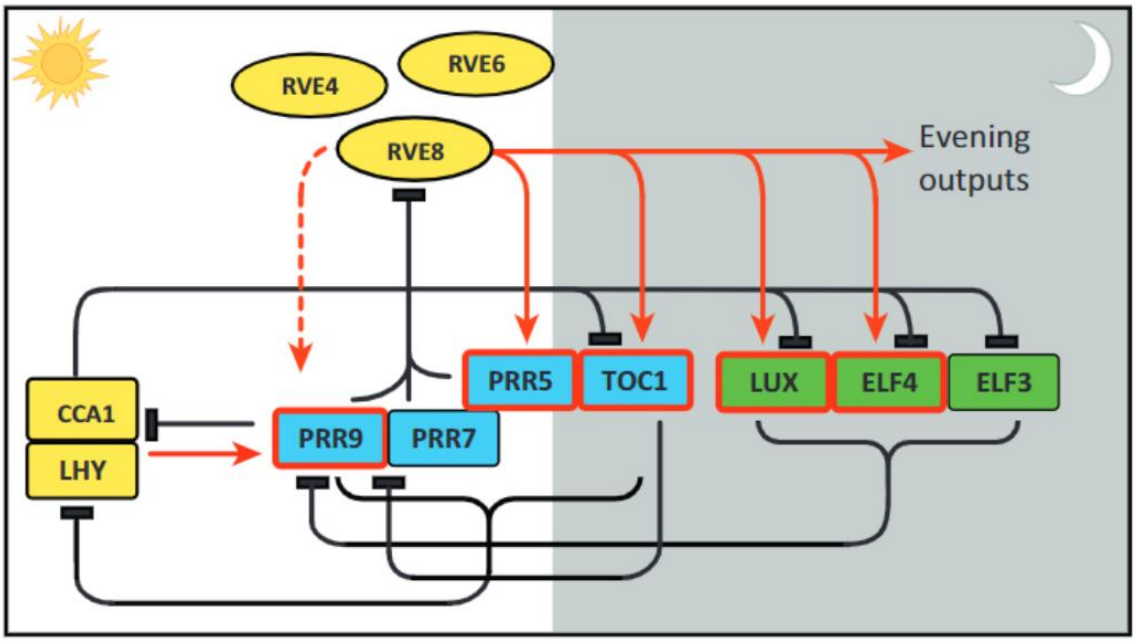

Figure 1.5 The core components of the *Arabidopsis* clock. Each color represents the proteins from the same family. The red lines show activation, and the black lines show repression. Adapted from (Hsu & Harmer, 2014).

1.2.6 Neurospora Clock

1.2.6.1 Neurospora crassa as a model organism

The ascomycete filamentous fungi *Neurospora crassa* is one of the primary model organisms that has been studied for many years (Baker et al., 2012) and as a model organism evolutionarily related to animals, has advanced our understanding of the circadian rhythm's architecture (Loros, 2020). This filamentous fungus *Neurospora crassa* possesses various properties that make it an ideal model for studying circadian rhythms. *Neurospora* is a

haploid microorganism, hence genetic analysis is much easier due to no complexity of dominance relationship between alleles. Also, the phenotype of the different mutations can be easily observed. This organism can be easily grown on media in a lab and a large amount of fungal mat can be harvested and used for biochemical analysis. The genome has been sequenced and a variety of genetic methods are available for *Neurospora*. Different imaging methods like luciferase and GFP tag methods can be applied for this fungus. In addition, knockout mutants can be easily constructed and can be found in the Fungal Genetics Stock Center (Lakin-Thomas et al., 2011).

1.2.6.2 Neurospora life cycle

Neurospora is a filamentous fungus from the Ascomycota phylum. This saprophytic fungus is known as a bread mold and is able to grow on carbohydrate rich substrates (Davis, 2004). The hyphae of this fungus exist in a multicellular and multinuclear network of tube-shaped cells (Fischer & Glass, 2019). *Neurospora*'s life cycle has two phases: sexual and asexual (Figure 1.6).

The asexual phase of the *Neurospora* life cycle starts with the growth of a sexual or asexual spore on a substrate. The spore generates hyphae, and then aerial hyphae start growing. At the tip of the aerial hyphae two types of asexual spores (conidia) can be produced by budding and segmentation, which are not very different morphologically. One type which is more abundant is called macroconidia that usually contains four nuclei. The other type is called microconidia which contains one nucleus only and is less viable. These conidiospores can spread easily by the wind and start growing on a new substrate (Davis, 2004). These

conidia are bright orange due to the carotenoid pigments and are highly hydrophobic (Baker et al., 2012).

The sexual phase is more complicated and happens when conditions are unfavorable to vegetative growth like in low nitrogen, low temperature, and low light (Wallen & Perlin, 2018). Two different mating types of mycelia should be present for sexual reproduction, mating types A and a, and each of these mating types can act as the female structure. Female mycelium makes a structure called Protoperithecium that contains the female gamete. The male gamete can be any viable spore. A bridge-like hypha called Trichogyne is made to connect the female and male gametes. Meanwhile the hyphae of the Protoperithecium keep growing until they make the mature female structure (Perithecium) which will contain the ascus inside. After conjugation of the female and male gametes, the new diploid nucleus undergoes two meioses to produce four haploid nuclei and then a final mitosis takes place and results in eight ascospores in one ascus. When octads are mature, they will be shot out of the hole on top of the Perithecium which is called Ostiole. These ascospores can stay dormant for a long time and then start germinating when the conditions are optimal. A heat shock or chemical stimulus is needed for their germination (Davis, 2004).

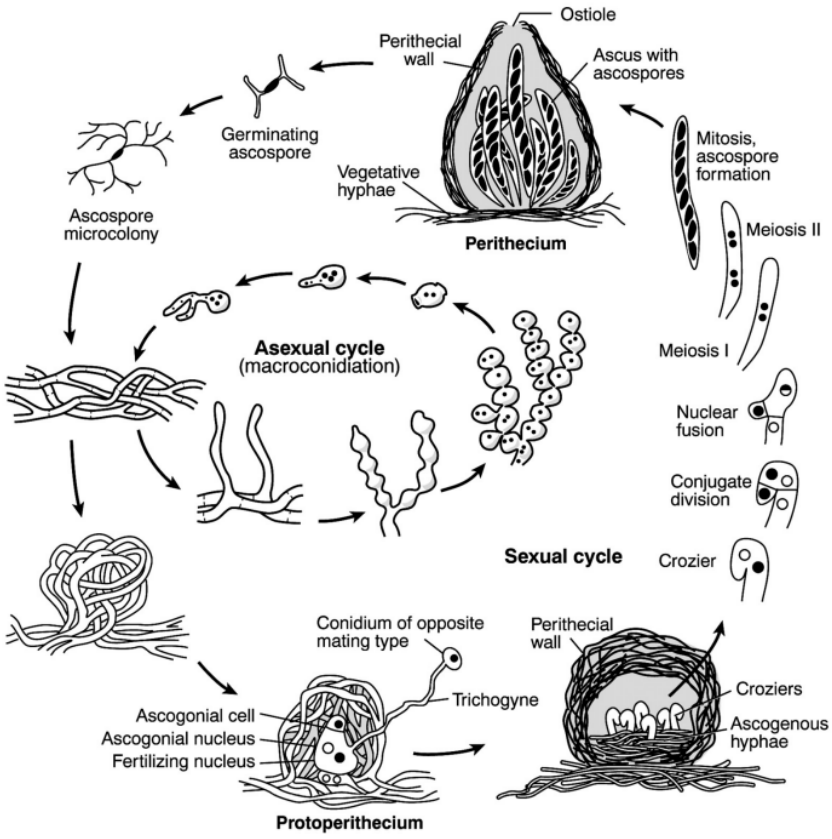

Figure 1.6 *Neurospora* life cycle. Both Sexual and asexual phases are depicted in the figure. Adapted from Davis (2004).

1.2.6.3 TTFL in Neurospora

It has been a consensus among scientists for many years that the main oscillator of the circadian rhythms in *Neurospora* is the well-known TTFL (Figure 1.7) (Lakin-Thomas, 2006b). The key genes in *Neurospora*'s clock are frequency (*frq*), white-collar1 (*wc1*), and white-collar 2 (*wc-2*). The protein products of these genes are FREQUENCY (FRQ), WHITE COLLAR-1 (WC-1), and WHITE COLLAR-2 (WC-2) respectively.

WC-1 and WC-2 proteins interact via PAS domains upon translation and make a transcription factor complex (WCC). WCC is hypophosphorylated and active in the absence of FRQ protein (Schafmeier et al., 2005) and acts as the positive arm of the clock and promotes the *frq* gene transcription. FRQ protein is an inherently disordered protein (IDP) and immediately after translation binds to its protein partner Frequency Interacting RNA helicase (FHR) and makes a complex known as FRQ/FHR complex (FFC). FRQ gets phosphorylated at about 100 phosphorylation sites in an orchestrated manner over a 22 hour period, a process facilitated by CK1a. At some point FFC enters the nucleus and interacts with WCC (Bartholomai et al., 2022) and removes it from the *frq* promoter (Baker et al., 2012; Dunlap & Loros, 2006) by modulating WCC phosphorylation to make it hyperphosphorylated and inactive (Schafmeier et al., 2005). FRQ protein level is highest between late night and morning, and it is lowest at the early night (Dunlap & Loros, 2006). This protein level is controlled by ubiquitin-dependent degradation in the cytoplasm (Srikanta & Cermakian, 2021). WCC arises from de novo synthesis or the dephosphorylated WCC can again start the feedback loop by promoting transcription of the *frq* gene (Bartholomai et al., 2022). WC-1 is a blue light photoreceptor that resets the clock upon receiving light cues and its transcription is induced by light, while WC-2 helps in the light-signaling pathway (Schafmeier et al., 2005).

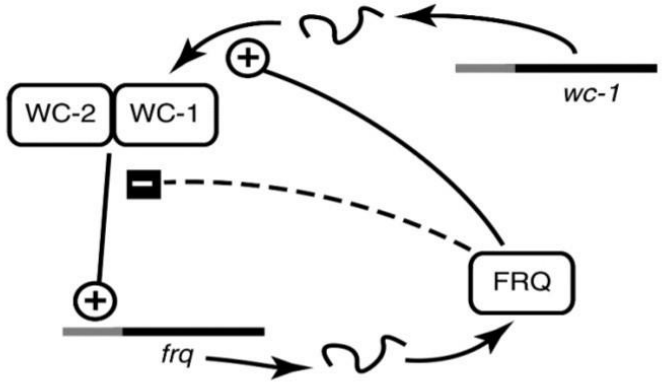

Figure 1.7 Circadian clock of *Neurospora crassa*. Adapted from Lakin-Thomas (2006b).

1.3 Oscillator(s) outside of the TTFL

Despite of the fact that transcription/translation feedback loops have been known to be responsible for driving circadian rhythms in various organisms, some anomalous observations seen in many different organisms changed this consensus.

1.3.1 Anomalous Observations in many organisms

A marine unicellular green alga, *Acetabularia*, which can be found in shallow waters near coral reefs, was one of the pioneer model organisms in circadian rhythms research. However, it has fallen out of interest recently. This alga has a long rhizoid that helps it to attach to the seabed and a long 5 cm stalk in its vegetative phase of life cycle. Most of its life the alga has only one nucleus in the rhizoid. This alga can survive for many days after the removal of the nucleus-containing rhizoid and is able to photosynthesize with circadian rhythmicity up to 7 weeks without the nucleus. In addition, chloroplast rhythmic movements are demonstrated in enucleated cells. In the presence of both nuclear and organellar RNA

synthesis inhibitors, the photosynthesis rhythmicity is not abolished, albeit the presence of protein inhibitors shifts the phase and inhibits the phosphorylation rhythms (Lakin-Thomas, 2006b; Woolum, 1991).

In the cyanobacterium *Synechococcus*, as was mentioned earlier, there is a translation transcription feedback loop between the *kai A*, *B*, and *C* genes. These three clock genes are required for the rhythmicity in this cyanobacterium and mutation in any of these genes disrupts the rhythms and changes the period. The TTFL model in this prokaryote was weakened by the work that provided evidence that the inhibition of the *kai* genes does not require the specific *kai* genes promoters and is more influenced by the phosphorylation state of KaiC protein (Ditty et al., 2003). In other work which was conducted by Tomita and colleagues, they directly tested whether the rhythmic expression of *kaiBC* is required for rhythmicity of the organism. They found that the phosphorylation of the KaiC protein is rhythmic in constant darkness, where the metabolic activities including transcription and translation are suppressed because this organism is photosynthetic. KaiC phosphorylation is also rhythmic in the presence of the transcription inhibitors. These autophosphorylation rhythms of KaiC were circadian in period and temperature compensated (Tomita et al., 2005). In another work, Nakajima and colleagues found rhythms in a test tube! They purified recombinant Kai A, B, and C proteins and mixed them in vitro with the ratio of in vivo conditions and added some ATP in a test tube. They observed self-sustained, temperature compensated, circadian phosphorylation rhythms in KaiC protein (Nakajima et al., 2005). These results show that for the generation of robust rhythms in *Synechococcus*, transcription and translation are not necessary. The interaction between KaiABC proteins, and the ability

of autophosphorylation and autodephosphorylation of KaiC is enough to generate self-sustained 24-hour rhythms (Nakajima et al., 2005).

The circadian clock of *Drosophila*, as is mentioned before, consists of two interlocked feedback loops. CLK and CYC complex activates the transcription of *per* and *tim* genes. PER and TIM proteins inhibit the CLK-CYC transcriptional activity. The VRI protein represses *clk* transcription and *clk* cycles in antiphase to *per* and *tim* due to the inhibition of *vri* by PER-TIM complex (Hardin, 2004). In work carried out by Kim et al. (2002), they tested the functional role of *clk* RNA by expressing *clk* from the *per* or *tim* promoter. This way, *clk* would be expressed at the same phase as *per* and *tim* instead of antiphase. The results however, showed no major effects on the cycling of the CLK protein or the rhythmic behavior of the flies. In another crucial experiment conducted by Yang & Sehgal (2001), they demonstrated what happens if the *per* and *tim* genes are constitutively expressed. The results showed that both proteins (PER and TIM) continued to cycle, and the behavioral rhythmicity can be restored in null mutant flies. 42% of the double-constitutive flies were rhythmic and an additional 13% were weakly rhythmic. These results demonstrate that the RNA cycling of *per* and *tim* are necessary for the robustness, but it is not required for rhythmicity (Lakin-Thomas, 2006b).

In mammals studying the effects of the clock gene mutants is more complex than the simpler organisms and various combinations of different clock gene knockouts are being assayed which result in different phenotypes. Rhythmicity seems to depend on various criteria such as age, genetic background, light-dark conditions, and the length of the time in dark (Lakin-Thomas, 2006b). Some experiments have been focused on looking at the

phenotypes of negative arms of the clock in mammals. One study showed that single knockouts in *cry1* or *cry2* genes, are rhythmic in DD, but double knockouts are immediately arrhythmic (Van der Horst et al., 1999). Single knockouts of *mPer1* or *mPer2* are initially rhythmic in constant dark, but they may become arrhythmic upon extended exposure to darkness. Double mutant mice in *mPer1* and *mPer2* genes are immediately arrhythmic (Bae et al., 2001). Double mutants of *mPer1*/*mCry1* and *mPer2*/*mCry2* are rhythmic in constant darkness. One mutation combination that depends on age is *mPer1*/*mCry2*, that is rhythmic when the mouse is young and becomes arrhythmic as the mouse gets old. Furthermore, inactivation of *mCry2* in *mPer2* mutant mice, restores the rhythmicity and normal clock gene expression (Oster et al., 2002, 2003). In addition, mutants in positive arms of the mammalian clock including *clock* and *Bmal1* mutants, have been assayed. Mice with mutation in *clock* become arrhythmic in DD after several days, but the rhythmicity can be restored by a light pulse. *Bmal1* mutants on the other hand, are immediately arrhythmic in DD. All these finding may suggest that the transcriptional control is not essential for rhythmicity in mice, but more research should be conducted on the circadian clock of mammals (Lakin-Thomas, 2006b).

1.3.2 *Frq*-less Oscillators in *Neurospora*

In *Neurospora crassa*, mutations in *frq*, *wc-1*, and *wc-2* genes alter the period, light sensitivity, temperature compensation, and expression of the conidiation rhythms. However, FRQ-WCC feedback loops are not required for rhythmicity under some conditions. The oscillators that generate rhythmicity in the absence of functional *frq* and *wc* genes, are called *frq*-less oscillators (FLO).

Rhythmicity in *frq*-null mutants were first demonstrated in frq^{9} and then in frq^{10} mutants, after growing for several days in extra-long race tubes on some special media. Also, *wc-1* and *wc-2* mutants show rhythmic conidiation after growing for several days on a glucose-free medium in extra-long race tubes. These rhythms are circadian in period but more variable than the wildtypes (Lakin-Thomas & Brody, 2004). More reliable rhythms can be observed when 10^{-4} to 10^{-5} M of farnesol or geraniol, which are related to the known intermediates in steroid pathway, are added to the media of each one of these arrhythmic mutants. The observed conidiation rhythms were robust free running, but insensitive to temperature and light (Granshaw et al., 2003). In addition, two mutants, *cel* (chain-elongation) and *chol-1* (choline-requiring) which are defective in lipid metabolism, are rhythmic under normal conditions. However, double mutation in any of *frq*, *wc-1*, or *wc-2* genes and *cel* or *chol-1* under lipid-deficient conditions generates robust rhythmicity (Lakin-Thomas, 2006a; Lakin-Thomas & Brody, 2000).

To investigate the presence of FLO and its connection with the FWO (FRQ-WCC oscillator), Hunt and colleagues knocked out all the key genes of FWO (*frq*, *wc-1*, and *wc-2*) and observed that the conidiation rhythm abolishes in constant conditions, yet conidiation stays rhythmic under entrainment by heat pulses and temperature cycles (Hunt et al., 2012).

In addition to rhythmicity in conidiation in clock gene null mutants, some molecular rhythms have been found in these mutants. Levels of sn-1,2-diacylglycerol (DAG) are rhythmic in a *frq* null mutant, driven by a light-sensitive oscillator (Ramsdale & Lakin-Thomas, 2000). The activity of the enzyme nitrate reductase is rhythmic in *Neurospora* when

the nitrate is the only nitrogen source. This activity stays rhythmic in constant dark or light, and in a *frq*^{9} mutant with no functional FRQ protein (Christensen et al., 2004).

The focus of our lab has been on identifying the components of the FLO(s) for many years. A mutagenesis screen was carried out on a FRQ-less strain. A mutation which was named UV90 was identified that affected both FRQ-less and FRQ-sufficient rhythms. UV90 mutation affects the free-running long-period rhythms in choline-depleted *chol-1* strain and makes it arrhythmic, and also alters the heat-entrained rhythms in *frq*^{10} severely. In FRQ-sufficient background, UV90 mutation reduces the amplitude of the FRQ protein rhythm, dampens the free-running conidiation rhythm, and increases the phase-resetting response to both heat pulses and light. The UV90 mutation has a small but significant effect on the period of conidiation and growth rate (S. Li et al., 2011). The *uv90* gene was mapped later in our lab and was identified as NCU05950, homologous to the TOR pathway (a highly conserved nutrient-sensing pathway in Eukaryotes) proteins EGO1 in yeast and LAMTOR1 in mammals. UV90 protein is anchored to the outer membrane of the vacuole and is required for the localization of TOR complex to the vacuolar membrane. Thus, this protein was named VTA (vacuolar TOR-associated) protein. Deletion of putative acylation sites of VTA destroys its localization to the vacuolar membrane as well as its role in rhythmicity. Also, deletion of VTA disrupts the growth responses to amino acids and glucose (Ratnayake et al., 2018).

Another gene that affects circadian rhythmicity which was identified by co-immunoprecipitation and mass spectrometry using VTA-FLAG strain, as a VTA protein binding partner, is *gtr2*. Δ*gtr2* affects both free-running FRQ-less rhythms and the FRQ-

sufficient rhythms and is very similar to Δ*vta*. Mutation in *gtr2* abolishes the free-running conidiation rhythms in a FRQ-less background, is defective in growth responses to amino acids, and is defective in heat entrainment when treated by cycles of heat pulses. In FRQ-sufficient background, the FRQ protein rhythmic levels dampen in the absence of GTR2. GTR2 protein levels are found to be rhythmic across two circadian cycles and this rhythmicity is depended on functional VTA protein. GTR2 is also a component of the TOR pathway and homologous to the yeast protein GTR2 and RAG C/D in mammals (Eskandari et al., 2021).

Four other genes *prd-1*, *prd-2*, *prd-3*, and *prd-4* (*period*) are found to have effects on FRQ-less rhythms. *Prd-3* and *prd-4* have subtle effects, while *prd-1* and *prd-2* have crucial effects on the FRQ-less rhythms in two genetic backgrounds. In *chol-1; frq*^{10} backgrounds on low choline media, *prd-1* and *prd-2* mutations abolished the free-running conidiation rhythmicity and significantly affected the entrained peak timing under heat entrainment conditions in *frq*^{10} background (Li, & Lakin-Thomas, 2010). *Prd-1* also disrupts the free-running rhythms in *wc-1* null mutant. This mutation influences the FRQ-sufficient rhythmicity by lengthening the period of the rhythms. Our lab mapped this gene and identified it as NCU07839, a DEAD-box RNA helicase *dbp-2*. A PRD-1-GFP fusion protein shows localization in the cell nucleus (Adhvaryu et al., 2016). Results of coimmunoprecipitation and mass spectrometry showed that one of the protein partners of PRD-1 is the ribosomal protein S6, a component of the TOR pathway which is involved in metabolism (unpublished data).

Also, in the fungus *Verticillium dahlia,* which is from the same class as *Neurospora*, the homologues of the key clock genes are identified, although no conidiation rhythms are observed in this plant pathogen fungus. However, in the *frq* gene mutants of this fungus (Δvdfrq) disruption in metabolism, transport, and redox processes are reported. Also, growth defects and reduced pathogenicity are displayed (Cascant-Lopez et al., 2020). All this evidence shows a connection between the circadian oscillators and the nutritional and metabolic pathways.

1.4 TOR (target of rapamycin pathway)

TOR (Target of rapamycin) pathway is a highly conserved signaling pathway in eukaryotes which is linked to metabolism. TOR (called mTOR in mammals) is a serine/threonine kinase that can be found in two structurally and functionally different complexes, TORC1 and TORC2 (mTORC1 and mTORC2 in mammals). Only TORC1 is sensitive to rapamycin. This kinase is activated through the activation of a complex of other proteins that respond to nutrients such as glucose and amino acids (arginine and leucine), or growth factors such as insulin (Lakin-Thomas, 2019). In unicellular organisms, nutrients are important TORC1 activators and are alone sufficient for TOR activation (González & Hall, 2017). TOR pathway regulates cell cycle progression, protein synthesis, ribosome biogenesis, autophagy (Jiao et al., 2023; Kato, 2023), and cell number and size (Fumagalli & Pende, 2022). TOR pathway is extensively studied in yeast and mammals.

1.4.1 TOR in Yeast and Mammals

Early research on TOR and the mechanism by which rapamycin acts as an immunosuppressor drug has been conducted on the budding yeast, *Saccharomyces*

cerevisiae. Rapamycin was first discovered as an anti-fungal drug which is a lipophilic macrolide and a secondary metabolite produced by the bacterium *Streptomyces hygroscopicus*. Rapamycin was discarded later as an antifungal agent due to its immunosuppressive side effects, but years later it was introduced as a T-helper cell inhibitor and an immunosuppressor for the treatment of allograft rejection (Loewith & Hall, 2011). Rapamycin in complex with peptidyl-prolyl isomerase Fpr1 (known as FKBP, FK506 binding protein in mammals) inhibits the activity of TOR kinases (Dubouloz et al., 2005).

All TORs have the same structure. In order from the N terminal to the C terminal, there are repeats of the HEAT domain, the FAT domain, the FRB domain, the Kinase domain, and the FATC domain. The HEAT repeats are the binding site for the components of the TOR complexes and the FRB domain is the part that is affected by rapamycin and the Kinase domain is the catalytic part (Loewith & Hall, 2011). TORC1 components in yeast are either TOR1 or TOR2, kog1, Lst8, and Tco89 (González & Hall, 2017). TORC2 components are TOR2, Avo1, Avo2, Avo3, Bit61 or Bit2, and Lst8 (Figure 1.8) (Loewith & Hall, 2011). The essential core components of mTORC1 in mammals are RAPTOR (regulatory-associated protein of mTOR) and mLST8 (mammalian lethal with sec13 protein 8), and the core components of mTORC2 are RICTOR (rapamycin-insensitive companion of mTOR), SIN1 (SAPK-interacting 1), and mLST8 (Shimobayashi & Hall, 2014). Rapamycin sensitive TORC1 mediates the TOR-shared pathway and the rapamycin insensitive TORC2 mediates the TOR-unique pathway. TORC1 regulates protein synthesis, nutrient uptake, mRNA synthesis and degradation, and autophagy, while TORC2 regulates actin skeleton organization, endocytosis, and sphingolipid synthesis. Although TOR pathway is highly

conserved among the eukaryotes, two TOR genes are present in *S. cerevisiae* despite the mammals, flies, and plants that have only one gene for TOR (Loewith & Hall, 2011).

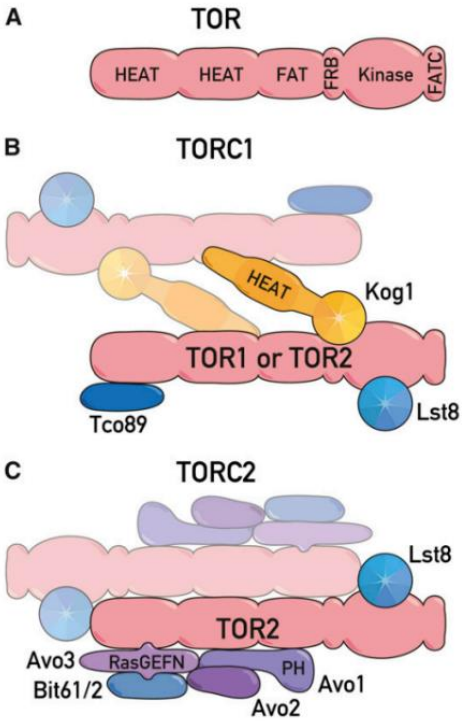

Figure 1.8 TORC domains. A) Conserved domain of TOR, B) composition of TOR Complex1 which is approximately 2 MDa in size, C) composition of TOR Complex2 which is approximately 2 MDa in size. Adapted from Loewith & Hall (2011).

GFP tagging of the TORC1 components has shown that the TORC1 localizes on the vacuolar membrane, which is a major nutrient reservoir. Rapamycin treatment on yeast alters the physiology of the yeast in the same way as nutrient starvation. It decreases protein synthesis dramatically, induces autophagy, and arrests the cell cycle (Barbet et al., 1996; Loewith & Hall, 2011). TOR activity is also regulated in response to environmental cues and noxious stressors such as a shift to a higher temperature, redox stress, and high salt. When

the environmental situation is inappropriate for growth, it results in the arrest of the cell cycle and division, the metabolism slows down, and energy stores get accumulated in the cells.

The EGO complex in yeast consists of Ego1, Ego3, Gtr1, and Gtr2 proteins. This complex resides on the vacuolar membrane and couples TORC1 with amino-acid signals such as intracellular Leucine levels and intravacuolar amino-acid levels (Figure 1.9). Gtr1 and Gtr2 are Ras-family GTPases and the combination of $Gtr1^{GTP}$ $Gtr2^{GDP}$ activates TORC1. AGC kinase Sch9, PP2A-like phosphatase Sit4 and Tap42-PP2A are the substrates of the activated TORC1 (Loewith & Hall, 2011; Urban et al., 2007).

The counterpart of EGO complex in mammals is the "Ragulator" complex, which is composed of p18/LAMTOR1 (homolog of Ego1) and p14+MP1/LAMTOR2+LAMTOR3 (homolog of Ego3). Ragulator complex with the Rags mediates amino-acid sufficiency signals to mTORC1 (Kuranda et al., 2006; Loewith & Hall, 2011; Shimobayashi & Hall, 2014).

mTORC1 is regulated by growth factors such as insulin-signaling pathway and nutrient sufficiency (Figure 1.9). Growth factors bind to a specific receptor tyrosine kinase and activate the PI3K-Akt and/or Ras-MAPK pathway. This pathway then activates the small GTPase Rheb (Ras homolog enriched in brain) through the phosphorylation of TSC2 (tuberous sclerosis complex 2). Activated Rheb activates mTORC1 (Kim et al., 2013; Shimobayashi & Hall, 2014). Activated mTORC1 regulates protein synthesis through phosphorylation and inactivation of eukaryotic initiation factor 4E-binding protein (4E-BP1) and phosphorylation and activation of S6 kinase 1(S6K1) (Kato, 2023). Activated S6K in

turn, phosphorylates several proteins which are involved in mRNA translation including ribosomal protein S6 (Cao, 2018).

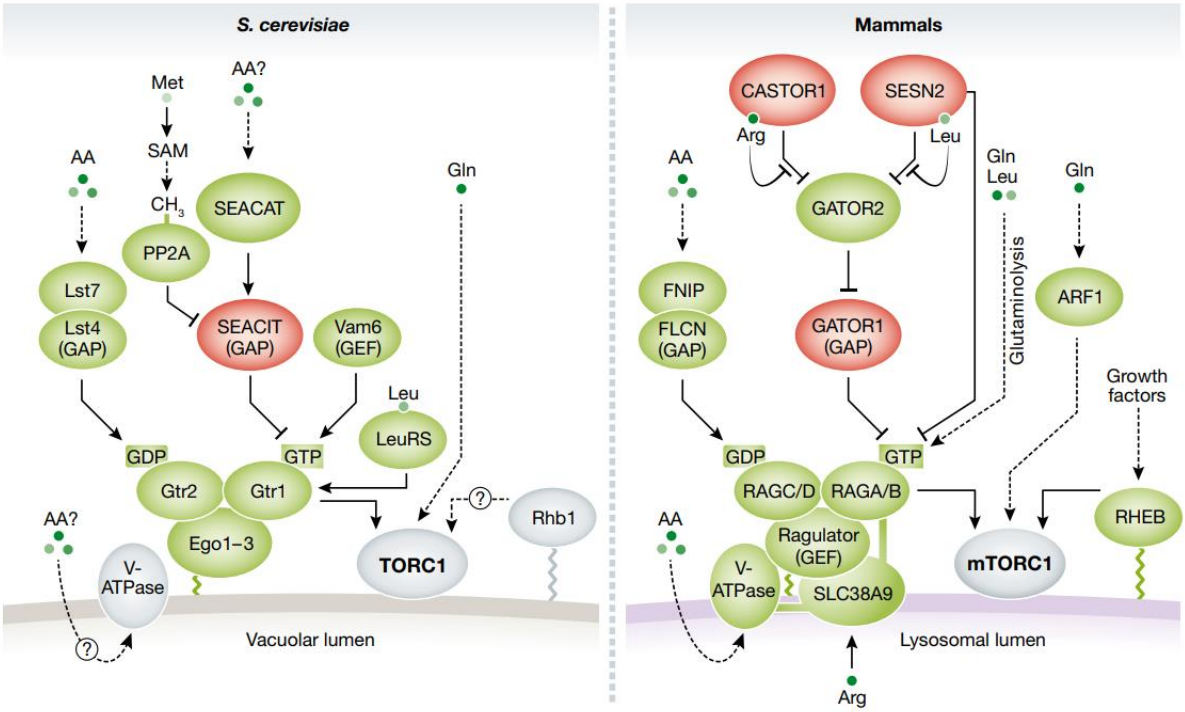

Figure 1.9 TORC1 regulation in *S. cerevisiae* and mammals. Green proteins activate TORC1 and red proteins inhibit TORC1. Dashed lines show indirect interaction. Adapted from González & Hall (2017).

1.4.2 Ribosomal Protein S6

One of the proteins which gets phosphorylated by S6K is 40S ribosomal protein S6. Ribosomal protein S6 (RPS6) exists in cells in multiple phosphorylated states, with different levels of activity. The active form of RPS6 is generally considered to be the hyper-

phosphorylated form, which has multiple phosphate groups attached to it. When RPS6 is hyper-phosphorylated, it can act as a regulator of protein synthesis by promoting the translation of mRNAs. This can occur through the activation of the mTORC1 pathway, which in turn activates ribosomal protein S6 kinase (S6K). Activated S6K can then phosphorylate RPS6 at multiple sites, leading to the hyper-phosphorylation and activation of RPS6 (Roux & Topisirovic, 2012).

RPS6 phosphorylation sites have been mapped to five cluster residues in mammals, with the majority of them located in the C-terminal region of the protein (Roux & Topisirovic, 2012; Ruvinsky & Meyuhas, 2006). These sites are serine residues that can be phosphorylated by different kinases, including ribosomal protein S6 kinases (S6Ks) and mitogen-activated protein kinases (MAPKs). The precise number of phosphorylation sites that are actually phosphorylated and the specific sites that are phosphorylated can vary depending on the cellular context and the signaling pathway involved. However, it is generally believed that the hyper-phosphorylation of RPS6 at multiple sites, including Ser235, Ser236, Ser240, Ser244, and Ser247, is required for its activation and its role in regulating protein synthesis (Roux & Topisirovic, 2012). It has been proposed that the S6 protein phosphorylation takes place in a defined order and the primary site which gets phosphorylated is the Ser236 residue, since the sequence context of this residue matches the recognition sequence of S6K (Ruvinsky & Meyuhas, 2006).

In yeast, S6 protein has two phosphorylation sites and in mammals it has five phosphorylation sites. Substituting all these 5 phosphorylatable serine residues with alanines in mice identified the role of S6 phosphorylation in cell size, cell proliferation, and glucose

homeostasis (Ruvinsky & Meyuhas, 2006). Figure 1.10 shows RPS6 phosphorylation sites in some eukaryotes.

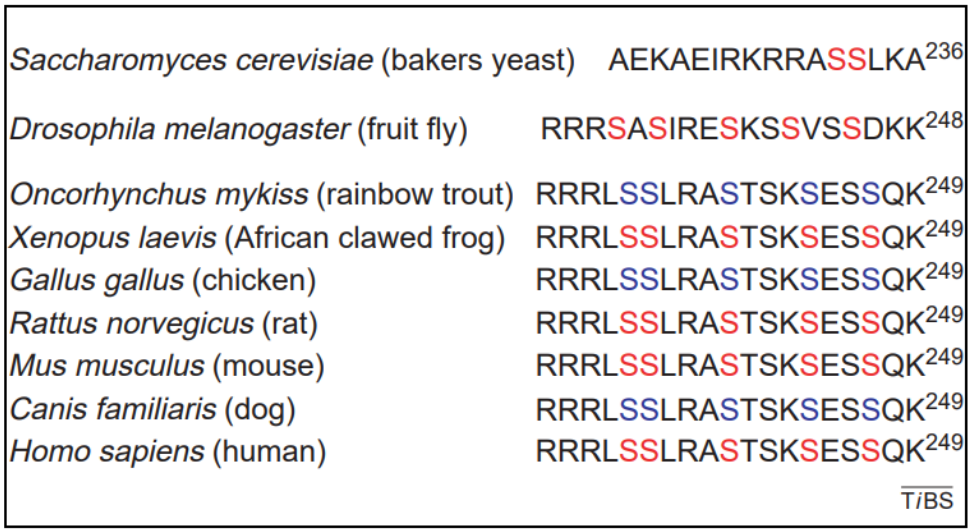

Figure 1.10 Ribosomal protein S6 Phosphorylation sites sequence in different organisms. The red residues show the phosphorylation sites, and the blue residues show the putative phosphorylation sites. Adapted from Ruvinsky & Meyuhas (2006).

In another study, the structure of the ribosome in *Neurospora crassa* was arrested using cycloheximide (CHX), which is a protein synthesis inhibitor. 40S ribosomal protein structure was determined in this study. The structure of RPS6 is shown in Figure 1.11. This protein has a sequence length of 239 and has α-helices and β-sheet structures. The putative phosphorylation sites are two serine residues on the α-helix tail (C-terminal) (Shen et al., 2021). The C-terminal sequence of *N. crassa* is VQKADARKRRASSMRK[239] (PDB: 7R81).

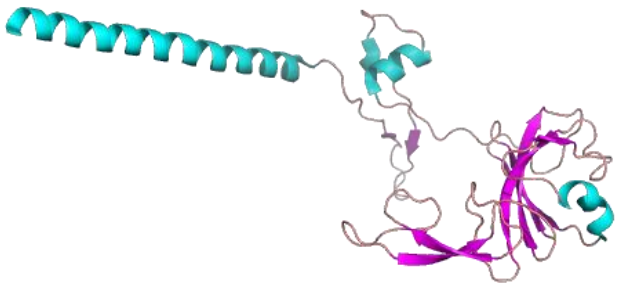

Figure 1.11 *Neurospora crassa* RPS6 structure. α-helices are shown in blue, and β-sheets are shown in magenta. The PDB number for this protein is 7R81. Generated by PyMOL.

1.4.3 TOR in *Neurospora*

TOR pathway is very well studied in yeast and mammals, albeit little is known about TOR in filamentous fungi such as *Neurospora*. The best studied organisms in the fungal kingdom are *S. cerevisiae*, *Schizosaccharomyces pombe*, and the human pathogen *Candida albicans* (Shertz et al., 2010). A global analysis of 86 serine/threonine kinases genes in *Neurospora* identified a homolog of yeast TOR1/TOR2 in this filamentous fungus. TOR deletion in *Neurospora* is lethal as indicated by the fact that a homokaryon is not available in Fungal Genetics Stock Center (Park et al., 2011). STK-10 was identified in the same study as the homolog of Sch9 in yeast and S6K in mammals. STK-10 knock-out showed impaired growth and osmoregulation (Park et al., 2011). We have identified two genes, *vta* and *gtr2*, in our lab, whose protein products are components of the TOR pathway in *Neurospora* (Figure 1.12), and knockouts of these genes do not exhibit robust normal conidiation rhythms

both in FRQ-sufficient and FRQ-less backgrounds (Eskandari et al., 2021; S. Li et al., 2011; Ratnayake et al., 2018). Some other basic components of the TOR pathway are also identified in *N. crassa* such as GTR1, GTR2, and KOG1 (Shertz et al., 2010). In addition, an ortholog of the mammalian CHK-2 (checkpoint kinase 2), which is involved in DNA-damage response, is identified in *Neurospora* as *prd-4*. The product of this *prd-4* (period-4) gene, which is a clock-controlled gene, advances the circadian phase by hyperphosphorylation of the FRQ protein. The kinase that phosphorylates and activates PRD-4 is the TOR kinase (Diernfellner et al., 2019).

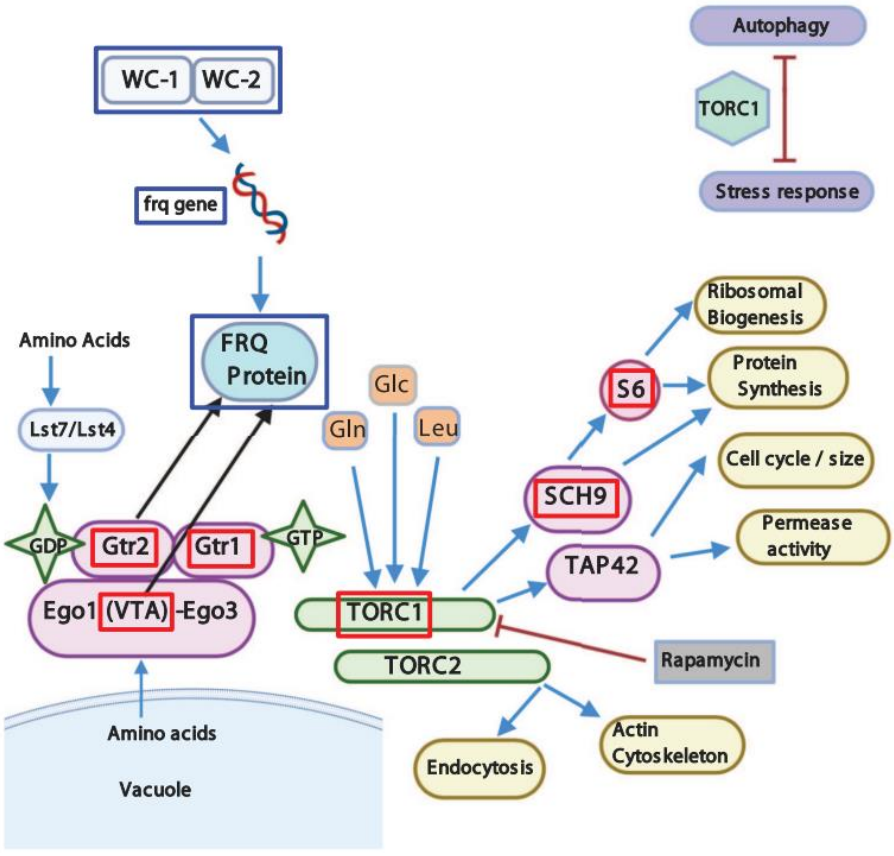

Figure 1.12 The TOR pathway based on *S. cerevisiae*. This figure highlights the connection between the TOR components and clock proteins in *N. crassa*. FRQ, WC-1, and WC-2 are Neurospora clock proteins and not found in yeast. The blue arrows show activation, and the red blunt-end lines

show inhibition. The proteins in red boxes show the probable TOR components in *Neurospora*. The black lines highlight the influence of VTA and GTR2 on the canonical clock proteins. Adapted from (Eskandari et al., 2021).

1.5 TOR and the Circadian Clock

There are many pieces of evidence that show the connection between the TOR signaling pathway and the circadian clock. Rhythmic TOR activity can be either the output of the circadian clock or another oscillator rather than TTFL which is working alongside of the well-known TTFL to generate the circadian rhythms (Lakin-Thomas, 2019). TOR (mTOR) is a typical signaling pathway that couples the environmental cues with the clock genes and their network. Research in mammals has uncovered 3 roles of the mTOR which are connected to the circadian clock: mTOR regulates the network between the coupled oscillators such as in SCN neurons, it is part of the photic entrainment pathway in the SCN, and it regulates autonomous clock properties in a range of oscillators (Cao, 2018).

mTOR regulates some fundamental clock properties in a variety of cells such as fibroblasts, hepatocytes, and adipocytes. mTOR inhibition leads to an increase in the period and a decrease in the amplitude, while its activation has an opposite effect (Ramanathan et al., 2018). Furthermore, the connection between mTOR and the circadian clock in diseases shows the relationship between the clock and TOR. In a study by Okazaki et al. (2014), they showed that everolimus treatment, which is a TOR inhibitor and is clinically approved to treat cancers such as kidney, pancreas, brain, and breast cancers, yields better results when it is applied at the time of the day that the mTOR is more activated. All these lines of evidence show the close relationship between the TOR/mTOR pathway and the circadian clock.

1.6 Circadian Rhythms and Human Health

Circadian disruption and misalignment (misalignment between the endogenous circadian cycle and the 24-hour environmental cues) is linked to many diseases and disorders in humans. Not having a regular sleep schedule, traveling between different time zones (jetlag), exposure to artificial light at night, consuming caffeine at night, and shifting light/dark schedule (shiftwork) are the most common reasons for circadian rhythms misalignment (Hower et al., 2018).

One example of the impact of circadian misalignment on human health is observed in shift workers. Shift work is a risk factor for developing hypertension, cardiovascular diseases, and inflammation (Morris et al., 2016). The activities which disrupt the circadian cycle such as irregular eating patterns and sleep/wake time can cause life-style diseases mediated by inflammation which result in diseases such as obesity, diabetes, hormonal imbalance, and neurological disorders (Fatima et al., 2022).

One of the neurodegenerative diseases which is connected to the circadian disturbance is Alzheimer's disease (AD). Memory impairment, sleep and circadian disruption are the common symptoms in AD patients. Many pieces of evidence suggest that the relationship between the circadian disruption and the Alzheimer's disease is bidirectional. Circadian disruption affects several parts of the brain through oxidative stress, neuronal metabolism, and proteostasis which might ultimately be one of the causes of Alzheimer's development (Adler et al., 2019). In addition, when the endogenous circadian pacing is at odds with the environmental cues, specifically light/dark cycle, due to jet lag, shift work, or

social obligations, the body may develop obesity and other metabolic diseases which are the major public health issues in industrialized societies (Woodie et al., 2022).

There is also a complex communication between the circadian cycle and the cell cycle. The circadian clock regulates cell division cycles, whose alteration can cause diseases like cancer (Bhadra et al., 2017). Cancers like breast, colorectal, and prostate cancer are among the diseases that occur with high rates in people with disrupted circadian rhythmicity (Roenneberg & Merrow, 2016). Considering the link between the circadian disruption and human diseases, knowing the circadian mechanism and its components is invaluable to human welfare and health.

1.7 Hypothesis and Objectives

Our hypothesis is that the TTFL is not the only oscillator in *Neurospora crassa* and there is one (or more than one) oscillator outside of the FRQ/WCC feedback loop which is working alongside the TTFL to generate the circadian rhythms. Our ultimate goal is to be able to identify this other FLO which is contributing to the circadian clock of this filamentous fungus.

My long-term objective is to identify the FRQ-less oscillator and its components and describe the interaction between the well-known TTFL and the FLO.

My short-term objective is to identify the role of the ribosomal protein S6 which is a component of the TOR pathway and as an assay of the TOR activity, and to investigate its rhythmicity in wild-type *Neurospora crassa* and the mutations which affect the wild-type conidiation rhythms. Also, to investigate the protein partners of S6 when it is highly

phosphorylated and when it is unphosphorylated to determine if there is a significant difference between the protein partners.

Chapter 2: Methods

2.1 *Neurospora crassa* Strains

Neurospora crassa strains which are used in this study are obtained either from Fungal Genetics Stock Centre (FGSC – Kansas State University, Manhattan, KS) or constructed in our laboratory using standard *Neurospora crassa* genetic crossing technique. All the strains used in this study carry *csp-1*, *ras-1*^{bd}, and *chol-1* mutations. The strains which only carry the mentioned mutations are referred to as Wild type in this study.

csp-1 (conidial separation-1) mutation is considered a morphological mutation and it prevents the conidiospores from separating from the aerial hyphae. Therefore, it protects the cultures from contamination by flying spores (Lakin-Thomas *et al*., 1990).

ras-1^{bd} (formerly *bd*) mutation is integrated in almost every *Neurospora* strain that is used for circadian research. This mutation influences circadian output of the clock and makes the fungus ideal for growth in glass race tubes with limited air flow. The growth rate is slower, and the banding is more visible in strains which carry *ras-1*^{bd} mutation. This mutation allows the fungus to continue conidiation when the CO_2 concentration is high in closed race tube cultures (Belden et al., 2007).

chol-1 mutant is defective in lipid synthesis. The conversion of phosphatidylethanolamine to phosphatidylmonomethylethanolamine is defective in this mutant and requires choline to be added to the culture of this mutant for normal growth. This mutation lengthens the period of circadian rhythms (Lakin-Thomas, 1996). Carried in almost all the strains in our lab, this mutation helps us to assay the FRQ-less rhythms in choline

dependent cultures (Lakin-Thomas & Brody, 2000). The list of the strains which are used in this study is found in Appendix I (Table 5.1).

S6-FLAG was constructed by one of the previous lab members, Milad Falahatchian, using knock-in technique to put the FLAG Tag on the endogenous S6 protein (Colot et al., 2006; Honda & Selker, 2009). The FLAG-tagged S6 gene was crossed into all of the strains used in this study using standard crossing techniques.

2.2 *Neurospora crassa* culture methods

2.2.1 Liquid culture

To investigate the effects of two of the activators of the TOR pathway (Glucose and Arginine) and two of the inhibitors of the TOR pathway (starvation and Rapamycin), spores were inoculated in 2 ml of liquid culture (2% glucose, 1X Vogel's salts, 10 mM choline) in 12-well plates and were grown in room temperature and constant light for 2 days. After 2 days of growth, the fungal mats were pressed between two layers of sterile filter papers to remove the excess medium and then transferred to fresh media for 4 hours before harvest. To investigate the effects of glucose on S6 phosphorylation, the fungal mats were transferred to fresh media plus glucose, to investigate the effect of arginine they were transferred to media plus arginine (5 mM final), to investigate the effect of starvation they were transferred to fresh media with only choline and no glucose, and to investigate the effect of rapamycin they were transferred to fresh media plus rapamycin (500 ng/ml final). The fungal mats were harvested over filter paper on a vacuum flask and were washed with distilled water. They were sucked almost dry over vacuum and frozen in microfuge tubes in liquid nitrogen and stored in -80^{o}C freezer.

2.2.2 Time Course experiment

To investigate the phosphorylation rhythms of S6 at the protein level, the fungus was grown on Maltose-Arginine media (MA) with 10mM choline, and 50x Vogel's salts (Appendix II) in large 15cm petri plates on top of a layer of sterile cellophane to prevent the hyphae from growing in the agar media; cellophane is made of cellulose and lets the fungus absorb the nutrients through it. Cellophane circles were cut using a lid from the 15cm petri plate, then they were soaked and washed with water, and autoclaved for 15 minutes at 121 ^{o}C to be sterilized. The sterile cellophane then was laid on the solidified agar media and kept under the UV light for one day to dry completely. Two starter plates per 20 cellophane plates were made using the same media but without any cellophane laid on them. The starter plates were inoculated on one edge with a few spores from the stock tubes and incubated in 30 ^{o}C and LL for 2 days. Then, the cellophane plates were inoculated on one edge by transferring plugs of the front growth with the hyphae on it from the starter plates using the circular end of a sterile pasture pipette. All the plates were incubated at 30^{o}C and constant light (LL) for at least 4 hours to synchronize the circadian clock of all the cells. Then the plates were moved to 22^{o}C and constant darkness (DD) at different times to cover a period of 20 to 80 hours of total growth in dark. The samples were harvested under the red safe light (*N. crassa* does not have any photoreceptors for the red light) using a plastic spatula that removes 1cm of the growth front at 4 hours intervals and were immediately dropped in liquid nitrogen and stored in -80^{o}C freezer (Schneider et al., 2009). A sample harvesting schedule is found in Appendix I, Table 5.2.

2.2.3 Race Tube Experiment

To investigate the rhythmic conidiation, period, and the linear growth rate of different strains of *N. crassa,* the fungus was grown on MA media in long glass "Race tubes". Race tubes are long 30cm hollow tubes that are bent in both ends and can contain 6ml of media. 5 sterile race tubes per each strain were filled with 6ml of media and after solidification were inoculated with small plugs cut from the starter plates, which were inoculated with the spores from the stock tubes and were kept at 30°C and LL to grow for at least one day. All the race tubes were incubated at 30°C and LL for one day. Then they were transferred to 22°C and DD. The growth front was marked everyday under the safe red light, noting the time and date. After growth was completed, the race tubes were removed from the incubators and were scanned. Using ImageJ, the growth marks and the band marks (middle of each band) were marked. Having the position and the timing of the growth marks, "Mac Tau" Excel program, which was developed by Dr. Lakin-Thomas (Lakin-Thomas, 1998), was used to calculate the linear growth rate. Period was calculated the same way using the positions of the band marks. Density of each tube was measured using the PlotProfile feature of ImageJ.

2.3 Protein Methods

2.3.1 Protein Extraction

The harvested time course samples were kept at -80°C. To extract protein from the frozen samples, they were ground with pre-cooled mortar and pestle in liquid nitrogen and the mycelia powder was transferred to 1.5 ml microfuge tubes on ice and then protein extraction buffer (50 mM Tris pH 6.8, 2% SDS, 10% Glycerol, and 1 mM PMSF) with the ratio of 1:1 v:v (buffer : mycelia powder) was added to the powder. The tubes were vortexed

for 20 seconds and then boiled for 5 minutes and then vortexed again, then were put on ice for 2 minutes. The samples were heated for 30 seconds in 80°C water and vortexed to redissolve and then were centrifuged for 5 minutes at 25°C and 12000g. The supernatant was transferred to a clean 1.5 ml tube for protein assay.

2.3.2 BioRad DC Protein Assay

To prepare the standard curve 0.5 mg/ml BSA (bovine serum albumin) was used. 0, 2.5, 5, 10, 15, and 20 µl of BSA was added to 25, 22.5, 20, 15, 10, and 5 µl of distilled water respectively in 1.5 ml tubes. The BioRad protein assay was performed following the manufacturer's instruction. 3x300 µl of 1/30 and 1/100 dilutions of the samples were loaded on 96-well plates and were read on a plate reader spectrophotometer. The protein concentrations were calculated in mg/ml.

2.3.3 Protein Electrophoresis by SDS-PAGE

SDS-PAGE was performed to separate different phosphorylated forms of the ribosomal S6 protein. Protein concentration was calculated for each time-point and 10 µg of total protein was used. 0.1 M DDT and 0.4% bromophenol blue were added to the samples and SDS extraction buffer was used to adjust the volume of all the samples to 10 µl. 12.5% acrylamide gel (Appendix II) was prepared and 50 µl of the phos binding reagent acrylamide (PhosTag, from APExBIO) and 50 µl of $MnCl_2$ were added to the gel to separate the S6 phosphorylated forms. The samples were heated for 2 minutes at 100 °C and loaded on the gel. Tris-glycine-SDS buffer (3.0 g Tris base, 14.4 g Glycine, 1.0 g SDS, 1 L water) was used as running buffer and the protein separation was performed for about 50 minutes at 200 V current.

2.3.4 Western Blotting

After electrophoresis, the gel was washed 3 times in cathode buffer (25 mM tris base, 40 mM glycine, 10% methanol, pH 9.4) and EDTA to remove MnCl2. Then proteins were transferred to a PVDF membrane (Millipore Immobilon-P transfer membrane) using three blotting buffers including Anode buffer I (0.3 M tris base, 10% methanol, pH 10.4), Anode buffer II (25 mM tris base, 10% methanol, pH 10.4), and Cathode buffer. The transfer was performed on a semi-dry blotter at 2 mA per cm^2 of the gel area for 40 minutes and at 14-15 V. After transfer, the blot was dried by soaking in 100% methanol for 10 seconds and stored at 4 ^oC.

2.3.5 Immunodetection

For immunodetection, the blot was wetted in 100% methanol for 15 seconds and rinsed with water briefly. The membrane was incubated in 1X blocking buffer (10X blocking buffer: 10% BSA in 1X TBST) for one hour with gentle agitation in room temperature. After blocking the membrane, primary anti-FLAG antibody (Monoclonal Anti-FLAG® M2 from Sigma F3165) was added to 1X blocking buffer with the 1:10,000 ratio and incubated for one hour with gentle agitation. Then the membrane was washed with TBST buffer (50 mM tris, 150 mM NaCl, 0.05% Tween-20, pH 7.5) 3 times for 15 minutes each. The secondary antibody (BioRad goat anti-mouse HRP-conjugated) was added to 1X blocking buffer with the 1:50,000 ratio and was agitated for 1 hour. Then the membrane was washed with TBST buffer 4x15 minutes. After washing the membrane with TBST, chemiluminescent detection reagents (immobilon® Western Chemiluminescent HRP Substrate from Millipore) were added on the membrane and incubated with gentle agitation for 5 minutes. The blot was

exposed to MicroChemi imager to detect the light produced by chemiluminescent substrate. 3 separate bands were detectable for each time-point. ImageJ was used to quantitate the results by measuring the mean grey value of the bands within a box of constant dimensions. The brightness of each band was determined by subtracting the brightness of the background. To normalize the values, the mean grey value of each separate band was divided by the sum of all 3 bands in each lane.

2.3.6 Staining of PVDF Membrane with Colloidal Gold Total Protein Stain

The membrane was washed in distilled water briefly after immunodetection. The membrane was then incubated in TTBS buffer (20 mM Tris, 500 M NaCl, 0.3% Tween-20, pH 7.5) with gentle agitation 3 times for 20 minutes. Then it was washed with distilled water 3 times for 2 minutes each. The membrane was then incubated with enough Colloidal Gold stain to cover the membrane completely with gentle agitation until the bands were visible. The membrane was washed with water 3 times for 1 minute after the staining.

2.4 Phosphatase Treatment

To determine that the three separate bands on the western blot results are different phosphorylated forms of the ribosomal protein S6, a few spores of the wildtype strain were grown in liquid media (2% glucose, 1X Vogel's salts, 10 mM choline) for 2 days in room temperature. The fungal mats were rinsed with water and dried over vacuum and frozen in liquid nitrogen. They were ground in pre-cooled mortar and pestle and then the powder was transferred to two microfuge tubes on ice. An equal volume of SDS-free phosphatase protein extraction buffer (50 mM HEPES, 100 mM NaCl, 2 mM DTT, 1% Triton X-100, plus protease inhibitors 1% PMSF and 1% protease inhibitor cocktail (NEB)) with PhosSTOP

(phosphatase inhibitor cocktail from Sigma-Aldrich, one PhosSTOP tablet per per 10 ml PMP buffer) was added to one of the tubes and extraction buffer without PhosSTOP was added to the other tube. PhosSTOP was added as a control for the phosphatase-treated samples as it inhibits the activity of any endogenous phosphatase. The tubes were kept on ice and then the supernatant was recovered by centrifuging at 12000xg and 4 ^{o}C for 5 minutes.

The samples which were extracted with extraction buffer without PhosSTOP were incubated on ice for 10, 30, and 60 minutes with 2.5 µl of 10X NEBuffer for protein MetalloPhosphatase and 2.5 µl of 10 mM $MnCl_2$ and 1 µl of Lambda Protein Phosphatase in 20 µl of total volume. After the incubation, the phosphatase protein extraction buffer was removed by centrifuging at 12000xg and 4 ^{o}C for 5 minutes and then 20 µl of SDS-containing protein extraction buffer was added to the pelleted proteins. The samples were loaded on a SDS-PAGE gel and then western blot and immunodetection were performed.

2.5 Immuno-precipitation (IP) & Mass-Spectrometry

Growth of the fungus for immunoprecipitation and mass-spectrometry were performed as described for the time-course experiment. Two of the time-points, one with more highly phosphorylated S6 and one with the least phosphorylated S6 (unphosphorylated) were selected for IP analysis.

Mortar and pestle were rinsed by ice-cold IP buffer (50 mM HEPES, pH 7.5, 150 mM NaCl, 10% (v/v) glycerol, 0.02% (v/v) NP40, 1 mM EDTA, 1 mg/ml leupeptin, 1 mg/ml pepstatin A, and 1 mM PMSF plus 1 tablet of PhosSTOP per 10 ml of the IP buffer to inhibit the endogenous phosphatases) and the fungal mycelia were ground in them with liquid

nitrogen being added to the mortar. Then the powder was transferred to 1.5 ml tubes containing 500 µl of IP buffer on ice. The tubes were inverted for 20 seconds to mix and then incubated for 5 minutes at 4 °C. The tubes were then centrifuged for 10 minutes at 4 °C and 12000g to remove the cell debris. Supernatants were collected in 5 ml tubes and the concentration of proteins was measured using BioRad DC protein assay. 100µl of the supernatant was collected for SDS-PAGE electrophoresis and Western blotting. The supernatant then was stored in -80 °C freezer.

To pre-clear the cell lysate and reduce the non-specific interactions, Sepharose 4B beads from Sigma-Aldrich were used. 50 µl of Sepharose 4B beads were washed 5 times with 1 ml of IP lysis buffer by centrifuging at 500xg at 4 °C for 1 minute each time. 5 ml of the IP extract with 10 mg total protein was added to the 50 µl pre-washed beads and the IP extract and the beads were incubated for 1 hour at 4°C with end-over-end agitation. Sepharose 4B beads were pelleted by centrifuging at 500xg at 4 °C for 1 minute and the supernatant was recovered.

10 µl of Anti-FLAG M2 Affinity Gel beads from Sigma-Aldrich were washed with 1 ml of cold IP lysis buffer by centrifuging at 500xg at 4 °C for 1 minute. Then the beads were incubated at room temperature for 10 minutes with 1 ml of 0.1 M glycine-HCl at pH 3.5. Beads were washed 3 times after the incubation with 1 ml of IP lysis buffer by centrifuging at 500xg at 4 °C for 1 minute each time.

The pre-cleared cell lysate was added to the pre-washed Anti-FLAG M2 Affinity Gel beads and incubated at 4 °C overnight with end-over-end gentle agitation. After the

incubation, the beads were pelleted by centrifuging at 750xg at 4 °C for 1 minute. 100 µl of the supernatant was collected for SDS-PAGE electrophoresis and Western blotting. The pelleted Anti-FLAG beads were washed 3 times with IP lysis buffer and 2 times with FLAG rinsing buffer (0.5 M NH_4HCO_3, 1 M KCl, 200 mM Na_2EDTA) by centrifuging at 500xg at 4 °C for 1 minute each time.

Washed beads were stored at -80 °C freezer and the frozen beads were sent to SPARC BioCentre (SickKids Proteomics, Analytics, Robotics & Chemical Biology Centre, Hospital for Sick Children, Toronto, Canada) for Mass-spectrometry analysis. The results were received as a Scaffold file.

Chapter 3: Results

3.1 TOR Assay Validation

3.1.1 Effects of activators and inhibitors of TOR on S6 Phosphorylation

To determine the effects of two of the activators and two of the inhibitors of the TOR pathway on the phosphorylation of the S6 protein, the wildtype strain (#667 S6-FLAG *csp-1; ras^{bd}; chol-1*) was treated with glucose, arginine, rapamycin, and starvation. The spores were grown for two days in liquid media and then they were transferred to fresh media for 4 hours before harvest. The results (Figures 3.1 and 3.2) showed that the activators of TOR, which are glucose and arginine, increase the phosphorylation of the S6 protein and the inhibitors of TOR, starvation and rapamycin, decrease the S6 protein phosphorylation, and so increase and decrease the activity of the TOR pathway. This result confirms that the S6-FLAG phosphorylation state responds as predicted and is therefore a valid assay for TOR activity.

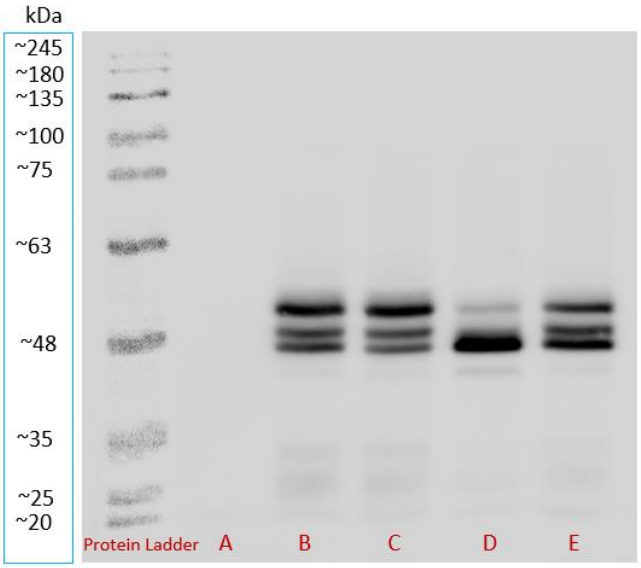

Figure 3.1 Western blot of the effects of activators and inhibitors of the TOR pathway A) Negative Control (#26 *csp-1; ras^{bd}; chol-1*) without S6-FLAG, B) S6-FLAG #667 grown in Minimal Media + Glucose, C) S6-FLAG #667 grown in Minimal Media + Arginine D) S6-FLAG #667 grown in Minimal Media only (starvation), E) S6-FLAG #667 grown in Minimal Media + Rapamycin

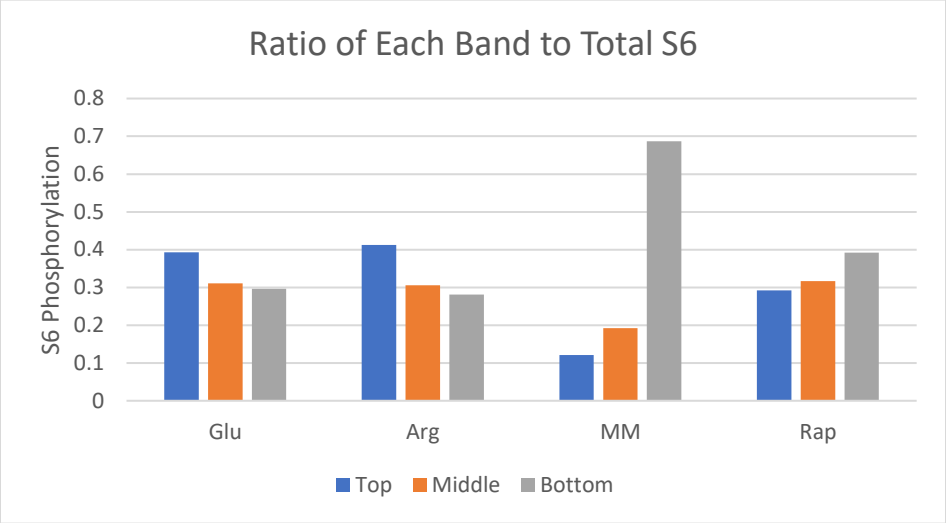

Figure 3.2 Quantified Western blot of activators and inhibitors experiment. Ratio of each band: top band (di-phosphorylated), middle band (monophosphorylated), and bottom band (dephosphorylated) to the total amount of S6. Glu: Glucose, Arg: Arginine, MM: Minimal Media or Starvation, Rap: Rapamycin. S6 Phosphorylation is higher when the fungus is treated with Glucose and Arginine.

3.1.2 Phosphatase treatment

To determine if the 3 bands on the gels represent the 3 different phosphorylated forms of the S6 protein, samples of the wildtype strain (#667) were extracted with SDS-free protein extraction (PMP) buffer and were treated with Lambda Phosphatase. As a control for this experiment, strain #667 was grown in the same liquid medium for 2 days and then the proteins were extracted with the SDS-containing extraction buffer and were boiled for 5 minutes (in this case endogenous phosphatases and proteases lose their activity). Another sample was treated with the PhosSTOP phosphatase inhibitor as another control to determine

if 3 separate bands will show on the gel using the PMP extraction buffer and extracting the proteins on ice rather than boiling the samples. The results (Figure 3.3) showed that 3 separate bands were visible for both controls and all the bands collapsed into one bottom band after the phosphatase treatment. The results show that the 3 bands which are detectable on the membrane are 3 different phosphorylated forms of the S6 protein.

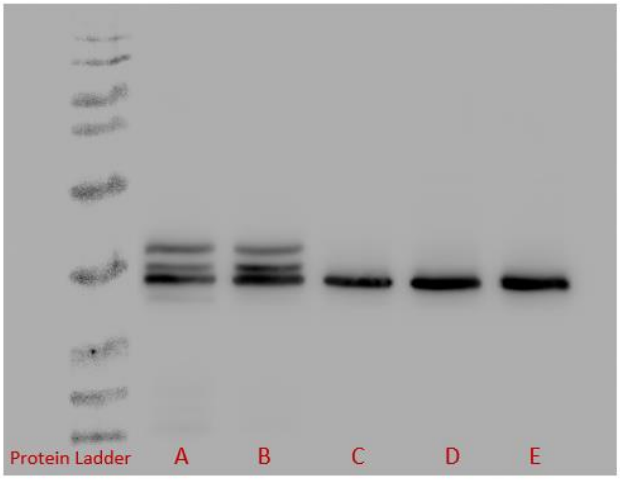

Figure 3.3 Phosphatase treatment. A) Control. Strain #667 extracted with SDS-containing extraction buffer B) Strain #667 treated with PhosSTOP C) Strain #667 treated with Lambda phosphatase for 10 minutes D) Strain #667 treated with Lambda phosphatase for 30 minutes E) Strain #667 treated with Lambda phosphatase for 60 minutes.

3.2 Time-courses

To investigate the rhythms in S6 phosphorylation, time-course experiments were performed for the wild-type, *vta*^{ko}, *gtr2*^{ko}, *prd-1*, *frq*^{7}, and *frq*^{10} strains.

To optimize the period of growth in dark and to capture the peaks and troughs of phosphorylation, time-courses were conducted covering a period of 0 to 96 hours in dark for

the wildtype strain (Figure 3.4). The best duration of growth in dark was determined to be 20 to 80 hours of growth in dark, since this duration covers 3 peaks and 2 troughs of S6 phosphorylation (Figure 3.5). As shown in Figure 3.5, the top band (hyper or diphosphorylated S6) and the bottom band (unphosphorylated S6) are rhythmic, and the middle band (monophosphorylated) is not rhythmic. Due to the fact that hyperphosphorylated S6 is the active form of the S6, only the top band is quantitated and shown in the next time-courses.

Neurospora crassa strains were grown on top of cellophane and were harvested every 4 hours across a 20–80-hour total growth in dark and at 22 ^{o}C. Each of the experiments was repeated for 3 biologically separate trials. After harvest, the proteins were extracted and separated on an SDS-PAGE gel using PhosTag as a phos-binding reagent.

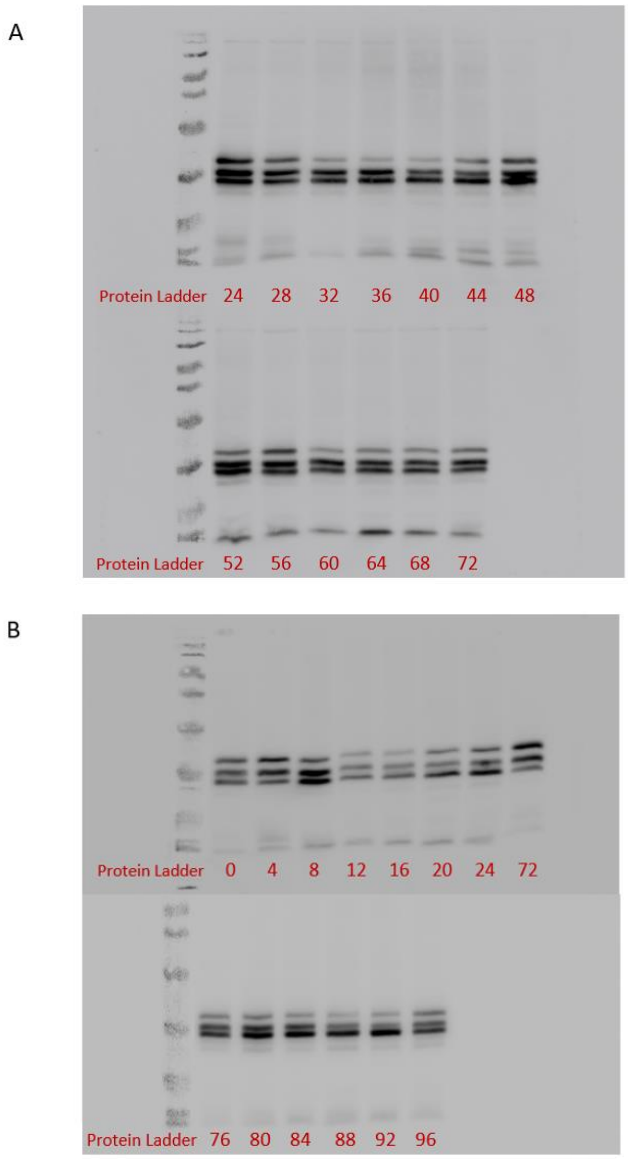

Figure 3.4 Western blot of the first time-course for the wildtype strain. A) 24-72 time-points, B) 0-24 and 72-96 time-points. The fungus was grown in dark for 0 to 96 hours and was harvested every 4 hours. The numbers represent the hours of growth in dark. One time-course was done covering 24-72 hours of growth and another time-course was done covering 0-24 and 24-96 hours of growth. 24-hour and 72-hour time-points were repeated in each set of the experiments.

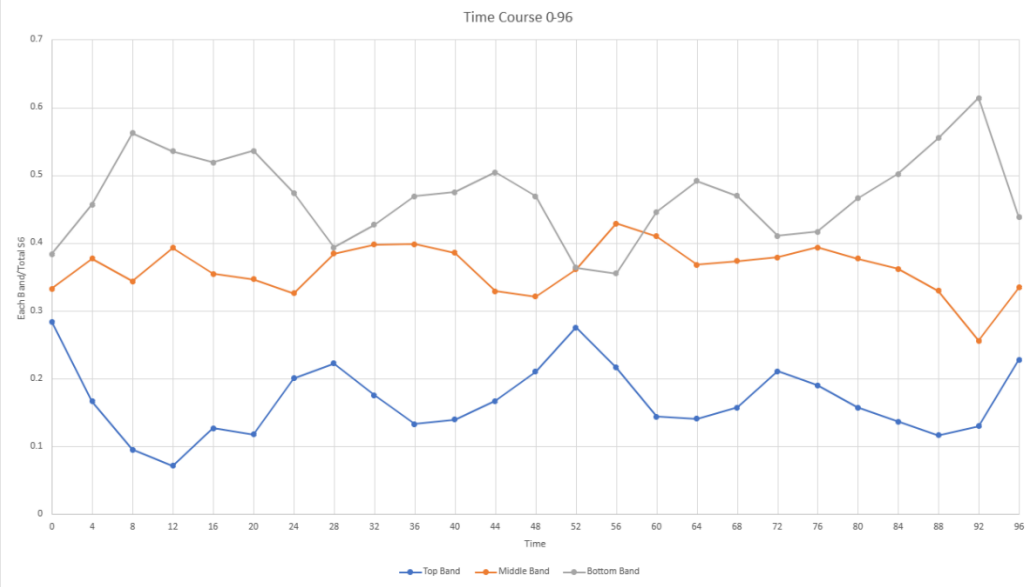

Figure 3.5 Time-course 0-96 hours. Top band (blue) shows the hyperphosphorylated S6, middle band (orange) shows the monophosphorylated S6, and bottom band (grey) shows the unphosphorylated S6.

The western blot of one of the trials of the *vta*^{ko} (*csp-1*; *ras*^{bd}; *chol-1*; *vta*) strain is shown in Figure 3.6 as an example. The rest of the western blots were done the same way.

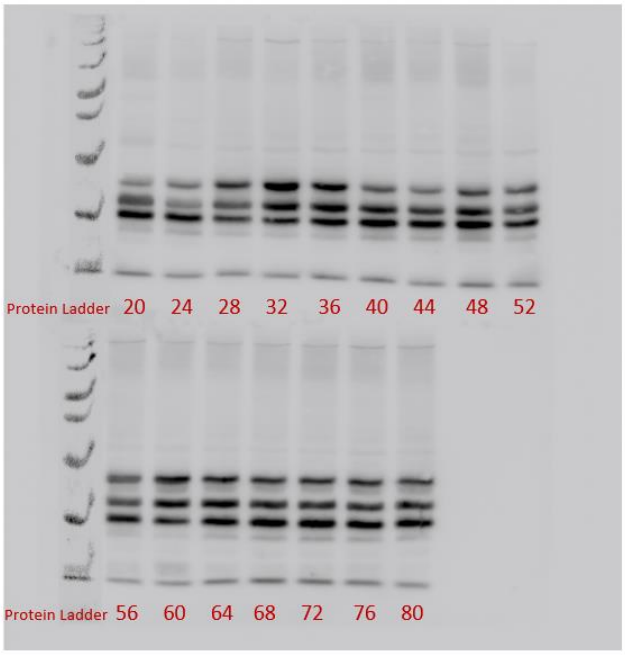

Figure 3.6 Western blot result of the third trial of *vta*^{ko} strain time-course. Numbers at the bottom of each lane represents the hours that the fungus was grown in dark. The rhythms in phosphorylation are noticeable in the bands. 50 µl of PhosTag was added to each gel.

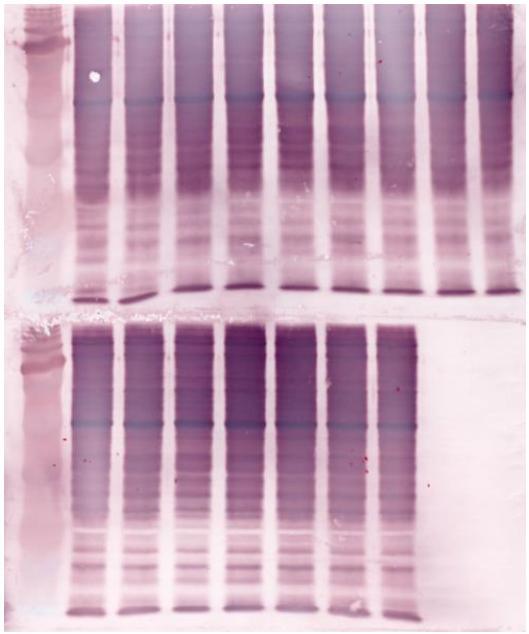

Figure 3.7 Total protein staining with Colloidal Gold stain.

Wildtype S6-FLAG time-course

Ribosomal protein S6 phosphorylation is rhythmic in the wildtype strain (*chol-1*; *csp-1*; *ras*^{bd}) with a period about 22 hours (Figure 3.8). Normalized total S6 protein levels are shown in Figure 3.9. Total S6 levels are rhythmic, although there is a high variation between the separate trials.

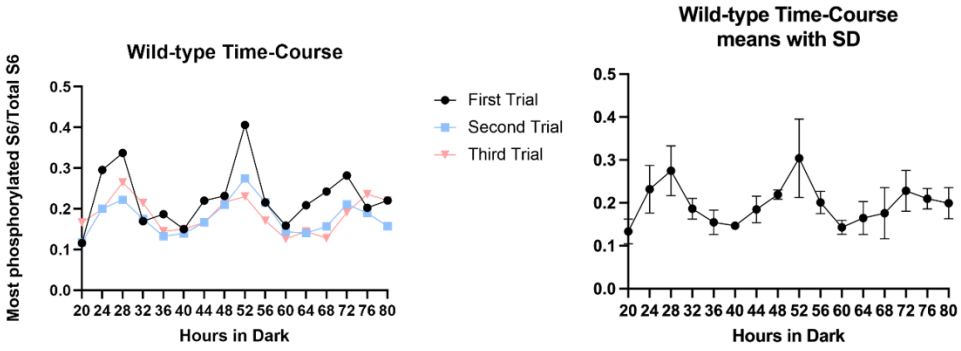

Figure 3.8 Time-course experiment for the wildtype strain. All 3 biologically separate trials are plotted on the graph on the left. The average of all trials with standard deviation are plotted on the right graph.

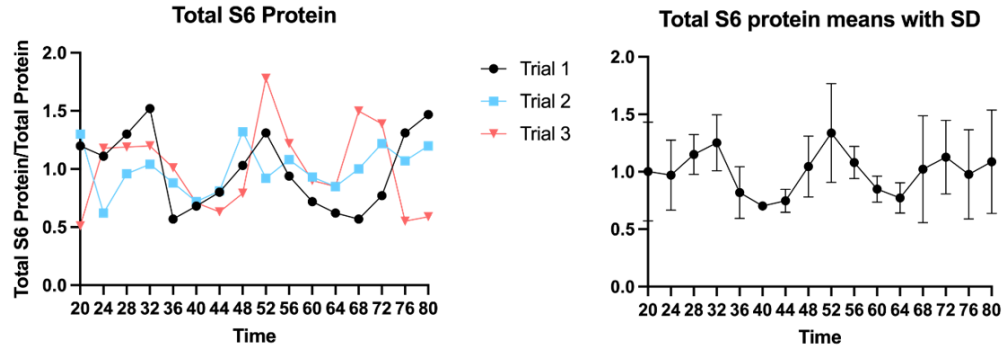

Figure 3.9 Normalized total S6 protein levels in wildtype. All 3 biologically separate trials are plotted on the graph on the left. The average of all trials with standard deviation are plotted on the right graph.

vta^{ko} S6-FLAG time-course

The S6 phosphorylation in *vta*^{ko} is rhythmic with a period about 28 hours and dampens out in the third cycle (Figure 3.10).

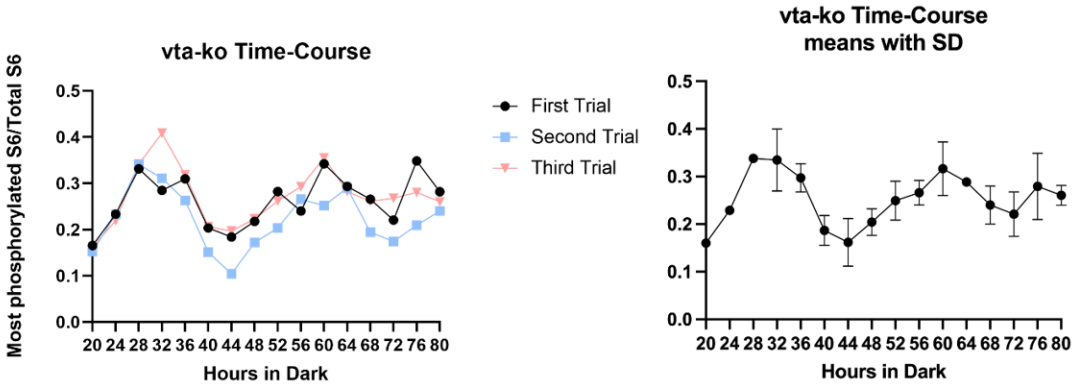

Figure 3.10 Time-course experiment for the *vta*^{ko} strain. All 3 biologically separate trials are plotted on the graph on the left. The average of all trials with standard deviation are plotted on the right graph.

gtr2^{ko} S6-FLAG time-course

The S6 phosphorylation in *gtr2*^{ko} (*csp-1*; *ras*^{bd}; *chol-1*; *gtr2*) is rhythmic with a period about 28 hours and dampens out after the second peak (Figure 3.11).

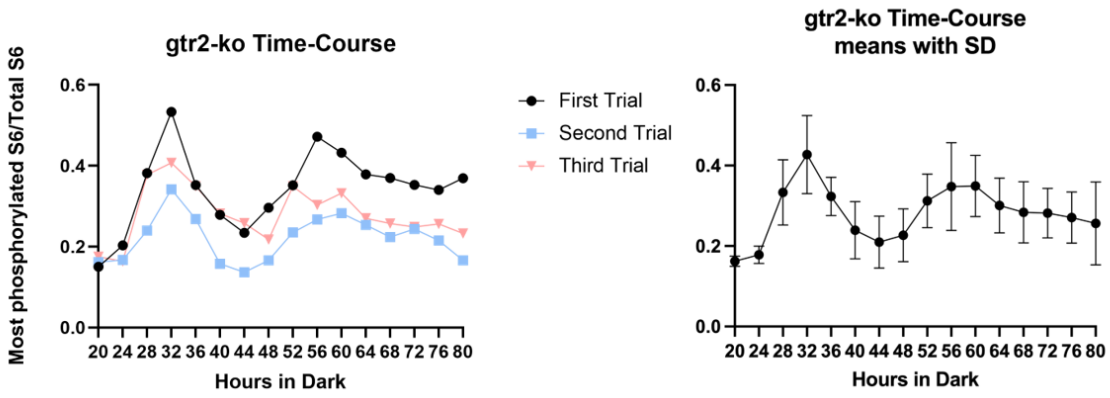

Figure 3.11 Time-course experiment for the *gtr2*^{ko} strain. All 3 biologically separate trials are plotted on the graph on the left. The average of all trials with standard deviation are plotted on the right graph.

prd-1 S6-FLAG time-course

S6 phosphorylation in the *prd1* (*csp-1*; *ras*^{bd}; *chol-1*; *prd-1*) strain is rhythmic with a period about 24 hours with a high amplitude (Figure 3.12).

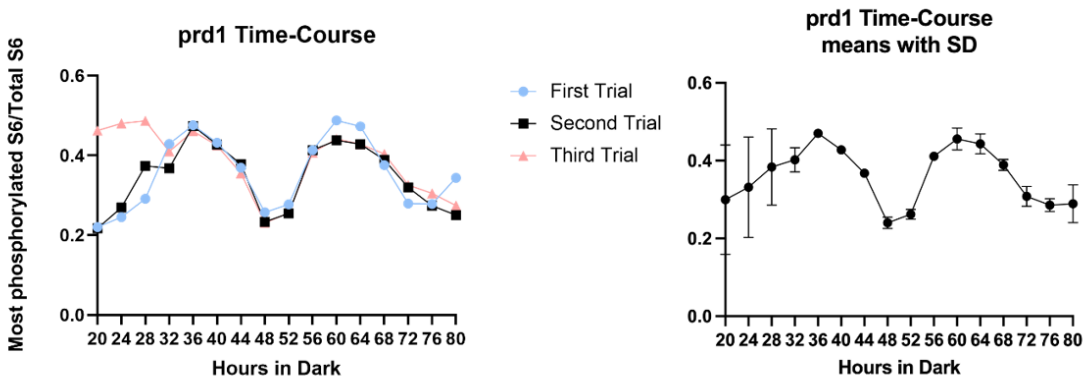

Figure 3.12 Time-course experiment for the *prd-1* strain. All 3 biologically separate trials are plotted on the graph on the left. The average of all trials with standard deviation are plotted on the right graph.

frq^{7} S6-FLAG time-course

S6 phosphorylation in the long-period (Diegmann et al., 2010) mutant *frq*^{7} (*csp-1*; *ras*^{bd}; *chol-1*; *frq*^{7}) shows a low amplitude rhythm with a period about 32 hours (Figure 3.13).

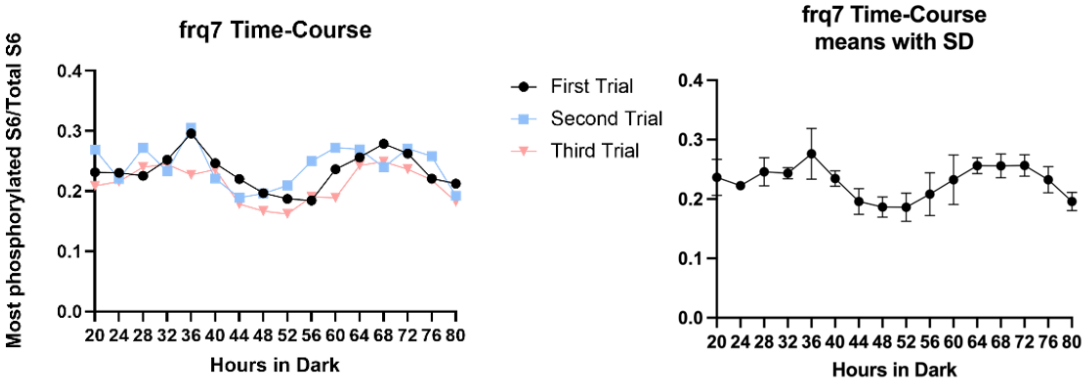

Figure 3.13 Time-course experiment for the *frq*^{7} strain. All 3 biologically separate trials are plotted on the graph on the left. The average of all trials with standard deviation are plotted on the right graph.

frq^{10} S6-FLAG time-course

S6 phosphorylation in *frq*-null background (*csp-1*; *ras*^{bd}; *chol-1; frq*^{10}) is not clearly rhythmic. Individual trials appear rhythmic but are not synchronized (Figure 3.14).

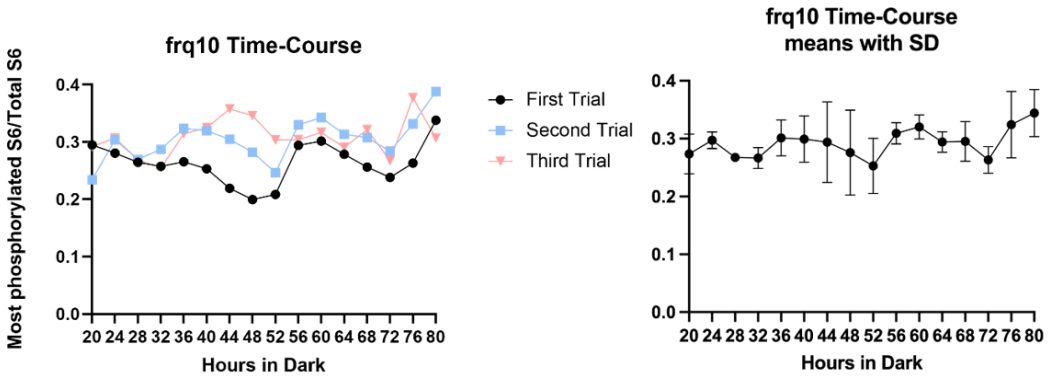

Figure 3.14 Time-course experiment for the *frq*^{10} strain. All 3 biologically separate trials are plotted on the graph on the left. The average of all trials with standard deviation are plotted on the right graph.

3.2.1 Statistical Analysis for Time-courses

3.2.1.1 One-Way ANOVA test

To determine whether the time is a significant variable in time-course experiments, one-way ANOVA test was performed for all the strains (Table 3.1).

Table 3.2 One-way ANOVA test p-values for the time variable. All the p-values are significant ($p<0.5$) except for *frq*^{10} strain.

Strain	**p-value**
Wild type	1.15e-03
frq^{7}	1.12e-03
frq^{10}	0.595
vta^{ko}	1.6e-05
gtr2^{ko}	1.32e-02
prd1	1.91e-04

The one-way ANOVA test results show that the time is a significant variable for all the strains except the *frq*^{10} mutant.

To determine if there is a difference of the total S6 phosphorylation between all the strains, one-way ANOVA test was performed, comparing strains to each other. The p-value of this test is **1.76e-12**. This value shows that the difference is very significant. To depict this difference, a box plot of the S6 phosphorylation values was plotted using R Studio (Figure 3.15).

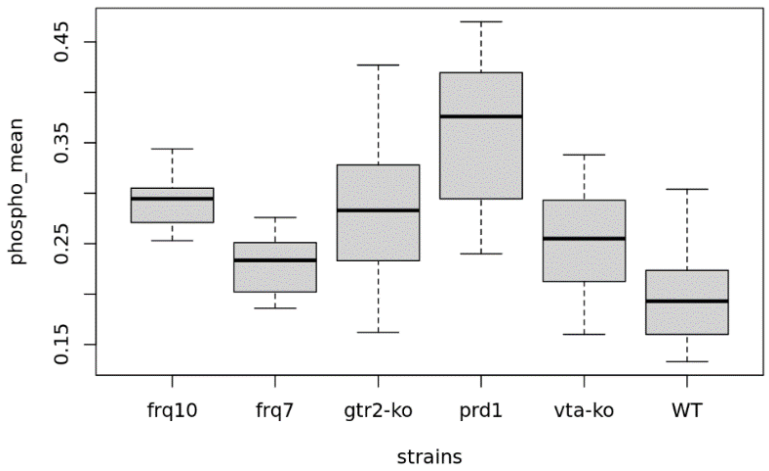

Figure 3.15 Box plot of the total S6 phosphorylation. This box plot shows the difference of total S6 phosphorylation among 6 strains. The whiskers show the minimum and maximum values of S6 phosphorylation, and the horizontal lines in the boxes show the median of each group.

3.2.1.2 Post hoc Analysis

The one-way ANOVA test is followed by a Post hoc analysis to investigate the difference between strains two by two (Table 3.2). From the table below that shows the adjusted p-values, the most interesting one is the p-value for *vta*^{ko} and *gtr2*^{ko} strains that is not significant and depicts that the total S6 phosphorylation between these two mutants is similar (this is also observable from the box plot). These two mutants are also very similar in phenotype and banding when they are grown on long race tubes (Eskandari et al., 2021).

Table 3.2 Post hoc analysis (Tuekey HDS) adjusted p-values results.

Strains	Adjusted p-value
frq7-frq10	1.3e-2
gtr2-ko-frq10	9.9e-2
prd1-frq10	5.9e-3
vta-ko-frq10	0.27
WT-frq10	3.2e-5

gtr2-ko-frq7	6.8e-2
prd1-frq7	0.7e-6
vta-ko-frq7	0.82
WT-frq7	0.54
prd1-gtr2-ko	8.08e-4
vta-ko-gtr2-ko	0.62
WT-gtr2-ko	3.13e-4
vta-ko-prd1	1.6e-6
WT-prd1	0.5e-6
WT-vta-ko	0.04

3.2.1.3 Cosinor test

To determine how the circadian rhythms of each of the time-courses fit a cosine curve as a test for rhythmicity, the Cosinor test was performed using the circacompare package in R programming language (the R code is provided in Appendix III section) (Figure 3.16).

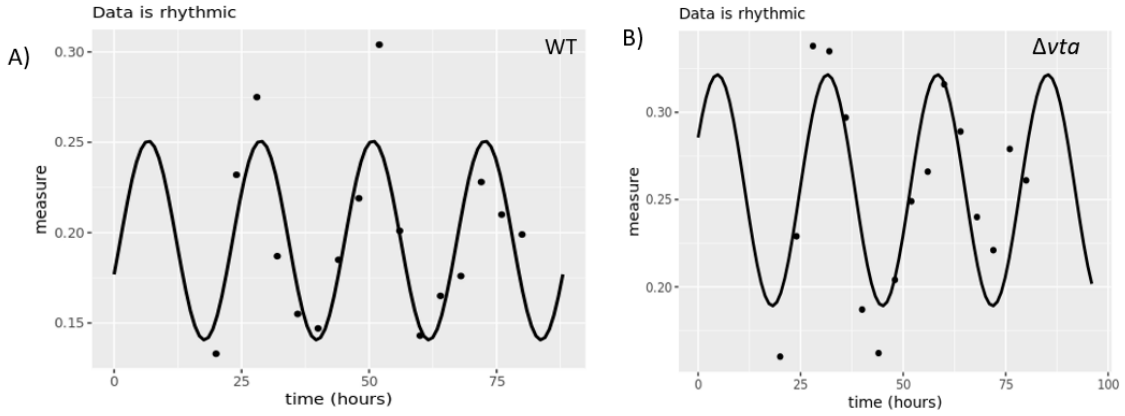

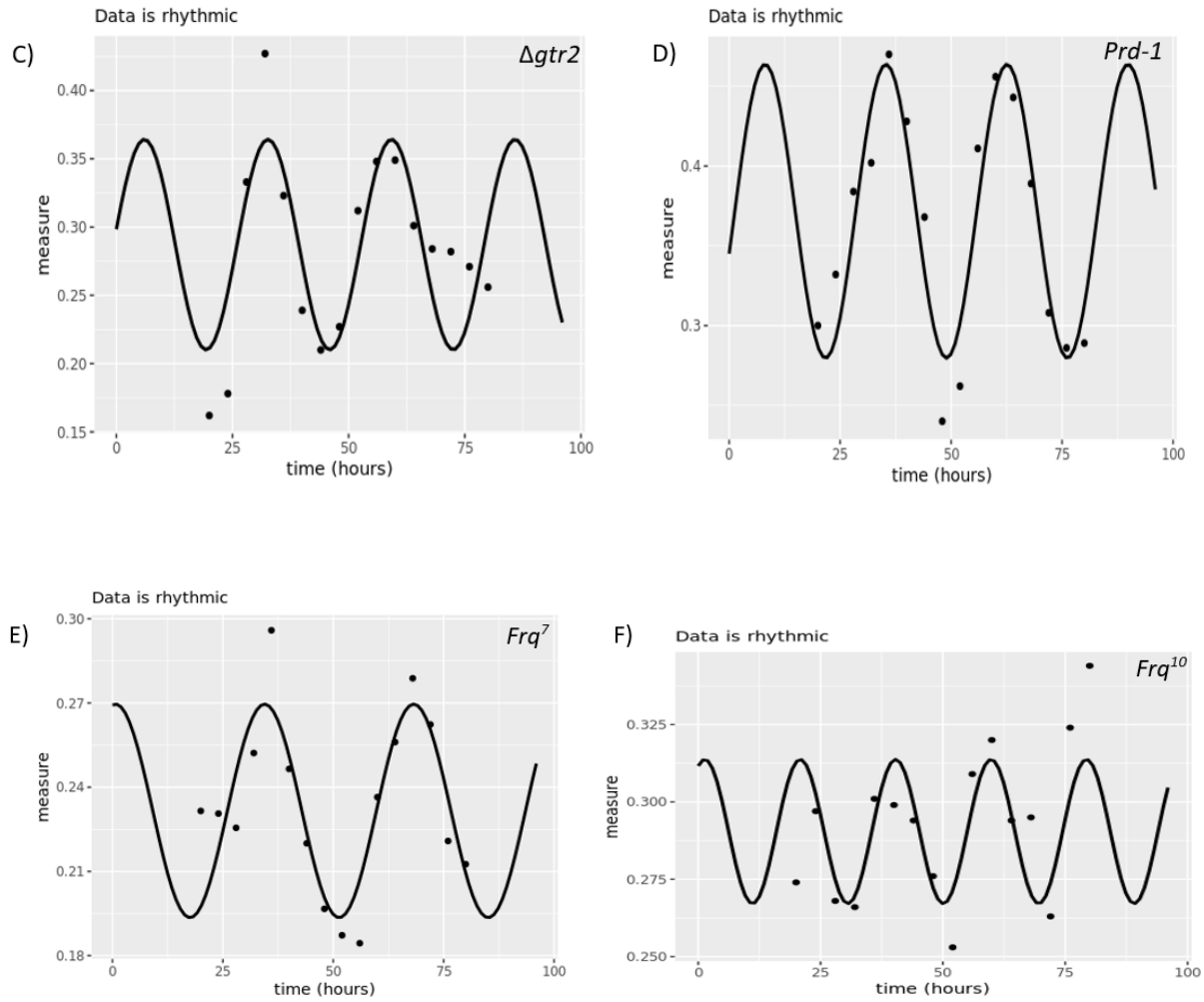

Figure 3.16 Circacompare package results (cosinor fit). Using R Studio, the time-course data was fitted on a cosine curve. All the time-courses were determined to be rhythmic by R.

All the time-course data was determined to be rhythmic by R. This package also calculated the p-value and suggested the period duration for the time-courses (Table 3.3).

Table 3.3 p-value and suggested period by R for each of the time-courses.

Strain	p-value	Suggested period (h)
WT	9.97e-05	22.00
Δvta	1.64e-04	26.85
Δgtr2	5.36e-04	26.59
prd-1	1.40e-06	27.24
frq^7	7.01e-05	33.76
frq^{10}	4.77e-03	19.50

3.3 Race tubes

To observe the conidiation rhythms in different strains and measure the conidiation period to compare it to the S6 phosphorylation period, they were grown in long glass race tubes. As it is shown in Figure 3.17, the wildtype is rhythmic, Δ*vta* and Δ*gtr2* look different from the wildtype and rhythms dampen out after a while. *prd-1* is rhythmic with smaller bands (prd-1 has a slow growth rate), frq^7 is also rhythmic, but frq^{10} is totally arrhythmic. Race tube results were analyzed as previously described in section 2.2.3. The average conidiation periods and growth rates of the strains are listed in Table 3.4.

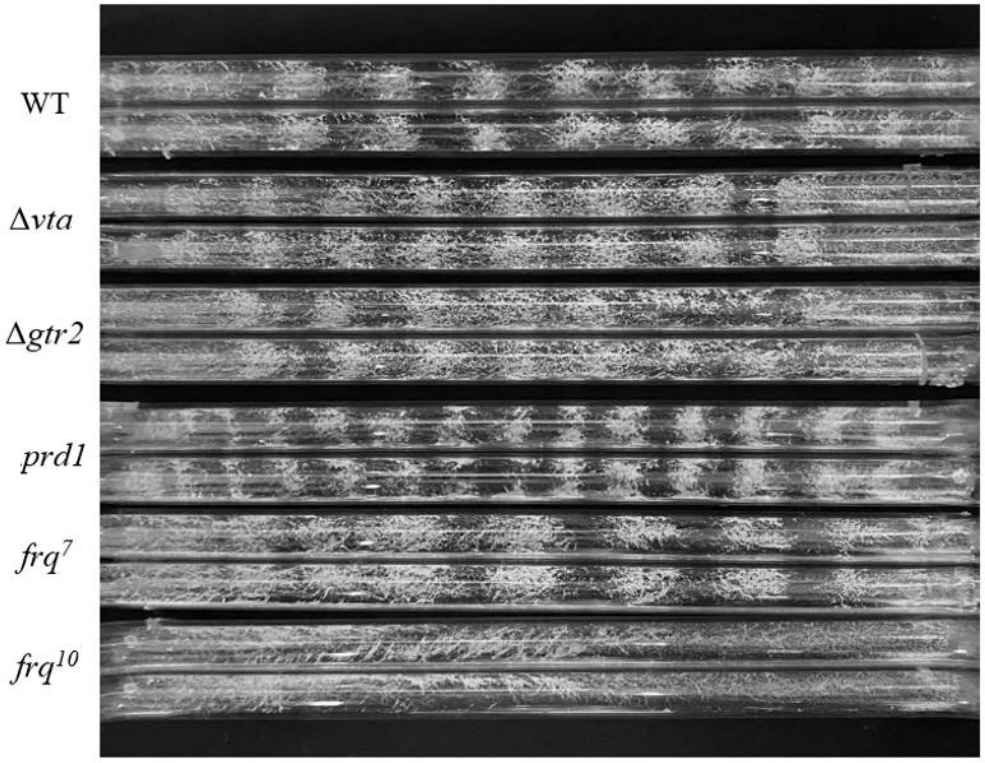

Figure 3.17 Race tube experiment. Two replicates are shown for each strain. The fungal plugs were inoculated on the left end of the tubes. All the tubes were grown in dark and 22 °C for one week, except the *prd-1* strain that was kept in dark for 2 weeks to complete growing (*prd-1* has a slow growth rate).

Table 3.4 The average period of banding and the growth rate

Strain	**Conidiation period (h)**	**Growth Rate (mm/h)**
Wildtype	22.80 ± 0.08	1.11 ± 0.008
vta^{ko}	24.48 ± 0.07	1.08 ± 0.008
$gtr2^{ko}$	23.82 ± 0.07	1.04 ± 0.005
prd-1	24.95 ± 0.11	0.77 ± 0.003

frq^{7}	32.34 ± 0.17	1.12 ± 0.006
frq^{10}	-	1.292 ± 0.005

Values are mean ± SEM of N=5 tubes.

3.4 Comparison of Race Tube Density with S6 Phosphorylation

To compare the peaks in conidiation rhythms with the S6 phosphorylation rhythms and see if they correlate, race tube density was plotted between 20 to 80 hours of growth in the dark and was compared to S6 phosphorylation rhythms. As mentioned in the methods section, the race tube density was measured using the scanned race tube pictures and Mac Tau Excel program developed by Dr. Lakin-Thomas. The S6 phosphorylation data was acquired from the time-course results.

In the wildtype, S6 phosphorylation peaks happen a few hours before the density peaks (Figure 3.18). In the Δ*vta*, S6 phosphorylation peaks happen a few hours before or at the same time as the density peaks, and both rhythms dampen out after the second peak (Figure 3.19). The Δ*gtr2* strain looks very similar to the Δ*vta.* The S6 phosphorylation peaks happen a few hours before or at almost the same time as the density peaks and both rhythms dampen out after the second peak (Figure 3.20). In the prd-1 strain, the S6 phosphorylation peaks happen a few hours before the density peaks and both rhythms show high amplitude (Figure 3.21). In comparison to the wildtype, S6 phosphorylation amplitude is higher in the *prd-1* strain. In the *frq*^{7} strain, the S6 phosphorylation peaks happen many hours before the density peaks and the amplitude of both S6 rhythms and density rhythms are lower than the

wildtype (Figure 3.22). Conidiation is completely arrhythmic in *frq*^{10} strain, and the S6 phosphorylation shows a low amplitude rhythm (Figure 3.23).

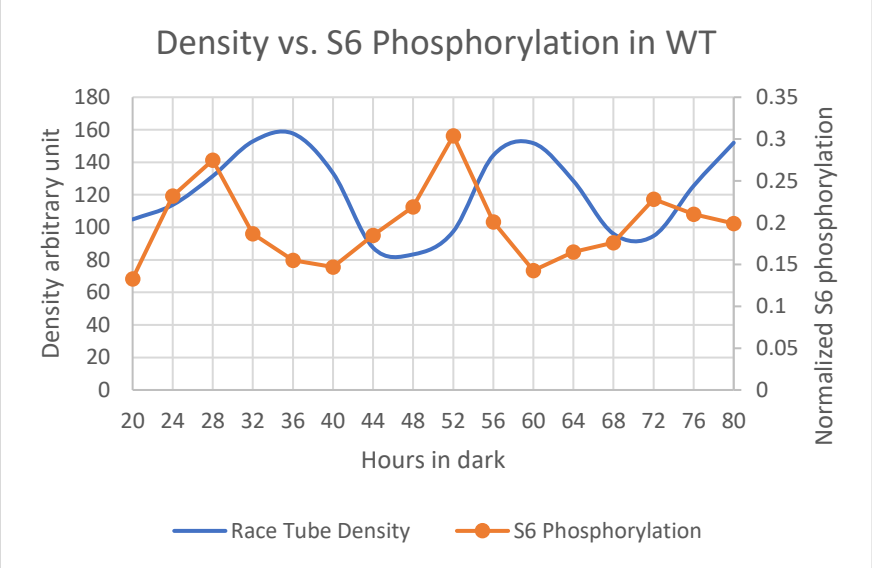

Figure 3.18 Race tube density and S6 phosphorylation rhythms in the Wildtype strain

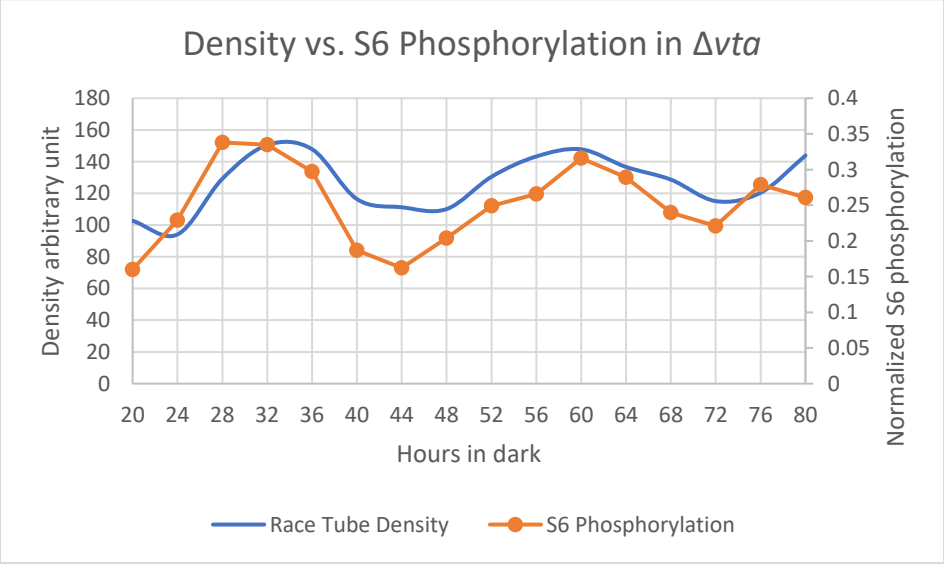

Figure 3.19 Race tube density and S6 phosphorylation rhythms in the *vta*^{ko} strain.

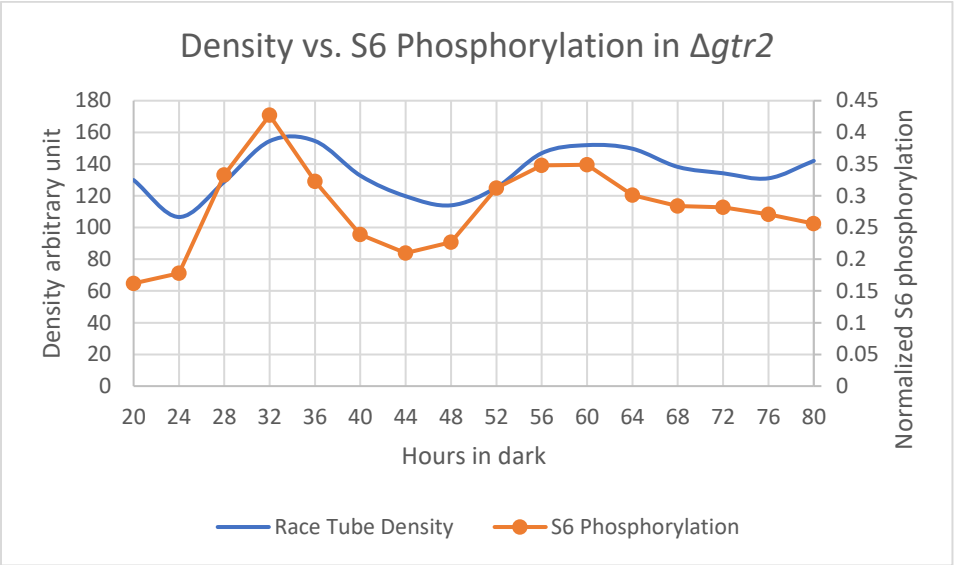

Figure 3.20 Race tube density and S6 phosphorylation rhythms in the *gtr2*^{ko} strain.

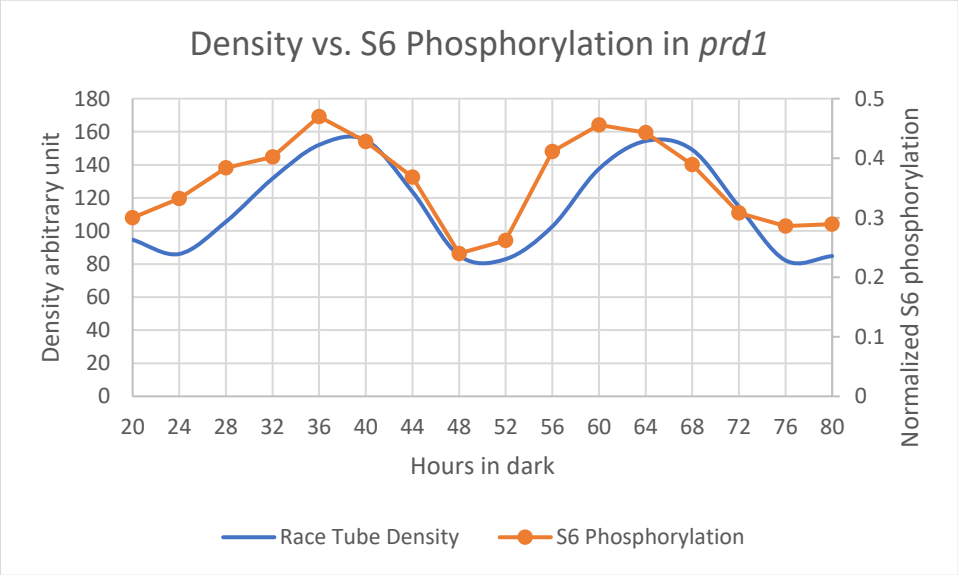

Figure 3.21 Race tube density and S6 phosphorylation rhythms in the *prd-1* strain.

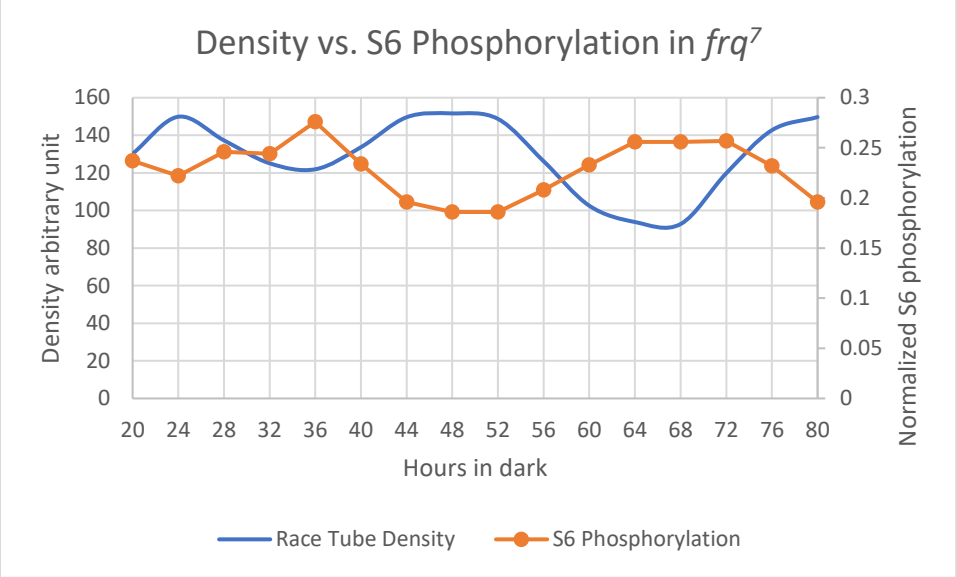

Figure 3.22 Race tube density and S6 phosphorylation rhythms in the *frq*^{7} strain.

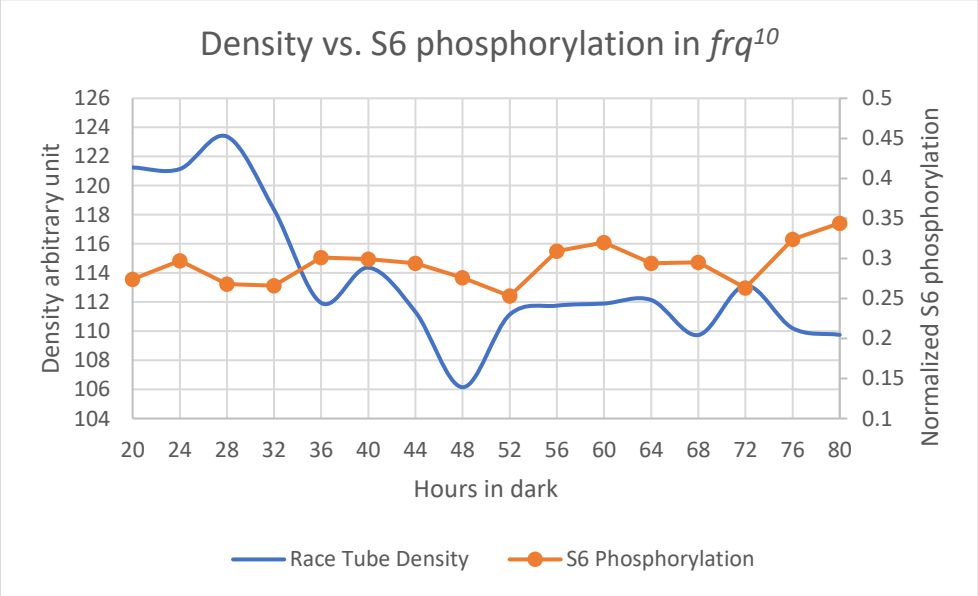

Figure 3.23 Race tube density and S6 phosphorylation rhythms in the *frq*^{10} strain.

3.5 Immunoprecipitation and Mass-spectrometry

To determine the protein partners of the S6 protein in the wildtype strain in two different phosphorylated states, at 52 hours of growth in dark and at 60 hours of growth in

dark, immunoprecipitation and mass-spectrometry were conducted. 52-hour time-point has the highest diphosphorylated (highly phosphorylated) S6 and the 60-hour time-point has the least diphosphorylated S6 (as shown in figure 3.5). Another purpose for doing the mass-spectrometry experiment was to determine if PRD-1 is one of the protein partners of S6 protein. As it was previously mentioned, our lab found that the ribosomal protein S6 is one of the protein partners of the PRD-1 protein (unpublished data). Therefore, I decided to check whether PRD-1 is S6 protein's partner when the reciprocal experiment is done. This experiment was done two times (2 trials). The results of mass-spectrometry were received as a scaffold file from the SPARC BioCentre (SickKids Hospital). Western blot results of samples before and after precipitation are shown in Figure 3.24.

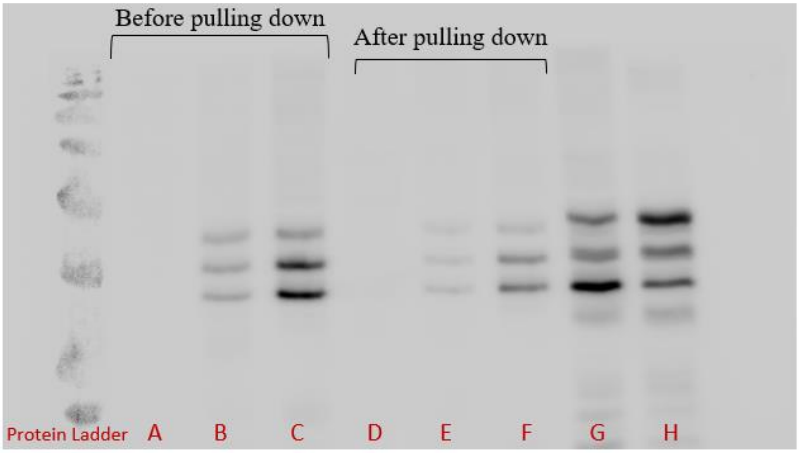

Figure 3.24 Western blot of mass-spectrometry samples and controls. A) #26 wildtype without FLAG-Tag before immunoprecipitation, B) 52-hour time-point before immunoprecipitation, C) 60-hour time-point before immunoprecipitation, D) #26 wildtype without FLAG-Tag after immunoprecipitation, E) 52-hour time-point after immunoprecipitation, F) 60-hour time-point after immunoprecipitation, G) 60-hour time-point extracted with SDS-containing protein extraction buffer as a control, H) 52-hour time-point extracted with SDS-containing protein extraction buffer as a control.

The control for this experiment was the #26 strain which is the wildtype strain without the S6-FLAG Tag. 376 proteins were detected as the partners of S6 protein. The majority of them are ribosomal proteins and the proteins which are associated with ribosomal biogenesis and protein translation. 5 proteins were detected as S6 partners only when it is highly phosphorylated (52-hour time-point), and 4 proteins were detected as S6 partners when it is mostly dephosphorylated (60-hour time-point). Among these proteins only one of each group was present in both trials (Table 3.5). 146 proteins were detected as S6 partners which were present for both time-points (Figure 3.25). This shows that the phosphorylation state of the S6 protein does not make a significant difference in its binding partners. A list of the first 5 protein partners of both time-points is provided in Table 3.6. One interesting protein which was detected as a partner of the hyperphosphorylated time-point (52hrs) is Casein kinase II. This protein phosphorylates FRQ protein.

In addition, PRD-1 protein (ATP-dependent RNA helicase dbp-2) was not found among the protein partners of the S6 protein.

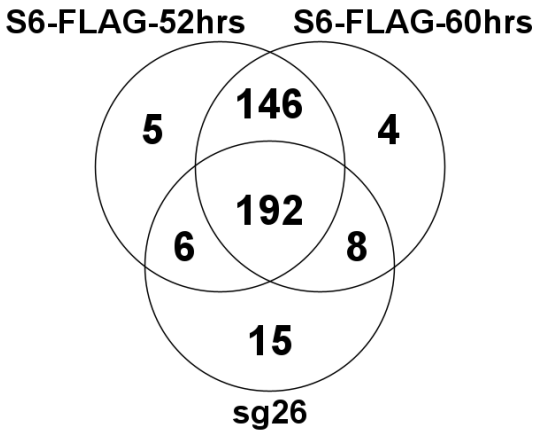

Figure 3.25 Venn diagram of the mass-spectrometry results. Sg26 represents the control (wildtype without the S6 FLAG) for this experiment. S6-FLAG-52hrs represents the 52-hour time-point (highly phosphorylated), and the S6-FLAG-60hrs represents the 60-hour time-point (dephosphorylated S6).

Table 3.5 Mass-Spectrometry Results. The protein partners which are found only for the 52-hour time-point or the 60-hour time-point. The highlighted proteins were found in both trials.

S6-FLAG-52hrs			
Gene Name	**ID**	**Molecular weight (kDa)**	**Total Spectrum Count Trial1/Trial2**
Casein Kinase II	Q8TG12	37	2/1
Uncharacterized Protein	A0A0B0EA19	10	2/0
Uncharacterized Protein	A0A0B0DNQ5	31	2/0
Glycosyltransferase	NCU01595	51	0/2
Uncharacterized Protein	Q6MUY5	36	2/0
S6-FLAG-60hrs			
Uncharacterized Protein	Q6MV08	69	2/3

Pre-mRNA processing splicing factor 8	NCU07832	275	0/2
Fe Superoxide dismutase	NCU07386	34	0/2
Cytochrome c oxidase subunit 2	A0A1W5YJY7	29	0/2

Table 3.6 Mass-Spectrometry results. The 5 top (higher counts) protein partners of both 52-hour and 60-hour time-points.

Gene Name	**ID**	**Molecular Weight (kDa)**	**Total Spectrum Count Trial1/Trail2**
Putative ribosomal protein S28	A0A0B0E2G8	16	67/128
Probable translation initiation factor eIF-2 beta chain	Q8NJ00	34	41/46
Eukaryotic translation initiation factor 2 beta subunit	NCU04640	32	39/43
Guanine nucleotide-binding protein subunit beta-like protein	Q01369	35	25/38
MurR/RpiR family transcriptional regulator	NCU06943	58	43/27

Chapter 4: Discussion

4.1 Conclusion and Discussion

In the filamentous fungus, *Neurospora crassa*, the main oscillator of the 24-hour circadian rhythms has been described as the Transcription/Translation feedback loop (TTFL) for many years. However, conditions where the circadian rhythms are still generated while the TTFL is not entirely functional, challenged this consensus, and drew scientists to the conclusion that another or many other oscillators should be involved in generating circadian rhythmicity in addition to the well-known TTFL. One potential candidate for this role is the TOR (target of rapamycin) pathway.

TOR (mTOR) pathway is a conserved translational control kinase which is highly regulated in the cell and has a close connection with the core clock genes. Protein synthesis and mRNA translation is the most energy demanding process in gene expression, and one of the networks in the cells which controls this process is the TOR pathway. mTOR in mammals is regulated in many ways in the cell, one of which is the BMAL1/CLOCK complex of core clock proteins (Guerrero-Morín & Santillán, 2020). On the other hand, mTOR activity has an effect on the clock at the cellular and tissue level. When mTOR is constantly active, it increases the amplitude and decreases the period of the rhythms, and when it is inhibited, it results in an increase in period and decrease in amplitude (Ramanathan et al., 2018). There is also a direct connection between the mTORC1 and BMAL1 protein. mTORC1 regulates the proteostasis of this clock protein by affecting its translation, degradation, and localization. When mTORC1 is constitutively active BMAL1 concentration is increased and when

rapamycin is used and the mTORC1 activity is blocked, BMAL1 expression in decreased (Lipton et al., 2017). A recent study showed that dysregulation of the clock gene *bmal1* in a part of the brain leads to overactivation of mTORC1 and may result in autism spectrum disorder-like symptoms in adult mice (Singla et al., 2022).

All this evidence shows the mutual effect and connection that the TTFL and the TOR pathway have. The main purpose of this project was to investigate the activity of the TOR pathway, using the ribosomal protein S6 as an assay, in the clock and TOR component mutant backgrounds.

Previously our lab demonstrated that the presence of functional VTA and GTR2 proteins (two components of the TOR pathway) is essential for the normal rhythmicity of the FRQ protein (Eskandari et al., 2021; Ratnayake et al., 2018). In Δ*gtr2* background, the expression levels of FRQ protein were lower and dampen over time (Eskandari et al., 2021).

The results from the time-course experiments using S6-FLAG Tag and PhosTag show a clear rhythm in S6 phosphorylation in the wildtype strain. This rhythmic S6 phosphorylation represents rhythmic TORC1 activity as has been observed in other eukaryotes like *Drosophila* (Allen et al., 2016) and mammals (Cao, 2018). S6 phosphorylation in the Δ*vta* and Δ*gtr2* backgrounds also shows rhythmicity with a different period from the wildtype and the rhythms dampen over time, especially in the Δ*gtr2* strain. In the race tube experiments, the same pattern is detectable. The rhythms of conidiation in Δ*gtr2* and Δ*vta* backgrounds are stronger in the beginning but they dampen over time. In the frq^7 background the rhythms in S6 phosphorylation show a long period and the same pattern

happens in conidiation of this strain. *frq*^{10} is totally arrhythmic on the race tubes, but a weak rhythmicity is detected for the S6 phosphorylation in this strain, although separate trials show different timings of the peaks and troughs in S6 phosphorylation. In the *prd-1* strain, S6 protein shows rhythmicity with a high amplitude. This strain has a slow growth rate and show clear banding on the race tubes.

To conclude from the time-course experiments, the rhythmicity in RPS6 phosphorylation and TOR activity with a period close to 24 hours in wildtype is detected. Also, in *Δvta*, *Δgtr2*, *prd-1*, and *frq*^{7} strains, rhythmicity in S6 phosphorylation with different periods from the wildtype is observed. Rhythmic S6 phosphorylation in these aforementioned strains is further confirmed by the cosinor test which was performed in R. However, for the *frq*^{10} (*frq* knockout background) strain, the results from the ANOVA test performed on the time-course data do not correlate with the cosinor results. The cosinor test showed the data as rhythmic for *frq*^{10}, but the p-value of the ANOVA was not significant. To further investigate the TOR activity in *frq*^{10} background more research should be conducted.

To compare the S6 phosphorylation rhythms with the conidiation rhythms (which are directly under the control of the clock (Sargent et al., 1966)), and to explore their correlation, the S6 rhythms and conidiation rhythms were plotted on the same graph covering 20 to 80 hours of growth in dark (Figure 3.18 – 3.23). Interestingly, the peaks in the S6 rhythms in the wildtype were a few hours before the peaks in the conidiation. This can be compared to the paper by Gooch et al. (2004) which investigated the circadian rhythms of conidiation and growth rate by time-lapse analysis in *Neurospora crassa*. When *N. crassa* is grown on an agar medium in a race tube in constant darkness, it makes thick bands which are the aerial

hyphae with conidiospores (spores) and interbands which are the thin mycelia with only a few spores. Watching a time-lapse video, as the growth front is going forward on the media, it grows past the region which will later become a conidial band and the conidia form in unison over a large area of the developing band. Gooch et al. (2004) also found that the growth rate in *N. crassa* is rhythmic, not linear. It is shown in figure 4.1 that the growth rate reaches its peak a few hours before the conidiation peak and slows down when the conidiation is at its highest level. Comparing this figure to figure 3.4 from the results section, if the TOR activity represents the growth rate (high TOR activity is associated with high growth rate (Saxton & Sabatini, 2017)) the same pattern is detectable from the two figures. TOR activity reaches its peak a few hours before the peak of density which shows as the thick bands of conidiation. Therefore, my results correlate with the findings in this paper (Gooch et al., 2004). Also, for the rest of the strains (*Δvta*, *Δgtr2*, *prd-1*, and frq^7) the peaks in S6 phosphorylation happen before the density peaks but the time difference between these two peaks is shorter (except frq^7) in comparison to the wildtype. Interestingly in the *Δvta* and *Δgtr2* strains, both the S6 phosphorylation rhythms and conidiation rhythms dampen out after growing for some time in constant darkness. This shows that, specifically in *Δvta* and *Δgtr2* strains, the same effect that these mutations have on the S6 phosphorylation and TOR activity, they have on the conidiation rhythms and the clock as well.

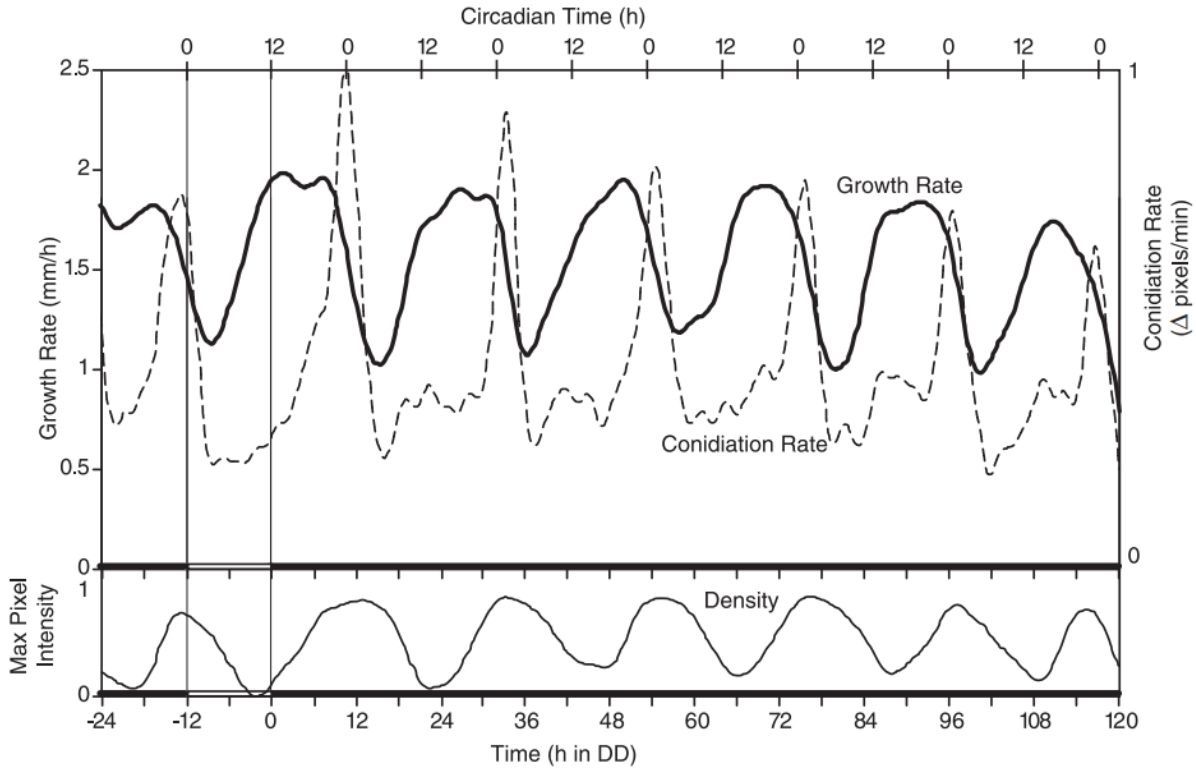

Figure 4.1 Growth rate, conidiation rate, and density in *Neurospora crassa*. The solid thick line shows the growth rate, the solid thin line shows the density, and the dotted line shows conidiation rhythms. Growth rate in *N. crassa* is rhythmic and the peaks of growth happen a few hours before the peaks in conidiation. Rhythms in growth rate and conidiation are measured by analyzing time-lapse videos. Adapted from (Gooch et al., 2004).

The comparison between the conidiation periods from table 3.5 and the S6 phosphorylation periods from table 3.4 shows a general correlation between these two sets of data. The periods of conidiation and S6 phosphorylation in the WT are very close to *N. crassa'*s circadian period (22 hours). These periods in Δ*vta* and Δ*gtr2* are a bit longer (~25 hours), and in frq^7 which is a long-period strain, both the conidiation and S6 phosphorylation periods are long and about 33 hours. The only strain in which the difference between these

two periods is more significant is the *prd-1* strain. The difference between the Tables 3.4 and 3.5 might be due to the fact that peaks are not accurate because the samples are 4 hours apart.

Using PhosTag as a phosphate-binding molecule gives us the ability to separate and detect the different phosphorylated forms of the S6 protein and it makes the quantification of the Western blots very effective. PhosTag has been used in other work as a powerful tool for studying protein phosphorylation (Kinoshita-Kikuta et al., 2021; Minh et al., 2021). The advantage of using PhosTag in SDS-PAGE electrophoresis is that by separating 3 different forms of phosphorylated S6, we can quantify and normalize the values without needing to compare the samples to a housekeeping gene or to stain the total protein on the membrane.

The immunoprecipitation and mass-spectrometry results did not show a difference in the presence and absence of the protein partners of S6 when it is hyperphosphorylated or unphosphorylated. Also, the PRD-1 protein was not found as a protein partner of the S6 protein.

All in all, the most important conclusions from the data are (1) RPS6 phosphorylation (TOR activity) in wildtype is rhythmic with a circadian period, and in Δ*vta*, Δ*gtr2*, *prd-1*, and frq^7 this rhythmicity happens with a different period than the wildtype, (2) the peaks in RPS6 phosphorylation happen a few hours before the peaks in density (conidiation) in WT, Δ*vta*, Δ*gtr2*, *prd-1*, and frq^7 with different timings, (3) the S6 phosphorylation periods and conidiation periods are very close in duration for WT, Δ*vta*, Δ*gtr2*, and frq^7 and these two rhythms follow the same pattern in each of these strains, (4) PRD-1 protein is not S6 protein's partner when S6 is either hyperphosphorylated or unphosphorylated.

To test my thesis hypothesis that the TOR pathway is a FRQ-less oscillator, further research should be conducted, although the results show that the TOR activity in *N. crassa* is rhythmic with a circadian period and mutations in the components of the TOR pathway (Δ*vta* and Δ*gtr2*) alter the normal conidiation and period the same way they change the RPS6 phosphorylation in *N. crassa*.

4.2 Future Experiments

The first question that arises after finding that the S6 phosphorylation is rhythmic is: Does the activation or inhibition of the TOR pathway have any effects on the period and phase of the clock (conidiation)? To answer this question experiments can be designed using activators of the TOR pathway like arginine and glucose or the inhibitors like Torin 1/2 or Rapamycin to observe the effects of TOR activation or inhibition on the clock. Appropriate concentrations of arginine or glucose can be used in liquid media to give a short pulse of TOR activation to *N. crassa* and then the fungus can be grown on the race tubes next to the controls to see if any phase shift happens after the treatment. The same experiment can be done using TOR inhibitors like Rapamycin and Torin1/2 to investigate the effects of the TOR inhibition on the conidiation in *N. crassa*. Rapamycin or Torin 1/2 can also be added to the solid agar media of the race tubes to observe the effect of these inhibitors on the period of the conidiation. If any effect is seen on the conidiation after using the activators or inhibitors of the TOR pathway, it further supports my hypothesis that TOR is a potential FRQ-less oscillator.

To further investigate the immunoprecipitation and mass spectrometry results, a quantitative analysis can be done. The analysis that I presented here was based on the

presence and absence of the protein partners. The present proteins in both replicates can be analysed further based on their quantitative levels in different samples. This experiment will show whether there is a difference in the quantitative levels of S6 proteins partners when it is hyperphosphorylated and when it is unphosphorylated.

Identifying S6 phosphorylation rhythm in *frq*^{10} background is important since it would be a new FRQ-less rhythm. One experiment to do with *frq*^{10} is to look at S6 phosphorylation under conditions that promote FRQ-less rhythms. Temperature pulses have already revealed an oscillation in *frq*^{10} background (Lakin-Thomas, 2006a). S6 phosphorylation rhythm in *frq*^{10} background and under the conditions which promote the FRQ-less rhythms can be investigated to observe whether it is rhythmic or not. Our lab also showed that the Δ*vta* and Δ*gtr2* mutants in *frq*^{10} destroyed the FRQ-less oscillator (Eskandari et al., 2021; Ratnayake et al., 2018). Double mutants of *frq*^{10}; *vta*^{ko} or *frq*^{10};*gtr2*^{ko} can be constructed with S6-FLAG to observe the effects of these two mutations on S6 phosphorylation under the conditions which promote the FRQ-less rhythms. If TOR is the oscillator driving these FRQ-less rhythms, double mutation of *frq*^{10} and Δ*vta* or Δ*gtr2* will eliminate S6 phosphorylation rhythms.

References

Adhvaryu, K., Firoozi, G., Motavaze, K., & Lakin-Thomas, P. (2016). PRD-1, a Component of the Circadian System of Neurospora crassa, Is a Member of the DEAD-box RNA Helicase Family. *Journal of Biological Rhythms*, *31*(3), 258–271. https://doi.org/10.1177/0748730416639717

Adler, P., Mayne, J., Walker, K., Ning, Z., & Figeys, D. (2019). Therapeutic Targeting of Casein Kinase 1Î/ϵ in an Alzheimer's Disease Mouse Model. *Journal of Proteome Research*, *18*(9), 3383–3393. https://doi.org/10.1021/acs.jproteome.9b00312

Allen, V. W., O'Connor, R. M., Ulgherait, M., Zhou, C. G., Stone, E. F., Hill, V. M., Murphy, K. R., Canman, J. C., Ja, W. W., & Shirasu-Hiza, M. M. (2016). Period-Regulated Feeding Behavior and TOR Signaling Modulate Survival of Infection. *Current Biology*, *26*(2), 184–194. https://doi.org/10.1016/j.cub.2015.11.051

Bae, K., Jin, X., Maywood, E. S., Hastings, M. H., Reppert, S. M., & Weaver, D. R. (2001). Differential functions of mPer1, mPer2, and mPer3 in the SCN circadian clock. *Neuron*, *30*(2), 525–536. https://doi.org/10.1016/s0896-6273(01)00302-6

Baker, C. L., Loros, J. J., & Dunlap, J. C. (2012). The circadian clock of Neurospora crassa. *FEMS Microbiology Reviews* (Vol. 36, Issue 1, pp. 95–110). https://doi.org/10.1111/j.1574-6976.2011.00288.x

Barbet, N. C., Schneider, U., Helliwell, S. B., Stansfield, I., Tuite, M. F., & Hall, M. N. (1996). TOR Controls Translation Initiation and Early GI Progression in Yeast FK506 in complex with its intracellular receptor. *Molecular Biology of the Cell* (Vol. 7). Liu.

Belden, W. J., Larrondo, L. F., Froehlich, A. C., Shi, M., Chen, C. H., Loros, J. J., & Dunlap, J. C. (2007). The band mutation in Neurospora crassa is a dominant allele of ras-1 implicating RAS signaling in circadian output. *Genes and Development*, *21*(12), 1494–1505. https://doi.org/10.1101/gad.1551707

Bhadra, U., Thakkar, N., Das, P., & Pal Bhadra, M. (2017). Evolution of circadian rhythms: from bacteria to human. *Sleep Medicine* (Vol. 35, pp. 49–61). Elsevier B.V. https://doi.org/10.1016/j.sleep.2017.04.008

Brown, T. M. (2016). Using light to tell the time of day: Sensory coding in the mammalian circadian visual network. *Journal of Experimental Biology* (Vol. 219, Issue 12, pp. 1779–1792). Company of Biologists Ltd. https://doi.org/10.1242/jeb.132167

Cao, R. (2018). mTOR signaling, translational control, and the circadian clock. *Frontiers in Genetics* (Vol. 9, Issue SEP). Frontiers Media S.A. https://doi.org/10.3389/fgene.2018.00367

Cascant-Lopez, E., Crosthwaite, S. K., Johnson, L. J., & Harrison, R. J. (2020). No Evidence That Homologs of Key Circadian Clock Genes Direct Circadian Programs of Development or mRNA

Abundance in Verticillium dahliae. *Frontiers in Microbiology*, *11*. https://doi.org/10.3389/fmicb.2020.01977

Cervela-Cardona, L., Alary, B., & Mas, P. (2021). The Arabidopsis Circadian Clock and Metabolic Energy: A Question of Time. *Frontiers in Plant Science* (Vol. 12). Frontiers Media S.A. https://doi.org/10.3389/fpls.2021.804468

Christensen, M. K., Falkeid, G., Loros, J. J., Dunlap, J. C., Lillo, C., & Ruoff, P. (2004). A nitrate-induced frq-less oscillator in Neurospora crassa. *Journal of Biological Rhythms*, *19*(4), 280–286. https://doi.org/10.1177/0748730404265532

Cohen, S. E., & Golden, S. S. (2015). Circadian Rhythms in Cyanobacteria. *Microbiology and Molecular Biology Reviews*, *79*(4), 373–385. https://doi.org/10.1128/mmbr.00036-15

Colot, H. V, Park, G., Turner, G. E., Ringelberg, C., Crew, C. M., Litvinkova, L., Weiss, R. L., Borkovich, K. A., & Dunlap, J. C. (2006). A high-throughput gene knockout procedure for Neurospora reveals functions for multiple transcription factors. *Proceedings of the National Academy of Sciences of the United States of America* (Vol. 103, Issue 5). www.pnas.orgcgidoi10.1073pnas.0601456103

Cumming, B. G., & Wagner, E. (1968). Rhythmic Processes in Plants,:l, In *Annu. Rev. Plant. Physiol* (Vol. 19). www.annualreviews.org

Davis, R. H. (2004). *The mycota : a comprehensive treatise on fungi as experimental systems for basic and applied research*. Springer.

Diegmann, J., Stck, A., Madeti, C., & Roenneberg, T. (2010). Entrainment elicits period aftereffects in neurospora crassa. *Chronobiology International*, *27*(7), 1335–1347. https://doi.org/10.3109/07420528.2010.504316

Diernfellner, A. C. R., Lauinger, L., Shostak, A., & Brunner, M. (2019). A pathway linking translation stress to checkpoint kinase 2 signaling in Neurospora crassa. *Proceedings of the National Academy of Sciences of the United States of America*, *116*(35), 17271–17279. https://doi.org/10.1073/pnas.1815396116

Ditty, J. L., Williams, S. B., & Golden, S. S. (2003). A Cyanobacterial Circadian Timing Mechanism. *Annual Review of Genetics* (Vol. 37, pp. 513–543). https://doi.org/10.1146/annurev.genet.37.110801.142716

Dubouloz, F., Deloche, O., Wanke, V., Cameroni, E., & de Virgilio, C. (2005). The TOR and EGO protein complexes orchestrate microautophagy in yeast. *Molecular Cell*, *19*(1), 15–26. https://doi.org/10.1016/j.molcel.2005.05.020

Dunlap, J. C. (1999). Molecular Bases for Circadian Clocks. *Cell* (Vol. 96).

Dunlap, J. C., & Loros, J. J. (2006). How fungi keep time: circadian system in Neurospora and other fungi. *Current Opinion in Microbiology* (Vol. 9, Issue 6, pp. 579–587). https://doi.org/10.1016/j.mib.2006.10.008

Eelderink-Chen, Z., Bosman, J., Sartor, F., Dodd, A. N., Kovács, Á. T., & Merrow, M. (2021). A circadian clock in a nonphotosynthetic prokaryote. Sci Adv. 2021 Jan 8;7(2):eabe2086. doi: 10.1126/sciadv.abe2086. PMID: 33523996; PMCID: PMC7793578.

Eskandari, R., Ratnayake, L., & Lakin-Thomas, P. L. (2021). Shared Components of the FRQ-Less Oscillator and TOR Pathway Maintain Rhythmicity in Neurospora. *Journal of Biological Rhythms*, *36*(4), 329–345. https://doi.org/10.1177/0748730421999948

Evans, J. A., & Gorman, M. R. (2016). In synch but not in step: Circadian clock circuits regulating plasticity in daily rhythms. *Neuroscience* (Vol. 320, pp. 259–280). Elsevier Ltd. https://doi.org/10.1016/j.neuroscience.2016.01.072

Fatima, N., Sonkar, G. K., & Singh, S. (2022). Circadian mechanism disruption is associated with dysregulation of inflammatory and immune responses: a systematic review. *Beni-Suef University Journal of Basic and Applied Sciences* (Vol. 11, Issue 1). Springer Science and Business Media Deutschland GmbH. https://doi.org/10.1186/s43088-022-00290-4

Fischer, M. S., & Glass, N. L. (2019). Communicate and fuse: How filamentous fungi establish and maintain an interconnected mycelial network. *Frontiers in Microbiology* (Vol. 10, Issue MAR). Frontiers Media S.A. https://doi.org/10.3389/fmicb.2019.00619

Fumagalli, S., & Pende, M. (2022). S6 kinase 1 at the central node of cell size and ageing. *Frontiers in Cell and Developmental Biology* (Vol. 10). Frontiers Media S.A. https://doi.org/10.3389/fcell.2022.949196

González, A., & Hall, M. N. (2017). Nutrient sensing and TOR signaling in yeast and mammals . *The EMBO Journal*, *36*(4), 397–408. https://doi.org/10.15252/embj.201696010

Gooch, V. D., Freeman, L., & Lakin-Thomas, P. L. (2004). Time-lapse analysis of the circadian rhythms of conidiation and growth rate in Neurospora. *Journal of Biological Rhythms*, *19*(6), 493–503. https://doi.org/10.1177/0748730404270391

Granshaw, T., Tsukamoto, M., & Brody, S. (2003). Circadian rhythms in Neurospora crassa: Farnesol or geraniol allow expression of rhythmicity in the otherwise arrhythmic strains frq10, wc-1, and wc-2. *Journal of Biological Rhythms*, *18*(4), 287–296. https://doi.org/10.1177/0748730403255934

Guerrero-Morín, J. G., & Santillán, M. (2020). Crosstalk dynamics between the circadian clock and the mTORC1 pathway. *Journal of Theoretical Biology*, *501*. https://doi.org/10.1016/j.jtbi.2020.110360

Hardin, P. E. (2004). Transcription regulation within the circadian clock: The E-box and beyond. In *Journal of Biological Rhythms* (Vol. 19, Issue 5, pp. 348–360). https://doi.org/10.1177/0748730404268052

Harmer, S. L., Panda, S., & Kay, S. A. (2001). Molecular bases of circadian rhythms. *Annual Review of Cell and Developmental Biology*, *17*, 215–253. https://doi.org/10.1146/annurev.cellbio.17.1.215

Honda, S., & Selker, E. U. (2009). Tools for fungal proteomics: Multifunctional neurospora vectors for gene replacement, protein expression and protein purification. *Genetics*, *182*(1), 11–23. https://doi.org/10.1534/genetics.108.098707

Hower, I. M., Harper, S. A., & Buford, T. W. (2018). Circadian rhythms, exercise, and cardiovascular health. *Journal of Circadian Rhythms* (Vol. 16). Ubiquity Press Ltd. https://doi.org/10.5334/jcr.164

Hsu, P. Y., & Harmer, S. L. (2014). Wheels within wheels: The plant circadian system. *Trends in Plant Science* (Vol. 19, Issue 4, pp. 240–249). Elsevier Ltd. https://doi.org/10.1016/j.tplants.2013.11.007

Hunt, S., Elvin, M., & Heintzen, C. (2012). Temperature-sensitive and circadian oscillators of Neurospora crassa share components. *Genetics*, *191*(1), 119–131. https://doi.org/10.1534/genetics.111.137976

Jiao, L., Liu, Y., Yu, X. Y., Pan, X., Zhang, Y., Tu, J., Song, Y. H., & Li, Y. (2023). Ribosome biogenesis in disease: new players and therapeutic targets. *Signal Transduction and Targeted Therapy* (Vol. 8, Issue 1). Springer Nature. https://doi.org/10.1038/s41392-022-01285-4

Kato, T. (2023). Role of mTOR1 signaling in the antidepressant effects of ketamine and the potential of mTORC1 activators as novel antidepressants. *Neuropharmacology*, *223*, 109325. https://doi.org/10.1016/j.neuropharm.2022.109325

Kim, E. Y., Bae, K., Ng, F. S., Glossop, N. R. J., Hardin, P. E., & Edery, I. (2002). Drosophila CLOCK protein is under posttranscriptional control and influences light-induced activity. *Neuron*, *34*(1), 69–81.

Kim, P., Kaur, M., Jang, H. I., & Kim, Y. I. (2020). The circadian clock—a molecular tool for survival in cyanobacteria. *Life* (Vol. 10, Issue 12, pp. 1–14). MDPI AG. https://doi.org/10.3390/life10120365

Kim, S. G., Buel, G. R., & Blenis, J. (2013). Nutrient regulation of the mTOR complex 1 signaling pathway. *Molecules and cells* (Vol. 35, Issue 6, pp. 463–473). https://doi.org/10.1007/s10059-013-0138-2

Kinoshita-Kikuta, E., Kinoshita, E., Suga, M., Higashida, M., Yamane, Y., Nakamura, T., & Koike, T. (2021). Characterization of phosphorylation status and kinase activity of src family kinases expressed in cell-based and cell-free protein expression systems. *Biomolecules*, *11*(10). https://doi.org/10.3390/biom11101448

Kippert, F. (2001). Cellular signalling and the complexity of biological timing: Insights from the ultradian clock of Schizosaccharomyces pombe. *Philosophical Transactions of the Royal*

Society B: Biological Sciences, *356*(1415), 1725–1733. https://doi.org/10.1098/rstb.2001.0935

Kuranda, K., Leberre, V., Sokol, S., Palamarczyk, G., & François, J. (2006). Investigating the caffeine effects in the yeast Saccharomyces cerevisiae brings new insights into the connection between TOR, PKC and Ras/cAMP signalling pathways. *Molecular Microbiology*, *61*(5), 1147–1166. https://doi.org/10.1111/j.1365-2958.2006.05300.x

Lakin-Thomas, P. L. (2019). Circadian rhythms, metabolic oscillators, and the target of rapamycin (TOR) pathway: the Neurospora connection. *Current Genetics* (Vol. 65, Issue 2, pp. 339–349). Springer Verlag. https://doi.org/10.1007/s00294-018-0897-6

Lakin-Thomas, P. L. (1996). Effects of choline depletion on the circadian rhythm in Neurospora crassa. *Biological Rhythm Research*, *27*(1), 12–30. https://doi.org/10.1076/brhm.27.1.12.12933

Lakin-Thomas P. L. (1998). Choline depletion, frq mutations, and temperature compensation of the circadian rhythm in Neurospora crassa. *Journal of biological rhythms*, *13*(4), 268–277. https://doi.org/10.1177/074873098129000101

Lakin-Thomas P. L. (2006). Circadian clock genes frequency and white collar-1 are not essential for entrainment to temperature cycles in Neurospora crassa. *Proceedings of the National Academy of Sciences of the United States of America*, *103*(12), 4469–4474. https://doi.org/10.1073/pnas.0510404103

Lakin-Thomas, P. L. (2006b). Transcriptional feedback oscillators: Maybe, maybe not... *Journal of Biological Rhythms* (Vol. 21, Issue 2, pp. 83–92). https://doi.org/10.1177/0748730405286102

Lakin-Thomas, P. L., Bell-Pedersen, D., & Brody, S. (2011). The genetics of circadian rhythms in Neurospora. *Advances in Genetics* (Vol. 74, pp. 55–103). Academic Press Inc. https://doi.org/10.1016/B978-0-12-387690-4.00003-9

Lakin-Thomas, P. L., & Brody, S. (2000). Circadian rhythms in Neurospora crassa: lipid deficiencies restore robust rhythmicity to null frequency and white-collar mutants. *Proceedings of the National Academy of Sciences of the United States of America*, *97*(1), 256–261. https://doi.org/10.1073/pnas.97.1.256

Lakin-Thomas, P. L., & Brody, S. (2004). Circadian rhythms in microorganisms: New complexities. *Annual Review of Microbiology* (Vol. 58, pp. 489–519). https://doi.org/10.1146/annurev.micro.58.030603.123744

Li, S., & Lakin-Thomas, P. (2010). Effects of prd circadian clock mutations on FRQ-less rhythms in Neurospora. *Journal of biological rhythms*, *25*(2), 71-80.

Li, S., Motavaze, K., Kafes, E., Suntharalingam, S., & Lakin-Thomas, P. (2011). A new mutation affecting frq-less rhythms in the circadian system of neurospora crassa. *PLoS Genetics*, *7*(6). https://doi.org/10.1371/journal.pgen.1002151

Li, W., Wang, Z., Cao, J., Dong, Y., & Chen, Y. (2023). Perfecting the Life Clock: The Journey from PTO to TTFL. *International Journal of Molecular Sciences*, *24*(3), 2402. https://doi.org/10.3390/ijms24032402

Lipton, J. O., Boyle, L. M., Yuan, E. D., Hochstrasser, K. J., Chifamba, F. F., Nathan, A., Tsai, P. T., Davis, F., & Sahin, M. (2017). Aberrant Proteostasis of BMAL1 Underlies Circadian Abnormalities in a Paradigmatic mTOR-opathy. *Cell Reports*, *20*(4), 868–880. https://doi.org/10.1016/j.celrep.2017.07.008

Loewith, R., & Hall, M. N. (2011). Target of rapamycin (TOR) in nutrient signaling and growth control. *Genetics* (Vol. 189, Issue 4, pp. 1177–1201). https://doi.org/10.1534/genetics.111.133363

Loros, J. J. (2020). Principles of the animal molecular clock learned from Neurospora. *European Journal of Neuroscience* (Vol. 51, Issue 1, pp. 19–33). Blackwell Publishing Ltd. https://doi.org/10.1111/ejn.14354

Minh, T. N., Lu, H., Zhang, P., Li, W., Zhong, S., Ding, X., Xiao, J., & Li, Q. (2021). Phosphorylation of Novel Interactors of Wild Soybean GsSnRK1 Protein Kinase. *Plant Molecular Biology Reporter*, *39*(4), 792–800. https://doi.org/10.1007/s11105-021-01288-5

Mohawk, J. A., Green, C. B., & Takahashi, J. S. (2012). Central and peripheral circadian clocks in mammals. *Annual Review of Neuroscience* (Vol. 35, pp. 445–462). https://doi.org/10.1146/annurev-neuro-060909-153128

Morris, C. J., Purvis, T. E., Hu, K., & Scheer, F. A. J. L. (2016). Circadian misalignment increases cardiovascular disease risk factors in humans. *Proceedings of the National Academy of Sciences of the United States of America*, *113*(10), E1402–E1411. https://doi.org/10.1073/pnas.1516953113

Nakajima, M., Imai, K., Ito, H., Nishiwaki, T., Murayama, Y., Iwasaki, H., Oyama, T., & Kondo, T. (2005). Reconstitution of circadian oscillation of cyanobacterial KaiC phosphorylation in vitro. *Science*, *308*(5720), 414–415. https://doi.org/10.1126/science.1108451

Nakamichi, N., Yamaguchi, J., Sato, A., Fujimoto, K. J., & Ota, E. (2022). Chemical biology to dissect molecular mechanisms underlying plant circadian clocks. In *New Phytologist* (Vol. 235, Issue 4, pp. 1336–1343). John Wiley and Sons Inc. https://doi.org/10.1111/nph.18298

Oakenfull, R. J., & Davis, S. J. (2017). Shining a light on the Arabidopsis circadian clock. *Plant, cell & environment* (Vol. 40, Issue 11, pp. 2571–2585). https://doi.org/10.1111/pce.13033

Okazaki, H., Matsunaga, N., Fujioka, T., Okazaki, F., Akagawa, Y., Tsurudome, Y., Ono, M., Kuwano, M., Koyanagi, S., & Ohdo, S. (2014). Circadian regulation of mTOR by the ubiquitin pathway in renal cell carcinoma. *Cancer Research*, *74*(2), 543–551. https://doi.org/10.1158/0008-5472.CAN-12-3241

Ono, D. (2022). Neural circuits in the central circadian clock and their regulation of sleep and wakefulness in mammals. *Neuroscience Research* (Vol. 182, pp. 1–6). Elsevier Ireland Ltd. https://doi.org/10.1016/j.neures.2022.05.005

Oster, H., Baeriswyl, S., van der Horst, G. T. J., & Albrecht, U. (2003). Loss of circadian rhythmicity in aging mPer1-/- mCry2-/- mutant mice. *Genes and Development*, *17*(11), 1366–1379. https://doi.org/10.1101/gad.256103

Oster, H., Yasui, A., van der Horst, G. T. J., & Albrecht, U. (2002). Disruption of mCry2 restores circadian rhythmicity in mPer2 mutant mice. *Genes and Development*, *16*(20), 2633–2638. https://doi.org/10.1101/gad.233702

Park, G., Servin, J. A., Turner, G. E., Altamirano, L., Colot, H. v., Collopy, P., Litvinkova, L., Li, L., Jones, C. A., Diala, F. G., Dunlap, J. C., & Borkovich, K. A. (2011). Global analysis of serine-threonine protein kinase genes in neurospora crassa. *Eukaryotic Cell*, *10*(11), 1553–1564. https://doi.org/10.1128/EC.05140-11

Partch, C. L., Green, C. B., & Takahashi, J. S. (2014). Molecular architecture of the mammalian circadian clock. *Trends in Cell Biology* (Vol. 24, Issue 2, pp. 90–99). https://doi.org/10.1016/j.tcb.2013.07.002

Patke, A., Young, M. W., & Axelrod, S. (2020). Molecular mechanisms and physiological importance of circadian rhythms. *Nature Reviews Molecular Cell Biology* (Vol. 21, Issue 2, pp. 67–84). Nature Research. https://doi.org/10.1038/s41580-019-0179-2

Paul, S., Hanna, L., Harding, C., Hayter, E. A., Walmsley, L., Bechtold, D. A., & Brown, T. M. (2020). Output from VIP cells of the mammalian central clock regulates daily physiological rhythms. *Nature Communications*, *11*(1). https://doi.org/10.1038/s41467-020-15277-x

Pittendrigh, C. S., & Miller, H. A. (1993). Temporal Organization: Reflections of a Darwinian Clock-Watcher. *Annu. Rev. Physiol* (Vol. 55)

Ramanathan, C., Kathale, N. D., Liu, D., Lee, C., Freeman, D. A., Hogenesch, J. B., Cao, R., & Liu, A. C. (2018). mTOR signaling regulates central and peripheral circadian clock function. *PLoS Genetics*, *14*(5). https://doi.org/10.1371/journal.pgen.1007369

Ramsdale, M., & Lakin-Thomas, P. L. (2000). sn-1,2-diacylglycerol levels in the fungus Neurospora crassa display circadian rhythmicity. *Journal of Biological Chemistry*, *275*(36), 27541–27550. https://doi.org/10.1074/jbc.M002911200

Ratnayake, L., Adhvaryu, K. K., Kafes, E., Motavaze, K., & Lakin-Thomas, P. (2018). A component of the TOR (Target Of Rapamycin) nutrient-sensing pathway plays a role in circadian rhythmicity in Neurospora crassa. *PLoS Genetics*, *14*(6). https://doi.org/10.1371/journal.pgen.1007457

Roenneberg, T., & Merrow, M. (2016). The circadian clock and human health. *Current Biology* (Vol. 26, Issue 10, pp. R432–R443). Cell Press. https://doi.org/10.1016/j.cub.2016.04.011

Roux, P. P., & Topisirovic, I. (2012). Regulation of mRNA translation by signaling pathways. *Cold Spring Harbor Perspectives in Biology*, *4*(11). https://doi.org/10.1101/cshperspect.a012252

Ruvinsky, I., & Meyuhas, O. (2006). Ribosomal protein S6 phosphorylation: from protein synthesis to cell size. *Trends in Biochemical Sciences* (Vol. 31, Issue 6, pp. 342–348). https://doi.org/10.1016/j.tibs.2006.04.003

Sargent, M. L., Briggs, W. R., & Woodward, D. 0. (1966). Circadian Nature of a Rhythm Expressed by an Invertaseless Strain of Neurospora crassa'. *Plant Physiol* (Vol. 41). https://academic.oup.com/plphys/article/41/8/1343/6090912

Saxton, R. A., & Sabatini, D. M. (2017). mTOR Signaling in Growth, Metabolism, and Disease. *Cell* (Vol. 168, Issue 6, pp. 960–976). Cell Press. https://doi.org/10.1016/j.cell.2017.02.004

Schafmeier, T., Haase, A., Káldi, K., Scholz, J., Fuchs, M., & Brunner, M. (2005). Transcriptional feedback of Neurospora circadian clock gene by phosphorylation-dependent inactivation of its transcription factor. *Cell*, *122*(2), 235–246. https://doi.org/10.1016/j.cell.2005.05.032

Schneider, K., Perrino, S., Oelhafen, K., Li, S., Zatsepin, A., Lakin-Thomas, P., & Brody, S. (2009). Rhythmic conidiation in constant light in Vivid mutants of Neurospora crassa. *Genetics* (Vol. 181, Issue 3, pp. 917–931). https://doi.org/10.1534/genetics.108.097808

Shen, L., Su, Z., Yang, K., Wu, C., Becker, T., Bell-Pedersen, D., Zhang, J., & Sachs, M. S. (2021). Structure of the translating *Neurospora* ribosome arrested by cycloheximide. *Proceedings of the National Academy of Sciences of the United States of America*, *118*(48), e2111862118. https://doi.org/10.1073/pnas.2111862118

Shertz, C. A., Bastidas, R. J., Li, W., Heitman, J., & Cardenas, M. E. (2010). Conservation, duplication, and loss of the Tor signaling pathway in the fungal kingdom. *BMC Genomics*, *11*(1). https://doi.org/10.1186/1471-2164-11-510

Shimobayashi, M., & Hall, M. N. (2014). Making new contacts: The mTOR network in metabolism and signalling crosstalk. *Nature Reviews Molecular Cell Biology*, *15*(3), 155–162. https://doi.org/10.1038/nrm3757

Singla, R., Mishra, A., & Cao, R. (2022). The trilateral interactions between mammalian target of rapamycin (mTOR) signaling, the circadian clock, and psychiatric disorders: an emerging model. *Translational psychiatry* (Vol. 12, Issue 1, p. 355). NLM (Medline). https://doi.org/10.1038/s41398-022-02120-8

Srikanta, S. B., & Cermakian, N. (2021). To Ub or not to Ub: Regulation of circadian clocks by ubiquitination and deubiquitination. *Journal of Neurochemistry* (Vol. 157, Issue 1, pp. 11–30). Blackwell Publishing Ltd. https://doi.org/10.1111/jnc.15132

Swan, J. A., Golden, S. S., LiWang, A., & Partch, C. L. (2018). Structure, function, and mechanism of the core circadian clock in cyanobacteria. *Journal of Biological Chemistry* (Vol. 293, Issue 14,

pp. 5026–5034). American Society for Biochemistry and Molecular Biology Inc. https://doi.org/10.1074/jbc.TM117.001433

Swift, J., Greenham, K., Ecker, J. R., Coruzzi, G. M., & Robertson McClung, C. (2022). The biology of time: dynamic responses of cell types to developmental, circadian and environmental cues. *Plant Journal* (Vol. 109, Issue 4, pp. 764–778). John Wiley and Sons Inc. https://doi.org/10.1111/tpj.15589

Tomita, J., Nakajima, M., Kondo, T., & Iwasaki, H. (2005). No transcription-translation feedback in circadian rhythm of KaiC phosphorylation. *Science (New York, N.Y.)*, *307*(5707), 251–254. https://doi.org/10.1126/science.1102540

Urban, J., Soulard, A., Huber, A., Lippman, S., Mukhopadhyay, D., Deloche, O., Wanke, V., Anrather, D., Ammerer, G., Riezman, H., Broach, J. R., de Virgilio, C., Hall, M. N., & Loewith, R. (2007). Sch9 Is a Major Target of TORC1 in Saccharomyces cerevisiae. *Molecular Cell*, *26*(5), 663–674. https://doi.org/10.1016/j.molcel.2007.04.020

Wallen, R. M., & Perlin, M. H. (2018). An overview of the function and maintenance of sexual reproduction in dikaryotic fungi. *Frontiers in Microbiology* (Vol. 9, Issue MAR). Frontiers Media S.A. https://doi.org/10.3389/fmicb.2018.00503

Welsh, D. K., Yoo, S. H., Liu, A. C., Takahashi, J. S., & Kay, S. A. (2004). Bioluminescence imaging of individual fibroblasts reveals persistent, independently phased circadian rhythms of clock gene expression. *Current biology : CB*, *14*(24), 2289–2295. https://doi.org/10.1016/j.cub.2004.11.057

Wollnik, F. (1989). Physiology and regulation of biological rhythms in laboratory animals: an overview. *Laboratory Animals* (Vol. 23).

Woodie, L. N., Oral, K. T., Krusen, B. M., & Lazar, M. A. (2022). The Circadian Regulation of Nutrient Metabolism in Diet-Induced Obesity and Metabolic Disease. *Nutrients* (Vol. 14, Issue 15). MDPI. https://doi.org/10.3390/nu14153136

Woolum, J. C. (1991). A re-examination of the role of the nucleus in generating the circadian rhythm in Acetabularia. *Journal of biological rhythms*, *6*(2), 129–136. https://doi.org/10.1177/074873049100600203

Yang, Z., & Sehgal, A. (2001). Role of molecular oscillations in generating behavioral rhythms in Drosophila. *Neuron*, *29*(2), 453–467. https://doi.org/10.1016/s0896-6273(01)00218-5

Yildirim, E., Curtis, R., & Hwangbo, D. S. (2022). Roles of peripheral clocks: lessons from the fly. *FEBS Letters* (Vol. 596, Issue 3, pp. 263–293). John Wiley and Sons Inc. https://doi.org/10.1002/1873-3468.14251

Appendix I:

Table 5.1 List of the *Neurospora crassa* strains used in this study. All strains carry the FLAG-tagged S6 gene.

Strain	Genotype	Lab Stock Number
Wildtype	*csp-1*; *chol-1*; *ras-1^{bd}*	667
Δ*vta*	*csp-1*; *chol-1*; *ras-1^{bd}*; *vta*	694
Δ*gtr2*	*csp-1*; *chol-1*; *ras-1^{bd}*; *gtr2*	42
prd-1	*csp-1*; *chol-1*; *ras-1^{bd}*; *prd-1*	10
frq^{7}	*csp-1*; *chol-1*; *ras-1^{bd}*; *frq^{7}*	702
frq^{10}	*csp-1*; *chol-1*; *ras-1^{bd}*; *frq^{10}*	668

Table 5.2 Sampling schedule for time-course. "Inoc" means "time of inoculation of the plate cultures" and "H" means "time of sample harvest".

Sample	**Hours in LL at 30°**	**Hours in DD at 22°**	**Total hours of growth**	**Mon 6 pm**	**Tues 10 am**	**Tues 2 pm**	**Tues 6 pm**	**Tues 10 pm**	**Wed 10 am**	**Wed 10 pm**	**Thurs 10 am**	**Fri 10 am**	**Fri 2 pm**	**Fri 6 pm**
A'- 20	24	20	44						Inoc		22°DD	H		
A - 24	24	24	48						Inoc		22°DD	H		
B - 28	24	28	52						Inoc		22°DD		H	
C - 32	24	32	56						Inoc		22°DD			H
D - 36	12	36	48						Inoc	22°DD		H		
E - 40	12	40	52						Inoc	22°DD			H	
F - 44	12	44	56						Inoc	22°DD				H
G - 48	16	48	64				Inoc		22°DD			H		
H - 52	16	52	68				Inoc		22°DD				H	

I - 56	16	56	72				Inoc		22°DD					H
J - 60	4	60	64				Inoc	22°DD				H		
K - 64	4	64	68				Inoc	22°DD					H	
L - 68	4	68	72				Inoc	22°DD						H
M - 72	4	72	76			Inoc	22°DD							H
N - 76	16	76	92	Inoc	22°DD								H	
O - 80	16	80	96	Inoc	22°DD									H

Appendix II:

Maltose-Arginine Media (MA)

Vogel's 50X	10 ml
Arginine 20 mg/ml	2.5 ml
Choline 10 mM	5 ml
Maltose	2.5 g
Bacto-Agar	10 g
Water	500 ml

%12.5 Acrylamide Gel

Water	2.02 ml
1.5M Tris PH 8.8	1.25 ml
%10 SDS	50 µl
%40 Acrylamide	1.56 ml
PhosTag	50 µl
10 mM $MnCl_2$	50 µl
%10 APS	25 µl
TEMED	2.5 µl

Appendix III:

R code used for Cosinor analysis

R Code

```
install.packages("readxl")
install.packages("circacompare")
library(tidyverse)
library(readxl)
library(circacompare)

#reading Wild-Type data (3 trials)
WT_TP <- read_excel("wt.xlsx")
str(WT_TP)

## tibble [48 × 2] (S3: tbl_df/tbl/data.frame)
##  $ time_point     : chr [1:48] "tp20" "tp20" "tp20" "tp24" ...
##  $ phosphorylation: num [1:48] 0.118 0.118 0.167 0.296 0.201 ...

# One-way ANOVA test for Wild-Type time-points for 3 trials
wt_anova <- aov(phosphorylation ~ time_point , data = WT_TP)
summary(wt_anova)

##             Df  Sum Sq  Mean Sq F value  Pr(>F)
## time_point  16 0.10190 0.006369   3.579 0.00115 **
## Residuals   31 0.05516 0.001779
## ---
## Signif. codes:  0 '***' 0.001 '**' 0.01 '*' 0.05 '.' 0.1 ' ' 1

#reading frq7 data (3 trials)
frq7_TP <- read_excel("frq7.xlsx")
str(frq7_TP)

## tibble [48 × 2] (S3: tbl_df/tbl/data.frame)
##  $ time_point     : chr [1:48] "tp20" "tp20" "tp20" "tp24" ...
##  $ phosphorylation: num [1:48] 0.232 0.269 0.209 0.231 0.221 ...

# One-way ANOVA test for frq7 time-points for 3 trials
frq7_anova <- aov(phosphorylation ~ time_point , data = frq7_TP)
summary(frq7_anova)

##             Df  Sum Sq   Mean Sq F value  Pr(>F)
## time_point  16 0.03463 0.0021646   3.589 0.00112 **
## Residuals   31 0.01870 0.0006032
## ---
## Signif. codes:  0 '***' 0.001 '**' 0.01 '*' 0.05 '.' 0.1 ' ' 1
```

```r
#reading frq10 data (3 trials)
frq10_TP <- read_excel("frq10.xlsx")
str(frq10_TP)
```

```
## tibble [48 × 2] (S3: tbl_df/tbl/data.frame)
##  $ time_point     : chr [1:48] "tp20" "tp20" "tp20" "tp24" ...
##  $ phosphorylation: num [1:48] 0.295 0.234 0.292 0.281 0.304 ...
```

```r
# One-way ANOVA test for frq10 time-points for 3 trials
frq10_anova <- aov(phosphorylation ~ time_point , data = frq10_TP)
summary(frq10_anova)
```

```
##             Df  Sum Sq  Mean Sq F value Pr(>F)
## time_point  16 0.02364 0.001478   0.881  0.595
## Residuals   31 0.05201 0.001678
```

```r
#reading vta-ko data (3 trials)
vta_TP <- read_excel("vta.xlsx")
str(vta_TP)
```

```
## tibble [48 × 2] (S3: tbl_df/tbl/data.frame)
##  $ time_point     : chr [1:48] "tp20" "tp20" "tp20" "tp24" ...
##  $ phosphorylation: num [1:48] 0.166 0.152 0.162 0.234 0.233 ...
```

```r
# One-way ANOVA test for vta-ko time-points for 3 trials
vta_anova <- aov(phosphorylation ~ time_point , data = vta_TP)
summary(vta_anova)
```

```
##             Df  Sum Sq  Mean Sq F value  Pr(>F)
## time_point  16 0.14308 0.008942   5.765 1.6e-05 ***
## Residuals   31 0.04808 0.001551
## ---
## Signif. codes:  0 '***' 0.001 '**' 0.01 '*' 0.05 '.' 0.1 ' ' 1
```

```r
#reading gtr2-ko data (3 trials)
gtr2_TP <- read_excel("gtr2.xlsx")
str(gtr2_TP)
```

```
## tibble [48 × 2] (S3: tbl_df/tbl/data.frame)
##  $ time_point     : chr [1:48] "tp20" "tp20" "tp20" "tp24" ...
##  $ phosphorylation: num [1:48] 0.15 0.162 0.175 0.203 0.167 ...
```

```r
# One-way ANOVA test for gtr2-ko time-points for 3 trials
gtr2_anova <- aov(phosphorylation ~ time_point , data = gtr2_TP)
summary(gtr2_anova)
```

```
##             Df Sum Sq  Mean Sq F value Pr(>F)
## time_point  16 0.2160 0.013497   2.523 0.0132 *
## Residuals   31 0.1658 0.005349
```

```
## ---
## Signif. codes:  0 '***' 0.001 '**' 0.01 '*' 0.05 '.' 0.1 ' ' 1

#reading prd-1 data (3 trials)
prd1_TP <- read_excel("prd1.xlsx")
str(prd1_TP)

## tibble [48 × 2] (S3: tbl_df/tbl/data.frame)
##  $ time_point     : chr [1:48] "tp20" "tp20" "tp20" "tp24" ...
##  $ phosphorylation: num [1:48] 0.22 0.217 0.462 0.245 0.269 ...

# One-way ANOVA test for prd-1 time-points for 3 trials
prd1_anova <- aov(phosphorylation ~ time_point , data = prd1_TP)
summary(prd1_anova)

##             Df Sum Sq  Mean Sq F value   Pr(>F)
## time_point  16 0.2404 0.015023   4.433 0.000191 ***
## Residuals   31 0.1051 0.003389
## ---
## Signif. codes:  0 '***' 0.001 '**' 0.01 '*' 0.05 '.' 0.1 ' ' 1

# Readeing the table of the average of 3 separate trials for all 6 strain
s
all_strain <- read_excel("strains.xlsx")
str(all_strain)

## tibble [16 × 6] (S3: tbl_df/tbl/data.frame)
##  $ WT     : num [1:16] 0.133 0.232 0.275 0.187 0.155 0.147 0.185 0.219
0.304 0.201 ...
##  $ frq7   : num [1:16] 0.237 0.222 0.246 0.244 0.276 0.234 0.196 0.186
0.186 0.208 ...
##  $ frq10  : num [1:16] 0.274 0.297 0.268 0.266 0.301 0.299 0.294 0.276
0.253 0.309 ...
##  $ vta-ko : num [1:16] 0.16 0.229 0.338 0.335 0.297 0.187 0.162 0.204
0.249 0.266 ...
##  $ gtr2-ko: num [1:16] 0.162 0.178 0.333 0.427 0.323 0.239 0.21 0.227
0.312 0.348 ...
##  $ prd1   : num [1:16] 0.3 0.332 0.384 0.402 0.47 0.428 0.368 0.24 0.2
62 0.411 ...

#preparing data for ANOVA
strains <- c(rep("WT", 16),rep("frq7", 16) , rep("frq10", 16) , rep("vta-
ko", 16) , rep("gtr2-ko", 16) , rep("prd1", 16))
phospho_mean <- c(all_strain$WT , all_strain$frq7 , all_strain$frq10 , al
l_strain$`vta-ko`, all_strain$`gtr2-ko`, all_strain$prd1)

# Box plot
strains_mean <- data.frame(strains , phospho_mean)
boxplot(phospho_mean ~ strains , data = strains_mean)
```

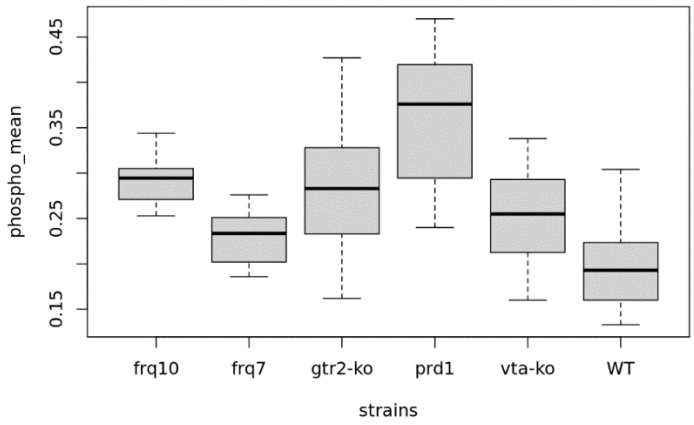


```
# One-way ANOVA test for different strains
strains_anova <- aov(phospho_mean ~ strains , data = strains_mean)
summary(strains_anova)

##              Df Sum Sq Mean Sq F value   Pr(>F)
## strains       5 0.2571 0.05143   18.28 1.76e-12 ***
## Residuals    90 0.2533 0.00281
## ---
## Signif. codes:  0 '***' 0.001 '**' 0.01 '*' 0.05 '.' 0.1 ' ' 1

# post hoc
TukeyHSD(strains_anova)

##   Tukey multiple comparisons of means
##     95% family-wise confidence level
##
## Fit: aov(formula = phospho_mean ~ strains, data = strains_mean)
##
## $strains
##                         diff          lwr           upr     p adj
## frq7-frq10      -0.0632500 -0.117865466 -8.634534e-03 0.0136076
## gtr2-ko-frq10   -0.0109375 -0.065552966  4.367797e-02 0.9919149
## prd1-frq10       0.0681875  0.013572034  1.228030e-01 0.0059730
## vta-ko-frq10    -0.0402500 -0.094865466  1.436547e-02 0.2736095
## WT-frq10        -0.0948750 -0.149490466 -4.025953e-02 0.0000321
## gtr2-ko-frq7     0.0523125 -0.002302966  1.069280e-01 0.0684589
## prd1-frq7        0.1314375  0.076822034  1.860530e-01 0.0000000
## vta-ko-frq7      0.0230000 -0.031615466  7.761547e-02 0.8228568
## WT-frq7         -0.0316250 -0.086240466  2.299047e-02 0.5444097
## prd1-gtr2-ko     0.0791250  0.024509534  1.337405e-01 0.0008088
## vta-ko-gtr2-ko -0.0293125 -0.083927966  2.530297e-02 0.6248109
## WT-gtr2-ko      -0.0839375 -0.138552966 -2.932203e-02 0.0003138
## vta-ko-prd1     -0.1084375 -0.163052966 -5.382203e-02 0.0000016
## WT-prd1         -0.1630625 -0.217677966 -1.084470e-01 0.0000000
## WT-vta-ko       -0.0546250 -0.109240466 -9.533970e-06 0.0499335
```

```r
#loading the table for circadian rhythm analysis (Wild Type)
WTcosinor <- read_excel("wtcosinor.xlsx")
str(WTcosinor)
```

```
## tibble [16 × 2] (S3: tbl_df/tbl/data.frame)
##  $ time           : num [1:16] 20 24 28 32 36 40 44 48 52 56 ...
##  $ phosphorylation: num [1:16] 0.133 0.232 0.275 0.187 0.155 0.147 0.1
85 0.219 0.304 0.201 ...
```

```r
# Checking the rhythmicity for the WT with a period of 22 hours
rhythmic_wt <- circa_single(x= WTcosinor, col_time="time", col_outcome="p
hosphorylation", period=22)
rhythmic_wt
```

```
## $fit
## Nonlinear regression model
##   model: measure ~ k + (alpha) * cos((1/period) * time_r - (phi))
##    data: x
##       k   alpha     phi
## 0.19568 0.05506 1.91855
##  residual sum-of-squares: 0.009995
##
## Number of iterations to convergence: 5
## Achieved convergence tolerance: 9.124e-09
##
## $summary
##         parameter        value
## 1      rhythmic_p 9.979105e-05
## 2           mesor 1.956817e-01
## 3       amplitude 5.506220e-02
## 4   phase_radians 1.918549e+00
## 5 peak_time_hours 6.717623e+00
## 6          period 2.200000e+01
##
## $plot
```

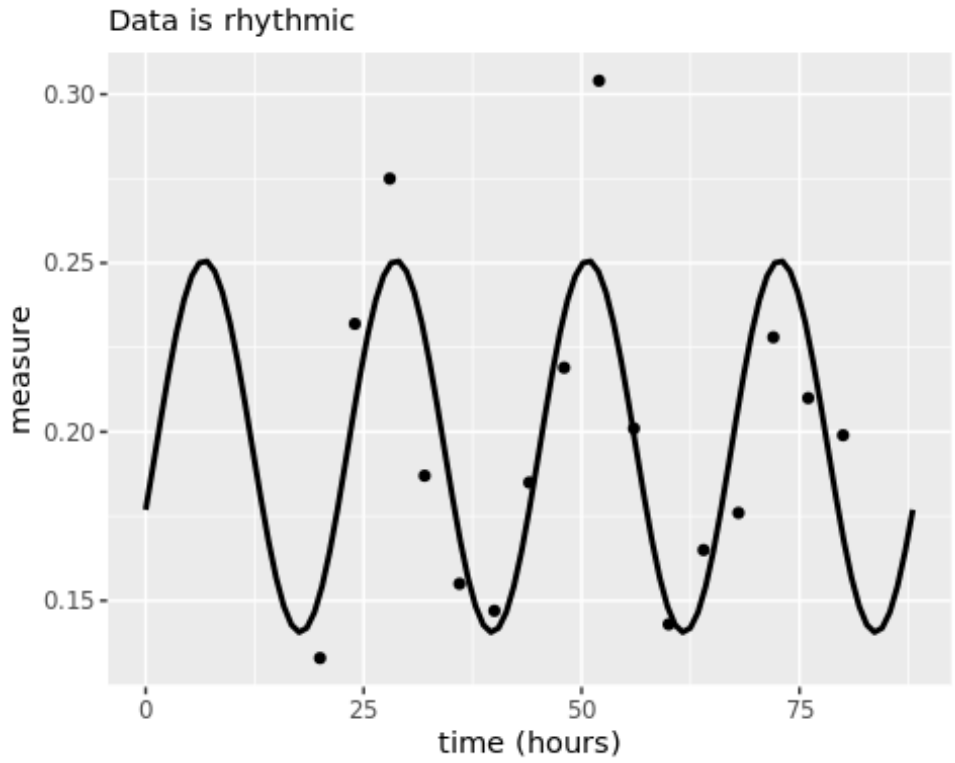


```
#loading the table for circadian rhythm analysis (vta-ko)
vtarhythm <- read_excel("vtarhythm.xlsx")
# Checking the rhythmicity for the vta-ko strain with an unknown period
rhythmicvta <- circa_single(x= vtarhythm, col_time="time", col_outcome="p
hosphorylation", control=list(period_param=TRUE))

## Error in stats::nls(formula = form, data = x, start = start_list(outco
me = x$measure,  :
##   number of iterations exceeded maximum of 50

rhythmicvta

## $fit
## Nonlinear regression model
##   model: measure ~ k + (alpha) * cos((1/(tau)) * time_r - (phi))
##    data: x
##        k    alpha      phi      tau
##  0.25535  0.06625  1.09750 26.85381
##  residual sum-of-squares: 0.01386
##
## Number of iterations to convergence: 15
## Achieved convergence tolerance: 8.282e-06
##
## $summary
##         parameter        value
```

```
## 1      rhythmic_p 1.646863e-04
## 2           mesor 2.553540e-01
## 3       amplitude 6.625374e-02
## 4   phase_radians 1.097504e+00
## 5 peak_time_hours 4.690641e+00
## 6          period 2.685381e+01
##
## $plot
```

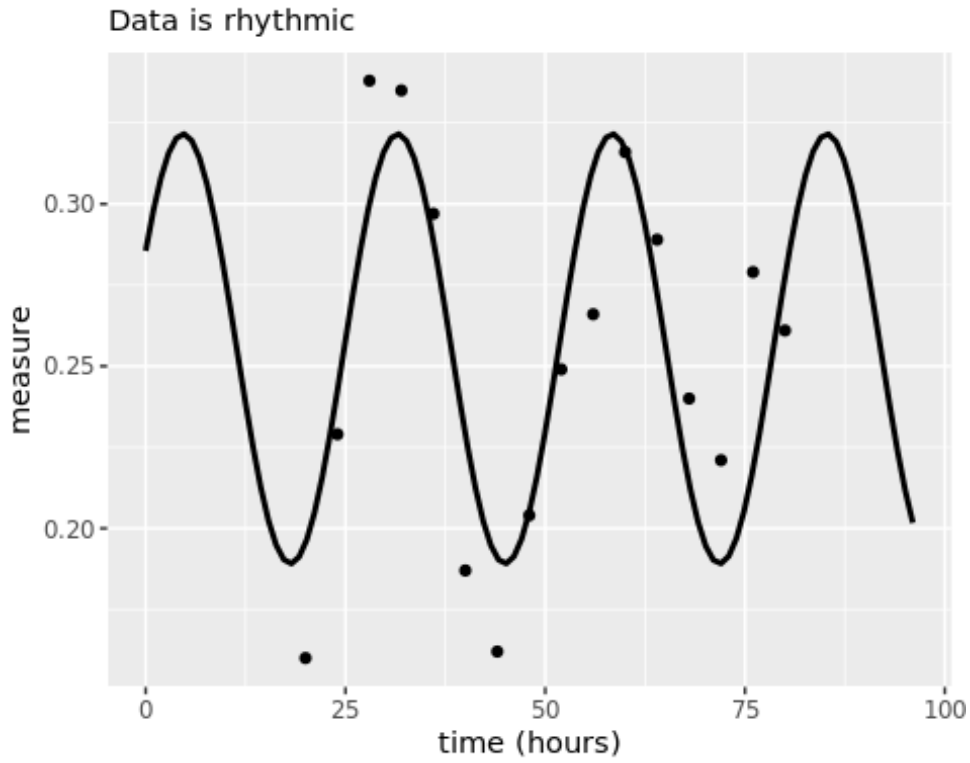


```
#Loading the table for circadian rhythm analysis (gtr2-ko)
gtr2rhythm <- read_excel("gtr2rhythm.xlsx")
# Checking the rhythmicity for the gtr2-ko strain with an unknown period
rhythmicgtr2 <- circa_single(x= gtr2rhythm, col_time="time", col_outcome=
"phosphorylation", control=list(period_param=TRUE))
rhythmicgtr2
```

```
## $fit
## Nonlinear regression model
##   model: measure ~ k + (alpha) * cos((1/(tau)) * time_r - (phi))
##    data: x
##        k    alpha      phi      tau
##  0.28716  0.07699  1.42416 26.59752
##  residual sum-of-squares: 0.0253
##
## Number of iterations to convergence: 23
```

```
## Achieved convergence tolerance: 9.762e-06
##
## $summary
##         parameter        value
## 1      rhythmic_p  0.000536916
## 2           mesor  0.287155901
## 3       amplitude  0.076989950
## 4   phase_radians  1.424157862
## 5 peak_time_hours  6.028640049
## 6          period 26.597516750
##
## $plot
```

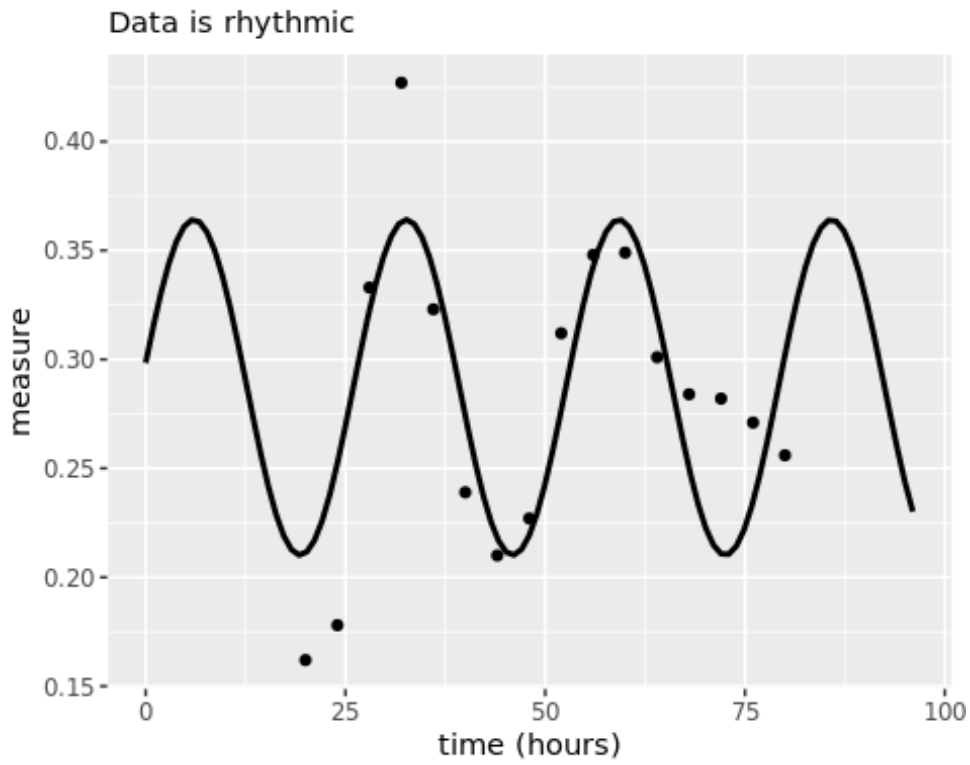


```
#loading the table for circadian rhythm analysis (prd1-ko)
prd1rhythm <- read_excel("prd1rhythm.xlsx")
# Checking the rhythmicity for the prd1 strain with an unknown period
rhythmicprd1 <- circa_single(x= prd1rhythm, col_time="time", col_outcome=
"phosphorylation", control=list(period_param=TRUE))
rhythmicprd1
```

```
## $fit
## Nonlinear regression model
##   model: measure ~ k + (alpha) * cos((1/(tau)) * time_r - (phi))
##    data: x
##        k    alpha      phi      tau
```

```
##  0.37166  0.09203  1.86438 27.24923
##  residual sum-of-squares: 0.01068
##
## Number of iterations to convergence: 8
## Achieved convergence tolerance: 3.075e-06
##
## $summary
##         parameter        value
## 1      rhythmic_p 1.403226e-06
## 2           mesor 3.716640e-01
## 3       amplitude 9.203454e-02
## 4   phase_radians 1.864383e+00
## 5 peak_time_hours 8.085547e+00
## 6          period 2.724923e+01
##
## $plot
```

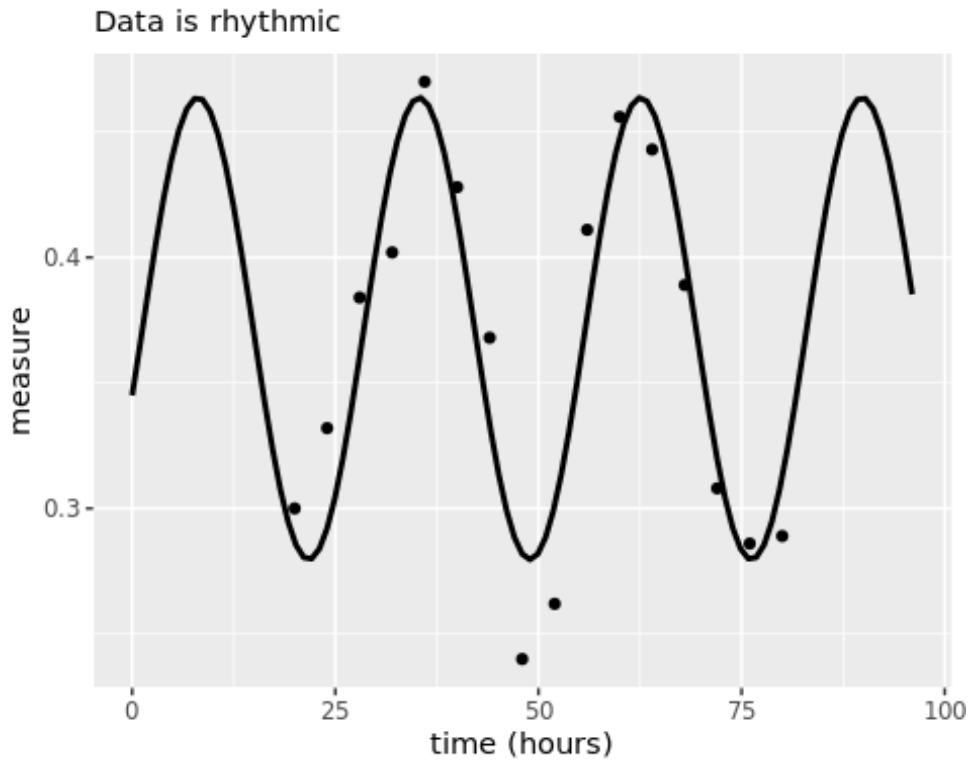


```
#loading the table for circadian rhythm analysis (frq7)
frq7rhythm <- read_excel("frq7rhythm.xlsx")
# Checking the rhythmicity for the frq7 strain with an unknown period
rhythmicfrq7 <- circa_single(x= frq7rhythm, col_time="time", col_outcome=
"phosphorylation", control=list(period_param=TRUE))
rhythmicfrq7
```

```
## $fit
## Nonlinear regression model
##   model: measure ~ k + (alpha) * cos((1/(tau)) * time_r - (phi))
##    data: x
##        k    alpha      phi      tau
##  0.23157  0.03803  0.12871 33.76148
##  residual sum-of-squares: 0.003644
##
## Number of iterations to convergence: 14
## Achieved convergence tolerance: 8.64e-06
##
## $summary
##         parameter        value
## 1      rhythmic_p 7.006741e-05
## 2           mesor 2.315699e-01
## 3       amplitude 3.803404e-02
## 4   phase_radians 1.287072e-01
## 5 peak_time_hours 6.915830e-01
## 6          period 3.376148e+01
##
## $plot
```

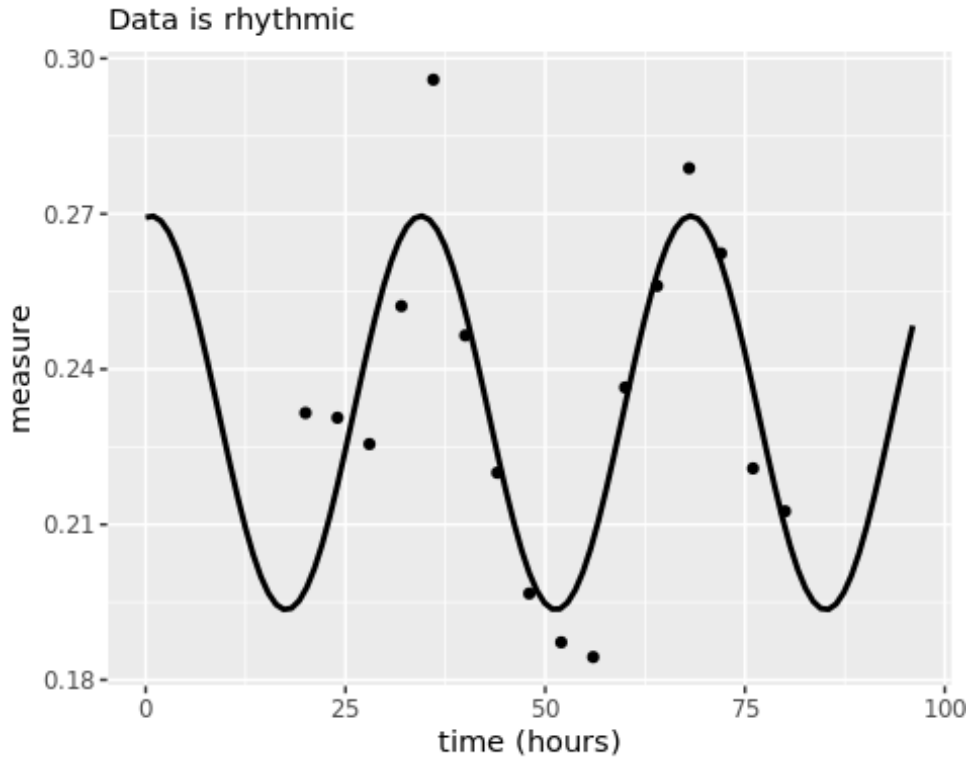


```
#loading the table for circadian rhythm analysis (frq10)
frq10rhythm <- read_excel("frq10rhythm.xlsx")
# Checking the rhythmicity for the frq10 strain with an unknown period
```

```
rhythmicfrq10 <- circa_single(x= frq10rhythm, col_time="time", col_outcom
e="phosphorylation", control=list(period_param=TRUE))

## Error in stats::nls(formula = form, data = x, start = start_list(outco
me = x$measure,  :
##   singular gradient

rhythmicfrq10

## $fit
## Nonlinear regression model
##   model: measure ~ k + (alpha) * cos((1/(tau)) * time_r - (phi))
##    data: x
##        k    alpha      phi      tau
##  0.29043  0.02332  0.43036 19.50141
##  residual sum-of-squares: 0.004593
##
## Number of iterations to convergence: 45
## Achieved convergence tolerance: 8.44e-06
##
## $summary
##         parameter        value
## 1      rhythmic_p  0.004778658
## 2           mesor  0.290434683
## 3       amplitude  0.023323707
## 4   phase_radians  0.430359562
## 5 peak_time_hours  1.335726342
## 6          period 19.501405020
##
## $plot
```

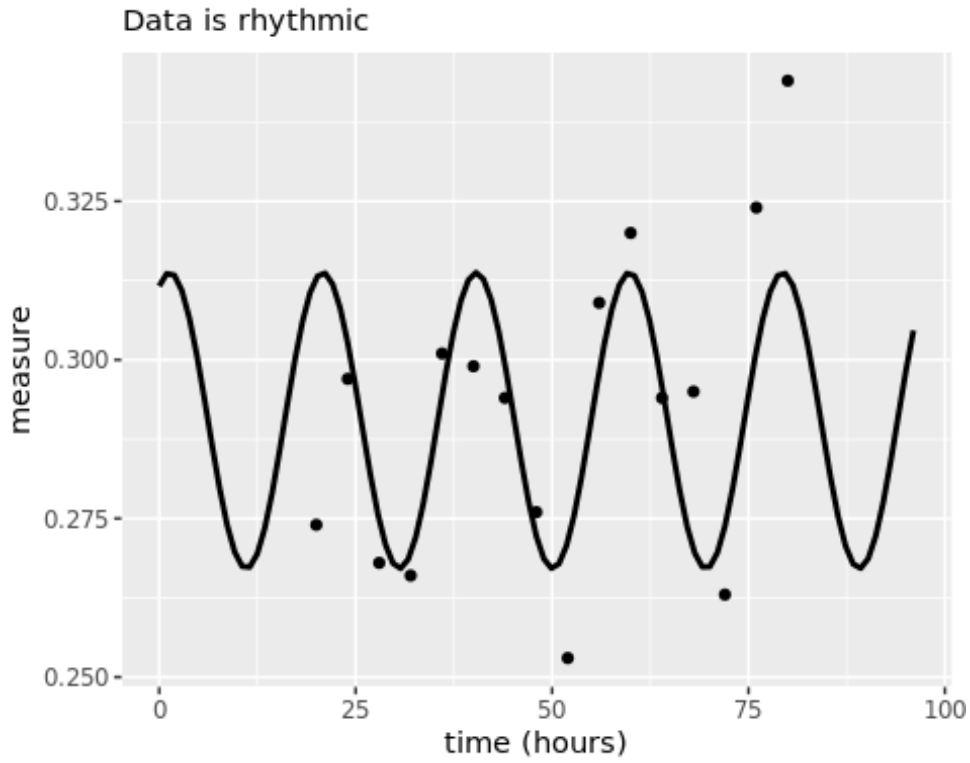
Data is rhythmic
0.325
0.300
0.275
0.250
measure
0
25
50
75
100
time (hours)